Scientific Reports

https://doi.org/10.1038/s41598-026-50541-y

Article in Press

Spectral energies of redefined Zagreb indices and comparative QSPR applications to anticancer and alcohol datasets

Received: 6 December 2025

Accepted: 21 April 2026

Published online: 29 April 2026

Cite this article as: Zeren Y., Çiçek E. & Alsharafi M. Spectral energies of redefined Zagreb indices and comparative QSPR applications to anticancer and alcohol datasets. *Sci Rep* (2026). https://doi.org/10.1038/s41598-026-50541-y

Yusuf Zeren, Erman Çiçek & Mohammed Alsharafi

We are providing an unedited version of this manuscript to give early access to its findings. Before final publication, the manuscript will undergo further editing. Please note there may be errors present which affect the content, and all legal disclaimers apply.

If this paper is publishing under a Transparent Peer Review model then Peer Review reports will publish with the final article.

ARTICLE IN PRESS

© The Author(s) 2026. **Open Access** This article is licensed under a Creative Commons Attribution-NonCommercial-NoDerivatives 4.0 International License, which permits any non-commercial use, sharing, distribution and reproduction in any medium or format, as long as you give appropriate credit to the original author(s) and the source, provide a link to the Creative Commons licence, and indicate if you modified the licensed material. You do not have permission under this licence to share adapted material derived from this article or parts of it. The images or other third party material in this article are included in the article's Creative Commons licence, unless indicated otherwise in a credit line to the material. If material is not included in the article's Creative Commons licence and your intended use is not permitted by statutory regulation or exceeds the permitted use, you will need to obtain permission directly from the copyright holder. To view a copy of this licence, visit http://creativecommons.org/licenses/by-nc-nd/4.0/.

ARTICLE IN PRESS

Spectral Energies of Redefined Zagreb Indices and Comparative QSPR Applications to Anticancer and Alcohol Datasets

Yusuf ZEREN[1], Erman Çiçek[2], and Mohammed Alsharafi [*3]

[1,2,3]Department of Mathematics Faculty of Arts and Science Yildiz Technical University, 34220 Esenler, Istanbul, Turkey
[3]Department of Mathematics, Sana'a University, Sana'a, Yemen

Abstract

This article develops a unified framework for the redefined Zagreb descriptors that combines graph theory, spectral analysis, and molecular structure–property applications. We study the basic redefined Zagreb descriptors together with their higher-order variants, introduce the associated weighted graph matrices, and investigate their spectral radii, energies, and related structural interpretations. For several standard graph families, including paths, cycles, complete graphs, stars, complete bipartite graphs, wheels, and friendship graphs, we derive explicit formulas and show how these descriptors reflect different degree patterns and connectivity structures. We also establish general bounds for the descriptors and their weighted spectral quantities, thereby clarifying their connections with classical degree-based indices and adjacency energy.

To examine chemical relevance, we first consider a small set of anticancer drug-like molecules and use it as an analytical descriptor study. In this setting, the redefined Zagreb descriptors and their energy-based analogues are strongly associated with size-related physicochemical quantities, while the mixed higher-order descriptor $ReZ_3^{2,1}$ shows the strongest relationship with the minimum universal force-field energy. This part of the study is intended to identify informative descriptor trends rather than to establish a fully validated predictive model.

We then carry out a broader QSPR study on 100 alcohol compounds with 17 physicochemical endpoints under repeated leakage-safe grouped external validation. The results show that the redefined Zagreb descriptor family and its derivative forms provide strong predictive performance for many targets, especially those related to molecular size, volume, and critical-property behavior. The derivative descriptors are therefore chemically meaningful and useful, while the combined representation shows where complementary information can be gained. Overall, the redefined Zagreb framework emerges as a mathematically rich and chemically useful family of descriptors whose combinatorial, spectral, and predictive roles can be studied in a unified way.

Keywords: redefined Zagreb indices; spectral graph theory; weighted adjacency matrices; graph energy; graph entropy; degree-based topological indices; QSPR; anticancer drug-like molecules; alcohol compounds.
MSC (2020): 05C09, 05C50, 05C92, 92E10.

1 Introduction

Graphs provide a flexible mathematical framework for modeling discrete structures arising in chemistry, physics, computer science, and complex networks. Standard background on graph structure and matrix representations may be found in [1, 2], while spectral aspects are treated in [3–5]. Structural and spectral invariants of graphs, such as degree sequences, eigenvalues, and various notions of graph energy, have been

*Corresponding author: alsharafi205010@gmail.com

ARTICLE IN PRESS

successfully used to describe physicochemical properties of molecules and to characterize complex systems. The concept of graph energy was introduced by Gutman and Trinajstić in the context of π–electron energies of conjugated hydrocarbons [6]. Since then, graph energy has developed into a broad research area; see, for example, [7–9]. More recent surveys and discussions may be found in [10–12]. In parallel, degree-based energies and their associated inequalities have become an active topic in spectral graph theory and mathematical chemistry [13, 14].

Among degree-based invariants, the Zagreb indices occupy a central position in chemical graph theory. Their origins go back to early work on molecular orbital theory [6, 15]. Later developments and surveys include [16–18], while broader discussions of degree-based indices appear in [19, 20]. Numerous generalizations and refinements have also been proposed. Sharp inequalities and extremal aspects were investigated in [21–23], whereas generalized Zagreb frameworks were considered in [24, 25]. Hyper-Zagreb indices and related coindices were introduced in [26, 27]. Further developments, including extremal and QSPR-oriented aspects, were reported in [28–30]. These studies illustrate the versatility of Zagreb-type quantities in capturing branching and degree heterogeneity in molecular graphs. Recent work has further broadened this area through explicit studies of Zagreb and multiplicative Zagreb indices on Eulerian graphs, as well as extremal investigations of the forgotten index and of graph classes maximizing or minimizing functions depending on adjacent vertex degrees [31–33].

A parallel line of research considers degree-based indices at the matrix level, where a graph is associated with a weighted adjacency matrix whose entries encode a symmetric function of endpoint degrees. Typical examples include the Randić matrix and Randić energy [34, 35], the ABC matrix [36], and matrices associated with the geometric-arithmetic index [37]. Related spectral and applicability aspects for graph descriptors were also investigated in [38]. From the viewpoint of complex networks, recent spectral work under noise disturbance has also highlighted the relevance of eigenvalue-based characteristics and coherence-type measures in the analysis of perturbed networked systems [39]. The spectral radius and energy of such matrices have been linked to QSPR/QSAR modeling and related applications [38, 40, 41]. Connections with Estrada-type quantities and broader spectral methods may be found in [4, 42, 43]. More generally, systematic studies of degree-based energies were developed in [13, 14]. These works complement the classical theory of graph energy and its variants, see [9, 44, 45] as well as [46–48].

Recently, new degree-based topological indices such as the Sombor index have attracted considerable attention. Gutman introduced the Sombor index through a geometric approach to degree-based descriptors [49]. Subsequent structural and chemical studies include [50–52], while spectral and energy aspects were investigated in [53–55]. Extremal and applicability results may also be found in [56–58]. On the applied side, contemporary QSPR studies continue to confirm the usefulness of topological descriptors for predicting physicochemical properties of medicinal and carbohydrate-related compounds [59, 60], while recent chemical variants further support the practical relevance of degree-based descriptors in molecular-property analysis [61, 62]. These developments reinforce the idea that many classical and new indices can be formulated in a unified way via edgewise kernels $F(x, y)$ of the endpoint degrees x and y, and that both their scalar values and associated matrix energies can carry chemically meaningful information.

Within this broader setting, the redefined Zagreb indices form a particularly interesting family of degree-based descriptors. Motivated by the search for degree parameters with improved discriminating power, several Zagreb–type modifications and extensions have been studied in the literature [26, 28, 29]. Related developments involving coindices, Zagreb–type energies, and Estrada–type quantities were reported in [27, 63]. From the viewpoint adopted in the present paper, these redefined Zagreb indices fit naturally into the edge–kernel paradigm, in which each index is written as a sum over edges of a symmetric kernel

$$F(\delta(u), \delta(v)),$$

where $\delta(u)$ and $\delta(v)$ are the degrees of the endpoints of the edge uv. They also admit hyper, general, and generalized–general extensions analogous to those known for the classical Zagreb family.

Despite this activity, most existing work on redefined Zagreb indices has focused on combinatorial structure, extremal behavior, and inequality theory. Comparatively less attention has been paid to their

ARTICLE IN PRESS

spectral aspects: how to associate weighted adjacency matrices to these kernels in a systematic way, how the resulting spectra and energies relate to classical graph energy and other degree-based energies, and how these spectral quantities behave on standard graph families such as paths, cycles, stars, complete graphs, complete bipartite graphs, wheels, and hypercubes. Related questions have been addressed for the Randić matrix [34,35], for degree–sum and ABC–type matrices [14,36,37], and for Zagreb energies and Zagreb Estrada–type indices [27,63]. Nevertheless, a unified treatment tailored specifically to the redefined Zagreb family still appears to be missing. At the same time, the broader topological-index literature also includes counting-based descriptors, such as subtree- and subpath-related parameters, which capture graph complexity from a perspective complementary to degree-based invariants. Related combinatorial investigations include expected subtree numbers of random hexagonal and phenylene chains, subpath numbers of cactus graphs, and extremal mean subtree order in trees [64–66].

The present paper contributes to this line of research by developing a unified F–weighted adjacency framework for redefined Zagreb indices and their hyper, general, and generalized–general variants. For each symmetric degree kernel $F(x,y)$, we associate a weighted adjacency matrix $W_F(G)$ whose (u,v)–entry equals $F\big(\delta_G(u),\delta_G(v)\big)$ whenever $uv \in E(G)$ and equals 0 otherwise. This perspective simultaneously encodes the scalar index

$$S_F(G) = \sum_{uv\in E(G)} F\big(\delta_G(u),\delta_G(v)\big),$$

its associated spectral radius $\rho_F(G)$, and the corresponding graph energy $E_F(G)$. In this way, the novelty of the present study lies not only in treating several redefined Zagreb variants within a single kernel-based setting, but also in linking their scalar forms, weighted spectral radii, and matrix energies in a unified and computationally tractable manner.

For regular and biregular graph families we prove a simple scaling law

$$W_F(G) = c\,A(G) \quad \text{with} \quad c = F(\delta_1,\delta_2),$$

which implies that the F–energy and F–spectral radius are obtained by scaling the classical adjacency energy and spectral radius. For general graphs we derive bounds in terms of the minimum and maximum degrees $\delta(G)$ and $\Delta(G)$, Frobenius–norm and row–sum estimates, and coindex relations that connect the energies of redefined Zagreb indices to other degree-based invariants and to basic structural parameters.

In addition, we provide closed formulas and explicit bounds for various redefined Zagreb–type energies on several standard graph classes, including complete graphs, complete bipartite graphs, stars, cycles, hypercubes, and certain chemical graph families. By expressing $S_F(G)$, $\rho_F(G)$, and $E_F(G)$ in terms of classical Zagreb indices, hyper–Zagreb indices, and related degree-based descriptors, we obtain inequalities that can be interpreted in both directions: known bounds for classical indices immediately translate into bounds for redefined Zagreb energies, and conversely, spectral information about $W_F(G)$ constrains traditional indices.

On the applied side, the manuscript contains two complementary case studies. First, for the anticancer-drug dataset, the UFF-related study is used as an analytical descriptor-comparison approach intended to explore structure–index–property relationships rather than as a fully developed predictive QSPR model. Second, for the alcohol dataset, we perform a broader comparative QSPR analysis with standardized descriptors and validation-based modeling across multiple physicochemical properties. This dual design aligns the scope of the applications with the actual level of statistical development in each part, while also showing that the proposed redefined Zagreb descriptors and their spectral analogues can be meaningfully examined in both exploratory and fully validated settings.

2 Basics: graphs, degree-based indices, spectra, energy and entropy

In this section we recall the basic concepts and notation that will be used throughout the paper. All graphs are assumed to be finite, simple, and undirected.

ARTICLE IN PRESS

2.1 Graphs and notation

Let $G = (V(G), E(G))$ be a simple graph with vertex set $V(G)$ and edge set $E(G)$. The *order* and *size* of G are denoted by

$$n := |V(G)|, \qquad m := |E(G)|.$$

For a vertex $v \in V(G)$, we write $\delta_G(v)$ (or simply $\delta(v)$) for its degree, i.e., the number of vertices adjacent to v. The minimum and maximum degrees of G are denoted by

$$\delta(G) := \min_{v \in V(G)} \delta(v), \qquad \Delta(G) := \max_{v \in V(G)} \delta(v).$$

A graph G is called *r-regular* if $\delta(v) = r$ for all $v \in V(G)$. A bipartite graph $G = (V_1 \cup V_2, E)$ is called *(r, s)-biregular* if each vertex in V_1 has degree r and each vertex in V_2 has degree s. The complement of G is denoted by $\overline{G}$; it has the same vertex set as G, and two distinct vertices are adjacent in $\overline{G}$ if and only if they are non-adjacent in G.

For an edge $uv \in E(G)$ we will often write

$$x = \delta(u), \qquad y = \delta(v)$$

for the degrees of its endpoints. This notation is convenient when we consider edge–based expressions of the form $F(x, y)$.

2.2 Some classical degree-based topological indices

Topological indices are numerical invariants of graphs that do not depend on the particular labelling of vertices. Many important indices in chemical graph theory are degree-based: they can be written as sums over vertices or edges involving vertex degrees. Such descriptors are especially useful because they encode local branching patterns and degree heterogeneity in a compact numerical form, which helps explain why they have remained central in both theoretical chemical graph theory and structure–property investigations.

Zagreb indices. The first and second Zagreb indices [6] of G are defined by

$$M_1(G) = \sum_{v \in V(G)} \delta(v)^2, \qquad M_2(G) = \sum_{uv \in E(G)} \delta(u)\,\delta(v). \tag{2.1}$$

Another frequently used degree-based quantity is the so–called forgotten index (or F–index) [67],

$$F(G) = \sum_{v \in V(G)} \delta(v)^3. \tag{2.2}$$

Randić–type and connectivity indices. The classical Randić index [68] is given by

$$R(G) = \sum_{uv \in E(G)} \frac{1}{\sqrt{\delta(u)\,\delta(v)}}. \tag{2.3}$$

Two closely related indices that will be useful for comparison are:

- the *harmonic index* [69]

$$H(G) = \sum_{uv \in E(G)} \frac{2}{\delta(u) + \delta(v)}, \tag{2.4}$$

- the *sum–connectivity index* [70]

$$\chi(G) = \sum_{uv \in E(G)} \frac{1}{\sqrt{\delta(u) + \delta(v)}}. \tag{2.5}$$

ARTICLE IN PRESS

GA and ABC indices. The first geometric–arithmetic index and the atom–bond connectivity index [71,72] are defined, respectively, by

$$GA(G) = \sum_{uv\in E(G)} \frac{2\sqrt{\delta(u)\,\delta(v)}}{\delta(u)+\delta(v)}, \qquad ABC(G) = \sum_{uv\in E(G)} \sqrt{\frac{\delta(u)+\delta(v)-2}{\delta(u)\,\delta(v)}}. \tag{2.6}$$

2.3 Spectral graph theory and energy of a graph

Let G be a simple graph of order n, and fix an ordering $V(G) = \{v_1, \dots, v_n\}$. The *adjacency matrix* of G [1] is the $n \times n$ matrix $A(G) = (a_{ij})$ defined by

$$a_{ij} = \begin{cases} 1, & \text{if } v_i v_j \in E(G), \\ 0, & \text{otherwise.} \end{cases}$$

Since G is undirected, $A(G)$ is real symmetric and has n real eigenvalues, which we list in nonincreasing order,

$$\lambda_1(G) \geq \lambda_2(G) \geq \cdots \geq \lambda_n(G).$$

The largest eigenvalue $\lambda_1(G)$ is called the *spectral radius* of G and is denoted by

$$\rho(G) := \lambda_1(G).$$

The *degree matrix* of G is the diagonal matrix

$$D(G) := \operatorname{diag}(\delta(v_1), \dots, \delta(v_n)).$$

The (combinatorial) Laplacian and the signless Laplacian of G [3,4] are defined by

$$L(G) := D(G) - A(G), \qquad Q(G) := D(G) + A(G).$$

Definition 2.1. *[9] Let G be a simple graph with adjacency eigenvalues $\lambda_1(G), \dots, \lambda_n(G)$. The* energy *of G is*

$$E(G) = \sum_{i=1}^{n} \bigl|\lambda_i(G)\bigr|. \tag{2.7}$$

Graph energy originates from Hückel molecular orbital theory, where the eigenvalues of $A(G)$ model the energy levels of π–electrons of a conjugated molecule. In our context, $E(G)$ will serve as a reference concept: later we will define and study analogous energies associated with matrices built from the redefined Zagreb kernels. This matrix-based viewpoint is one of the central ideas of the paper, because it allows scalar degree descriptors and their associated spectral quantities to be analyzed within a single framework.

More generally, if $M(G)$ is any real symmetric matrix associated with G (for instance, $L(G)$, $Q(G)$, or a weighted adjacency matrix), with eigenvalues $\mu_1, \dots, \mu_n$, one can define the corresponding *M–energy* by

$$E(M(G)) := \sum_{i=1}^{n} |\mu_i|.$$

This unified viewpoint will be used in Sections 5 and 6 for the matrices induced by the redefined Zagreb families.

ARTICLE IN PRESS

2.4 An entropy viewpoint for degree-based weights

Since the present work also refers to entropy-type interpretations, we briefly recall the basic probabilistic viewpoint that will be used later. If a finite family of nonnegative weights $\{w_i\}_{i=1}^N$ is given, with $\sum_{i=1}^N w_i > 0$, then the normalized quantities

$$p_i = \frac{w_i}{\sum_{j=1}^N w_j}, \qquad i = 1, \dots, N,$$

define a probability distribution. The associated Shannon entropy is

$$\mathcal{H}(p_1, \dots, p_N) = -\sum_{i=1}^N p_i \log p_i, \tag{2.8}$$

with the convention $0 \log 0 = 0$.

In degree-based graph settings, such weights may be constructed from vertex contributions, edge contributions, or kernel values such as $F(\delta(u), \delta(v))$. Entropy then measures how uniformly or non-uniformly the corresponding structural information is distributed across the graph. In particular, more uniform distributions are associated with larger entropy values, whereas strongly concentrated contributions lead to smaller entropy values.

Although the main emphasis of the paper is on weighted spectral radii and energies, this entropy viewpoint provides a complementary way to interpret the same kernel-based data and helps clarify the role of regular versus heterogeneous graph structure.

3 Redefined Zagreb indices for special graphs

In this section, we study the behavior of the redefined Zagreb indices on several classical graph families. We begin by recalling the closed forms of the basic redefined Zagreb indices ReZ_1, ReZ_2, and ReZ_3 for paths, cycles, complete graphs, stars, wheels, and related graph classes. For convenience, these known formulas, together with our newly derived explicit expressions for the hyper, general, and generalized–general variants $\mathrm{ReZ}_i^{2,1}$, $\mathrm{ReZ}_i^{1,2}$, and $\mathrm{ReZ}_i^{\alpha,\alpha}$, for $i \in \{1, 2, 3\}$, are collected in Proposition 3.3 and Table 1. In addition to the above classical families, the summary also covers complete bipartite graphs and friendship graphs. These closed forms play a dual role in the sequel: on the one hand, they provide exact values of the scalar descriptors themselves, and on the other hand, they reveal how degree patterns control the corresponding weighted energies and entropy-type quantities from both spectral and information–theoretic viewpoints.

Let $G = (V(G), E(G))$ be a simple graph with $|V(G)| = n$ and $|E(G)| = m$. For a vertex $u \in V(G)$ denote its degree by $\delta_G(u)$ (or simply $\delta(u)$ when there is no ambiguity). For an edge $uv \in E(G)$ write

$$x = \delta_G(u), \qquad y = \delta_G(v).$$

The redefined Zagreb indices are defined [73] by

$$\mathrm{ReZ}_1(G) = \sum_{uv \in E(G)} \frac{x+y}{xy}, \qquad \mathrm{ReZ}_2(G) = \sum_{uv \in E(G)} \frac{xy}{x+y}, \qquad \mathrm{ReZ}_3(G) = \sum_{uv \in E(G)} xy\,(x+y).$$

ARTICLE IN PRESS

The *hyper*, *general*, and *generalized–general* variants are given by

$$\mathrm{ReZ}_1^{2,1}(G) = \sum_{uv\in E(G)} \frac{(x+y)^2}{xy}, \quad \mathrm{ReZ}_1^{1,2}(G) = \sum_{uv\in E(G)} \frac{x+y}{(xy)^2},$$

$$\mathrm{ReZ}_1^{\alpha,\alpha}(G) = \sum_{uv\in E(G)} \frac{(x+y)^\alpha}{(xy)^\alpha}, \quad \mathrm{GReZ}_1^{\alpha,\alpha}(G) = \sum_{uv\in E(G)} \frac{(x^\alpha+y^\alpha)^\alpha}{(xy)^{\alpha^2}},$$

$$\mathrm{ReZ}_2^{2,1}(G) = \sum_{uv\in E(G)} \frac{(xy)^2}{x+y}, \quad \mathrm{ReZ}_2^{1,2}(G) = \sum_{uv\in E(G)} \frac{xy}{(x+y)^2},$$

$$\mathrm{ReZ}_2^{\alpha,\alpha}(G) = \sum_{uv\in E(G)} \frac{(xy)^\alpha}{(x+y)^\alpha}, \quad \mathrm{GReZ}_2^{\alpha,\alpha}(G) = \sum_{uv\in E(G)} \frac{(x^\alpha y^\alpha)^\alpha}{(x^\alpha+y^\alpha)^\alpha},$$

$$\mathrm{ReZ}_3^{2,1}(G) = \sum_{uv\in E(G)} (xy)^2(x+y), \quad \mathrm{ReZ}_3^{1,2}(G) = \sum_{uv\in E(G)} xy(x+y)^2,$$

$$\mathrm{ReZ}_3^{\alpha,\alpha}(G) = \sum_{uv\in E(G)} (xy)^\alpha(x+y)^\alpha, \quad \mathrm{GReZ}_3^{\alpha,\alpha}(G) = \sum_{uv\in E(G)} (xy)^{\alpha^2}(x^\alpha+y^\alpha)^\alpha,$$

where $\alpha > 0$.

Remark 3.1. If the edge set admits a partition by degree types

$$E(G) \;=\; \bigsqcup_{t=1}^{T} E_{(a_t,b_t)}, \qquad E_{(a,b)} := \{\, uv \in E(G) : \{\delta_G(u), \delta_G(v)\} = \{a,b\} \,\},$$

and $m_t := |E_{(a_t,b_t)}|$, then for any symmetric kernel $F : \mathbb{N}\times\mathbb{N} \to \mathbb{R}_{>0}$ one has

$$\sum_{uv\in E(G)} F\big(\delta_G(u), \delta_G(v)\big) \;=\; \sum_{t=1}^{T} m_t\, F(a_t, b_t).$$

This observation is fundamental for all subsequent calculations: once the edge set is decomposed according to degree types, each redefined Zagreb quantity reduces to a finite weighted sum depending only on the corresponding local degree pairs. In particular, the formulas in Table 1 reflect the interaction between graph structure and degree distribution rather than merely the total number of edges.

Remark 3.2. Since

$$\mathrm{ReZ}_1(G) = \sum_{uv\in E(G)} \left(\frac{1}{\delta_G(u)} + \frac{1}{\delta_G(v)}\right),$$

each non-isolated vertex contributes exactly 1, while isolated vertices contribute 0. Hence

$$\mathrm{ReZ}_1(G) = |V(G)| - \#\{\text{isolated vertices of } G\}.$$

Thus, unlike the higher-order variants, ReZ_1 does not distinguish between non-isomorphic graphs having the same set of non-isolated vertices. This simple identity helps explain why richer redefined Zagreb variants are needed when finer structural discrimination is desired.

Proposition 3.3. *For the graph families P_n, K_n, C_n, $S_n = K_{1,n-1}$, $K_{m,n}$, W_n, and F_n, the closed forms of the classical redefined Zagreb indices ReZ_i and of their hyper, general, and generalized–general variants $\mathrm{ReZ}_i^{2,1}$, $\mathrm{ReZ}_i^{1,2}$, and $\mathrm{ReZ}_i^{\alpha,\alpha}$, for $i = 1, 2, 3$, are listed in Table 1. Here $n \geq 3$ for P_n and C_n, $n \geq 2$ for K_n and S_n, $m, n \geq 1$ for $K_{m,n}$, $n \geq 4$ for W_n, and $n \geq 1$ for F_n.*

ARTICLE IN PRESS

Table 1: Closed forms of the classical redefined Zagreb indices and their variants for selected graph families.

Family	Degree pattern / assumptions	Index	Classical ReZ_i	Hyper $\mathrm{ReZ}_i^{2,1}$	General $\mathrm{ReZ}_i^{1,2}$	Generalized–general $\mathrm{ReZ}_i^{\alpha,\alpha}$
P_n	$n \geq 3$; two edges of type $(1,2)$ and $n-3$ edges of type $(2,2)$ (for $n=3$, only $(1,2)$-edges occur)	ReZ_1	n	$4n-3$	$\frac{n+3}{4}$	$(n-3)+2\left(\frac{3}{2}\right)^{\alpha}$
		ReZ_2	$n-\frac{5}{3}$	$\frac{12n-28}{3}$	$\frac{9n-11}{36}$	$(n-3)+2\left(\frac{2}{3}\right)^{\alpha}$
		ReZ_3	$16n-36$	$64n-168$	$64n-156$	$2\cdot 6^{\alpha}+(n-3)\cdot 16^{\alpha}$
K_n	$n \geq 2$; every edge has degree pair $(n-1,n-1)$	ReZ_1	n	$2n(n-1)$	$\frac{n}{(n-1)^2}$	$n\,2^{\alpha-1}(n-1)^{1-\alpha}$
		ReZ_2	$\frac{n(n-1)^2}{4}$	$\frac{n(n-1)^4}{4}$	$\frac{n(n-1)}{8}$	$\frac{n(n-1)^{\alpha+1}}{2^{\alpha+1}}$
		ReZ_3	$n(n-1)^4$	$n(n-1)^6$	$2n(n-1)^5$	$n\,2^{\alpha-1}(n-1)^{3\alpha+1}$
C_n	$n \geq 3$; all edges are of type $(2,2)$	ReZ_1	n	$4n$	$\frac{n}{4}$	n
		ReZ_2	n	$4n$	$\frac{n}{4}$	n
		ReZ_3	$16n$	$64n$	$64n$	$n\,16^{\alpha}$
$S_n = K_{1,n-1}$	$n \geq 2$; every edge has degree pair $(1,n-1)$	ReZ_1	n	n^2	$\frac{n}{n-1}$	$n^{\alpha}(n-1)^{1-\alpha}$
		ReZ_2	$\frac{(n-1)^2}{n}$	$\frac{(n-1)^3}{n}$	$\frac{(n-1)^2}{n^2}$	$\frac{(n-1)^{\alpha+1}}{n^{\alpha}}$
		ReZ_3	$n(n-1)^2$	$n(n-1)^3$	$n^2(n-1)^2$	$n^{\alpha}(n-1)^{\alpha+1}$
$K_{m,n}$	$m,n \geq 1$; all edges are of type (m,n)	ReZ_1	$m+n$	$(m+n)^2$	$\frac{m+n}{mn}$	$(m+n)^{\alpha}(mn)^{1-\alpha}$
		ReZ_2	$\frac{m^2n^2}{m+n}$	$\frac{m^3n^3}{m+n}$	$\frac{m^2n^2}{(m+n)^2}$	$\frac{(mn)^{\alpha+1}}{(m+n)^{\alpha}}$
		ReZ_3	$m^2n^2(m+n)$	$m^3n^3(m+n)$	$m^2n^2(m+n)^2$	$(mn)^{\alpha+1}(m+n)^{\alpha}$
W_n	$n \geq 4$; $n-1$ rim edges of type $(3,3)$ and $n-1$ spokes of type $(3,n-1)$	ReZ_1	n	$\frac{n^2+16n-8}{3}$	$\frac{2n^2-n+8}{27(n-1)}$	$(n-1)\left(\frac{2}{3}\right)^{\alpha}+\frac{(n+2)^{\alpha}}{3^{\alpha}}(n-1)^{1-\alpha}$
		ReZ_2	$\frac{9n(n-1)}{2(n+2)}$	$\frac{9(n-1)(2n^2-n+8)}{2(n+2)}$	$\frac{n-1}{4}+\frac{3(n-1)^2}{(n+2)^2}$	$(n-1)\left(\frac{3}{2}\right)^{\alpha}+\frac{3^{\alpha}(n-1)^{\alpha+1}}{(n+2)^{\alpha}}$
		ReZ_3	$3(n-1)(n^2+n+16)$	$9(n-1)[54+(n-1)^2(n+2)]$	$3(n-1)[108+(n-1)(n+2)^2]$	$(n-1)\left(2^{\alpha}3^{3\alpha}+3^{\alpha}(n-1)^{\alpha}(n+2)^{\alpha}\right)$
F_n	$n \geq 1$; order $2n+1$; n edges of type $(2,2)$ and $2n$ edges of type $(2,2n)$	ReZ_1	$2n+1$	$2n^2+8n+2$	$\frac{n^2+n+1}{4n}$	$n+2^{1-\alpha}n^{1-\alpha}(n+1)^{\alpha}$
		ReZ_2	$\frac{n(5n+1)}{n+1}$	$4n+\frac{16n^3}{n+1}$	$\frac{n}{4}+\frac{2n^2}{(n+1)^2}$	$n+\frac{2^{\alpha+1}n^{\alpha+1}}{(n+1)^{\alpha}}$
		ReZ_3	$16n(n^2+n+1)$	$64n+64n^3(n+1)$	$64n+32n^2(n+1)^2$	$n\,16^{\alpha}+2n\,8^{\alpha}n^{\alpha}(n+1)^{\alpha}$

Table 1 shows a clear structural pattern. For regular families such as K_n and C_n, every edge has the same degree type, so each redefined Zagreb quantity collapses to a constant multiple of the number of edges. This reflects a high degree of structural uniformity and anticipates the scaling relations for the associated weighted matrices developed later.

By contrast, for non-regular families such as paths, stars, wheels, and friendship graphs, multiple edge types coexist, and the corresponding formulas separate naturally into contributions from peripheral and central edges. In particular, the formulas for P_n isolate the effect of the two terminal $(1,2)$-edges, whereas those for S_n and W_n reveal how the presence of a hub vertex amplifies the higher-order variants, especially those involving products such as $\mathrm{ReZ}_3^{2,1}$ and $\mathrm{ReZ}_3^{\alpha,\alpha}$.

This distinction is important for the later spectral and applied parts of the paper. Kernels that emphasize products or higher powers of endpoint degrees respond much more strongly to degree imbalance and branching concentration, which helps explain why some redefined Zagreb variants are more sensitive than others in both energy-based comparisons and descriptor-analysis settings.

4 Bounds for redefined Zagreb indices and relations with other topological indices

Throughout this section, let $G = (V(G), E(G))$ be a simple graph of order $n = |V(G)|$ and size $m = |E(G)|$. For $v \in V(G)$ we denote its degree by $\delta_G(v)$, or simply $\delta(v)$. The minimum and maximum degrees are denoted by

$$\delta = \delta(G) := \min_{v \in V(G)} \delta(v), \qquad \Delta = \Delta(G) := \max_{v \in V(G)} \delta(v).$$

We use the notation

$$x = \delta(u), \quad y = \delta(v) \quad \text{for a generic edge } uv \in E(G), \qquad S = x + y, \quad P = xy.$$

ARTICLE IN PRESS

Recall that the basic redefined Zagreb indices are

$$\mathrm{ReZ}_1(G) = \sum_{uv\in E(G)} \frac{x+y}{xy}, \qquad \mathrm{ReZ}_2(G) = \sum_{uv\in E(G)} \frac{xy}{x+y}, \qquad \mathrm{ReZ}_3(G) = \sum_{uv\in E(G)} xy\,(x+y),$$

and that hyper, general, and generalized–general variants arise from replacing the kernel $(x,y) \mapsto \frac{x+y}{xy}$, $\frac{xy}{x+y}$ or $xy(x+y)$ by the corresponding modified kernels $\mathrm{ReZ}_i^{2,1}$, $\mathrm{ReZ}_i^{1,2}$, $\mathrm{ReZ}_i^{\alpha,\alpha}$ and $\mathrm{GReZ}_i^{\alpha,\alpha}$, $i \in \{1,2,3\}$, as defined in Section 3. The aim of this section is to connect these kernels with standard degree-based quantities and to derive bounds that make the later spectral analysis easier to interpret.

4.1 Inverse–degree evaluation of ReZ_1 and coindex relations

We first observe that ReZ_1 admits a particularly simple expression in terms of the degree sequence. This leads to direct relations with the inverse–degree index

$$S_{-1}(G) := \sum_{v\in V(G)} \frac{1}{\delta(v)},$$

a well–studied degree-based topological index.

Lemma 4.1. *Assume that every vertex of G has positive degree. Then*

$$\mathrm{ReZ}_1(G) = \sum_{uv\in E(G)} \left(\frac{1}{\delta(u)} + \frac{1}{\delta(v)}\right) = \sum_{v\in V(G)} \frac{\delta(v)}{\delta(v)} = |V(G)| = n.$$

If isolated vertices are present, $\mathrm{ReZ}_1(G)$ equals the number of non–isolated vertices.

Proof. Each vertex v is incident with exactly $\delta(v)$ edges, and each incident edge contributes $\frac{1}{\delta(v)}$ through the term $\frac{1}{\delta(u)} + \frac{1}{\delta(v)}$. Hence the total contribution of v is $\delta(v) \cdot \frac{1}{\delta(v)} = 1$. Summing over all non–isolated vertices gives the claim. □

Lemma 4.1 shows that ReZ_1 is structurally much more rigid than the higher redefined Zagreb variants: once isolated vertices are excluded, it depends only on the order of the graph and not on the finer arrangement of edges. This explains why ReZ_1 is useful as a normalization benchmark, whereas more refined discrimination must come from kernels such as ReZ_2, ReZ_3, and their variants.

As an immediate consequence, we recover classical order/size constraints in terms of n and m.

Corollary 4.2. *Let G be a graph with minimum degree at least 1, order n, and size m. Then*

$$\frac{2m}{n-1} \;\le\; \mathrm{ReZ}_1(G) = n \;\le\; 2m.$$

The left equality holds for $G \cong K_n$, and the right equality is attained when every edge joins two vertices of degree 1, i.e., by a matching (possibly plus isolated vertices; in particular, by a perfect matching if there are no isolated vertices).

Proof. For graphs without isolated vertices one has $1 \le \delta(v) \le n-1$, hence $2/(n-1) \le (1/\delta(u)+1/\delta(v)) \le 2$ for each edge uv. Summing over m edges and using Lemma 4.1 yields $2m/(n-1) \le n \le 2m$. □

The extremal cases in Corollary 4.2 have a clear interpretation. Complete graphs minimize the edgewise inverse-degree contribution because all degrees are as large as possible, whereas matchings maximize it because every contributing endpoint has degree 1. Thus the bound reflects the transition from highly dense uniform structures to maximally sparse nontrivial ones.

We now introduce the *coindex* corresponding to ReZ_1.

ARTICLE IN PRESS

Definition 4.3. *Assume that G has no isolated vertices. The coindex associated with* ReZ_1 *is defined by*

$$\overline{\mathrm{ReZ}_1}(G) := \sum_{\{u,v\}\notin E(G)} \left(\frac{1}{\delta(u)} + \frac{1}{\delta(v)}\right),$$

where the sum is taken over all unordered nonedges $\{u, v\}$.

Lemma 4.4. *If G has no isolated vertices, then*

$$\overline{\mathrm{ReZ}_1}(G) = (n-1) \sum_{v\in V(G)} \frac{1}{\delta(v)} - \mathrm{ReZ}_1(G) = (n-1)\, S_{-1}(G) - n.$$

Proof. Fix $v \in V(G)$. The vertex v has $n - 1 - \delta(v)$ non–neighbours, and each corresponding nonedge contributes $1/\delta(v)$ in the coindex. The total contribution of v is thus $(n - 1 - \delta(v))/\delta(v)$. Summing over all vertices, one obtains

$$\overline{\mathrm{ReZ}_1}(G) = \sum_{v\in V(G)} \frac{n-1-\delta(v)}{\delta(v)} = (n-1)\, S_{-1}(G) - \sum_{v\in V(G)} \frac{\delta(v)}{\delta(v)},$$

and Lemma 4.1 gives the result. □

Lemma 4.4 is important because it expresses the nonedge contribution entirely through the inverse-degree index. In this way, the pair $\mathrm{ReZ}_1(G)$ and $\overline{\mathrm{ReZ}_1}(G)$ separates the graph into edge and nonedge contributions while remaining linked by a single inverse-degree quantity.

Combining Lemma 4.4 with standard bounds for the inverse–degree index yields two–sided estimates for $\overline{\mathrm{ReZ}_1}(G)$ and for the mixed sum $\mathrm{ReZ}_1(G) + \overline{\mathrm{ReZ}_1}(G)$.

Theorem 4.5. *For any graph G with minimum degree $\delta \geq 1$ and maximum degree Δ, one has*

$$\frac{n^2}{2m} \leq S_{-1}(G) \leq \frac{n}{\delta}, \qquad \frac{n}{\Delta} \leq S_{-1}(G),$$

and consequently

$$(n-1)\frac{n^2}{2m} - n \leq \overline{\mathrm{ReZ}_1}(G) \leq (n-1)\frac{n}{\delta} - n,$$

as well as

$$(n-1)\frac{n}{\Delta} - n \leq \overline{\mathrm{ReZ}_1}(G).$$

Moreover,

$$\mathrm{ReZ}_1(G) + \overline{\mathrm{ReZ}_1}(G) = (n-1)\, S_{-1}(G)$$

satisfies

$$(n-1)\frac{n^2}{2m} \leq \mathrm{ReZ}_1(G) + \overline{\mathrm{ReZ}_1}(G) \leq (n-1)\frac{n}{\delta}.$$

Proof. The lower bound $S_{-1}(G) \geq n^2/(2m)$ follows from Cauchy–Schwarz:

$$\left(\sum_{v\in V(G)} 1\right)^2 \leq \left(\sum_{v\in V(G)} \delta(v)\right)\left(\sum_{v\in V(G)} \frac{1}{\delta(v)}\right) = 2m\, S_{-1}(G).$$

The upper and lower one–sided bounds $S_{-1}(G) \leq n/\delta$ and $S_{-1}(G) \geq n/\Delta$ are immediate from $\delta \leq \delta(v) \leq \Delta$. The inequalities for $\overline{\mathrm{ReZ}_1}(G)$ and $\mathrm{ReZ}_1(G) + \overline{\mathrm{ReZ}_1}(G)$ follow by substituting into Lemma 4.4. □

ARTICLE IN PRESS

Theorem 4.5 shows that the coindex of ReZ_1 is governed by the same degree extremal parameters that control the inverse-degree index. In dense graphs, where degrees are large, both $S_{-1}(G)$ and $\overline{\mathrm{ReZ}_1}(G)$ are comparatively small; in sparse graphs with small minimum degree, these quantities may become much larger. Thus the theorem makes explicit how inverse-degree information regulates the balance between adjacency and nonadjacency contributions.

The quantity $S_{-1}(G)$ thus provides a natural bridge between the redefined Zagreb index ReZ_1, its coindex, and other inverse–degree– based topological indices studied in the chemical graph theory literature. This bridge will also be useful later when interpreting weighted energies, because it illustrates how apparently different descriptors can often be traced back to a common degree-based core.

4.2 Degree–extreme bounds for ReZ_2 and ReZ_3

We next derive sharp bounds for the second and third redefined Zagreb indices in terms of m, δ, and Δ. These bounds already illustrate an important structural distinction between ReZ_1 and the higher redefined Zagreb indices: unlike ReZ_1, both ReZ_2 and ReZ_3 genuinely respond to the concentration of degree mass along the edges, and therefore encode nontrivial information on the degree heterogeneity of the graph.

Theorem 4.6. *Let G be a simple graph with minimum degree $\delta \geq 1$ and maximum degree Δ. Then*

$$\frac{\delta}{2}\, m \;\leq\; \mathrm{ReZ}_2(G) = \sum_{uv \in E(G)} \frac{xy}{x+y} \;\leq\; \frac{\Delta}{2}\, m,$$

and

$$2\,\delta^3\, m \;\leq\; \mathrm{ReZ}_3(G) = \sum_{uv \in E(G)} xy(x+y) \;\leq\; 2\,\Delta^3\, m.$$

Equality holds in either pair of bounds for ReZ_2 or ReZ_3 if and only if G is regular.

Proof. For $f_2(x,y) = \frac{xy}{x+y}$ one computes

$$\frac{\partial f_2}{\partial x} = \frac{y^2}{(x+y)^2} > 0, \qquad \frac{\partial f_2}{\partial y} = \frac{x^2}{(x+y)^2} > 0,$$

so f_2 is strictly increasing in each coordinate on $\mathbb{R}^2_{>0}$. Hence

$$f_2(\delta,\delta) \leq f_2(x,y) \leq f_2(\Delta,\Delta),$$

that is,

$$\frac{\delta}{2} \leq \frac{xy}{x+y} \leq \frac{\Delta}{2}.$$

Summing over all m edges yields the claimed bounds for ReZ_2.

For $f_3(x,y) = xy(x+y)$, monotonicity on $\mathbb{R}^2_{>0}$ is immediate, since

$$\frac{\partial f_3}{\partial x} = y(2x+y) > 0, \qquad \frac{\partial f_3}{\partial y} = x(x+2y) > 0,$$

and therefore

$$f_3(\delta,\delta) = 2\delta^3, \qquad f_3(\Delta,\Delta) = 2\Delta^3,$$

with

$$2\delta^3 \leq xy(x+y) \leq 2\Delta^3.$$

Summation over edges gives the bounds for ReZ_3.

ARTICLE IN PRESS

For the equality cases, note that equality in the lower or upper bound for ReZ_2 forces

$$\frac{xy}{x+y} = \frac{\delta}{2} \quad \text{or} \quad \frac{xy}{x+y} = \frac{\Delta}{2}$$

for every edge uv, which by strict monotonicity implies $(x, y) = (\delta, \delta)$ or $(x, y) = (\Delta, \Delta)$ for every edge. Since $\delta \geq 1$, every vertex is incident with an edge, so all vertices must have the same degree, and G is regular. The same argument applies to ReZ_3. Conversely, if G is r-regular, then

$$\mathrm{ReZ}_2(G) = m\frac{r^2}{2r} = \frac{r}{2}m, \qquad \mathrm{ReZ}_3(G) = mr^2(2r) = 2r^3 m,$$

so both bounds are attained with equality. □

Theorem 4.6 shows that the two indices react in different magnitudes to degree variation. The quantity ReZ_2 scales linearly with the degree level, whereas ReZ_3 scales cubically. Consequently, ReZ_3 is far more sensitive to the presence of high-degree vertices and concentrated branching, a feature that will later help explain why higher-order redefined Zagreb descriptors may display stronger variation in spectral and descriptor-based analyses.

4.3 A unified δ–Δ framework for hyper/general variants

The previous theorem is a special case of a general extremal principle for degree-based indices whose kernels are monotone on the degree rectangle $[\delta, \Delta]^2$. This unified point of view is particularly useful because it allows the basic, hyper, general, and generalized–general redefined Zagreb families to be handled within a single kernel-based framework rather than through separate case-by-case arguments.

Definition 4.7. *Let $F : \mathbb{R}^2_{>0} \to \mathbb{R}_{>0}$ be a symmetric kernel. Define the kernel–based indices and coindices as*

$$\mathcal{I}_F(G) := \sum_{uv \in E(G)} F(\delta(u), \delta(v)), \qquad \overline{\mathcal{I}}_F(G) := \sum_{\{u,v\} \notin E(G)} F(\delta(u), \delta(v)).$$

Every redefined Zagreb index (basic, hyper, general, or generalized–general) is of the form $\mathcal{I}_F(G)$ for a suitable choice of F.

Lemma 4.8. *Let $F : \mathbb{R}^2_{>0} \to \mathbb{R}_{>0}$ be continuous and symmetric.*

(i) If F is coordinatewise increasing, then

$$m\,F(\delta,\delta) \;\leq\; \mathcal{I}_F(G) \;\leq\; m\,F(\Delta,\Delta), \qquad \overline{m}\,F(\delta,\delta) \;\leq\; \overline{\mathcal{I}}_F(G) \;\leq\; \overline{m}\,F(\Delta,\Delta),$$

where $\overline{m} = \binom{n}{2} - m$. Equality in any of these inequalities forces G to be regular.

(ii) If F is coordinatewise decreasing, then

$$m\,F(\Delta,\Delta) \;\leq\; \mathcal{I}_F(G) \;\leq\; m\,F(\delta,\delta),$$

and similarly for $\overline{\mathcal{I}}_F(G)$, with equality again characterizing regular graphs.

(iii) If F attains its maximum on the diagonal $x = y$ and its minimum at the contrasted corner (δ, Δ), then

$$m\,F(\delta,\Delta) \;\leq\; \mathcal{I}_F(G) \;\leq\; m\,F(\delta,\delta) = m\,F(\Delta,\Delta),$$

and analogously for $\overline{\mathcal{I}}_F(G)$. The upper bound is attained by regular graphs, while the lower bound is attained by bipartite biregular graphs in which every edge joins a vertex of degree δ to a vertex of degree Δ.

ARTICLE IN PRESS

Proof. Since the degrees of endpoints of any edge lie in $[\delta, \Delta]$, the values $F(\delta, \delta)$, $F(\Delta, \Delta)$, and $F(\delta, \Delta)$ are extremal on the rectangle $[\delta, \Delta]^2$ under the corresponding monotonicity or diagonal-extremum hypothesis. Summing edgewise over $E(G)$ (or over the nonedges) yields the stated inequalities.

For the equality cases in (i) and (ii), equality in the lower or upper bound implies that every contributing edge realizes the corresponding extremal kernel value. By the strict extremal character on the degree rectangle, this forces all endpoint degrees to be equal, hence all vertices have the same degree and G is regular. In case (iii), the upper bound is attained precisely when all edges lie on the diagonal degree type, that is, in the regular case, while the lower bound is realized when every edge has the contrasted degree pair (δ, Δ), namely in bipartite biregular graphs of type (δ, Δ). □

Lemma 4.8 clarifies the role of regular and biregular structures in the extremal theory of kernel-based indices. Regular graphs maximize or minimize kernels whose extremum is attained on the diagonal, because every edge carries the same degree pair, whereas bipartite biregular graphs become extremal when the kernel favors maximal degree contrast. This observation will repeatedly simplify the analysis of hyper and generalized redefined Zagreb families.

By choosing F to be the kernels corresponding to the various redefined Zagreb families, Lemma 4.8 yields a complete set of δ–Δ bounds. The main consequences of this lemma for the specific redefined Zagreb kernels will be summarized explicitly in the next results, so that the general framework can be used as a quick reference rather than only as an abstract principle.

4.4 Compact δ–Δ bounds for all redefined families

For the reader's convenience, we now summarize in a single table the main degree–extreme bounds for the hyper, general, and generalized–general redefined Zagreb families. This compact presentation is intended to serve as a quick reference for the kernel-based estimates developed in the previous subsection.

In Table 2 we collect the extremal δ–Δ bounds for all hyper, general, and generalized–general redefined Zagreb indices. For each row the bounds follow from Lemma 4.8 applied to the corresponding kernel $F(x, y)$, using that $x, y \in [\delta, \Delta]$ for every edge $uv \in E(G)$. Thus, instead of treating each variant separately, the entire family can be analyzed through the same extremal mechanism once its defining kernel is identified.

Table 2 makes the structural dependence of the different families especially transparent. Variants derived from inverse-degree kernels decrease with increasing degree, whereas variants built from products or higher powers of endpoint degrees increase rapidly with degree concentration. In particular, the ReZ_3 family and its extensions are much more sensitive to high-degree vertices than the ReZ_1 family, which reflects their stronger response to branching intensity and degree heterogeneity.

This compact comparison is also useful for the later spectral sections: once the scalar kernel is known to be degree-increasing or degree-decreasing, one immediately anticipates how the corresponding weighted matrices and their energies will behave on regular, biregular, sparse, or highly branched graph families.

Remark 4.9 (Coindex version and equality patterns). For every entry in Table 2, the same bounds hold for the corresponding coindex with m replaced by $\overline{m} = \binom{n}{2} - m$, provided all denominators are well defined (in particular, $\delta \geq 1$ whenever inverse degrees appear). Whenever the kernel F is coordinatewise increasing (respectively decreasing), the lower (respectively upper) bound is attained when every edge joins vertices of minimum (respectively maximum) degree, and the opposite bound is attained when every edge joins vertices of maximum (respectively minimum) degree; in particular, regular graphs attain both extremal bounds in these cases. For the unimodal kernel corresponding to $\mathrm{ReZ}_2^{1,2}$, the upper bound $m/4$ is attained precisely when every edge joins two vertices of equal degree (in particular, by regular graphs), whereas the lower bound is attained by bipartite biregular graphs whose every edge joins a δ–vertex to a Δ–vertex.

The equality patterns emphasize once again that regular graphs play a canonical role in the extremal theory of redefined Zagreb kernels, while biregular graphs become natural extremizers whenever the kernel favors maximal contrast between endpoint degrees. This dichotomy will reappear in the weighted spectral

ARTICLE IN PRESS

Table 2: Bounds for redefined Zagreb indices in terms of $\delta = \delta(G)$, $\Delta = \Delta(G)$ and $m = |E(G)|$. Here $\alpha > 0$. For ReZ_1 one has the exact identity $\mathrm{ReZ}_1(G) = n$ by Lemma 4.1; the bounds shown are coarse degree–extreme estimates.

Variant	**Kernel** $F(x,y)$	**Lower bound**	**Upper bound**
ReZ_1	$\dfrac{x+y}{xy}$	$m\,\dfrac{2}{\Delta}$	$m\,\dfrac{2}{\delta}$
$\mathrm{ReZ}_1^{2,1}$	$\dfrac{(x+y)^2}{xy}$	$4\,m$	$m\,\dfrac{(\delta+\Delta)^2}{\delta\,\Delta}$
$\mathrm{ReZ}_1^{1,2}$	$\dfrac{x+y}{(xy)^2}$	$m\,\dfrac{2}{\Delta^3}$	$m\,\dfrac{2}{\delta^3}$
$\mathrm{ReZ}_1^{\alpha,\alpha}$	$\dfrac{(x+y)^\alpha}{(xy)^\alpha}$	$m\,\dfrac{2^\alpha}{\Delta^\alpha}$	$m\,\dfrac{2^\alpha}{\delta^\alpha}$
$\mathrm{GReZ}_1^{\alpha,\alpha}$	$\dfrac{(x^\alpha+y^\alpha)^\alpha}{(xy)^{\alpha^2}}$	$m\,\dfrac{2^\alpha}{\Delta^{\alpha^2}}$	$m\,\dfrac{2^\alpha}{\delta^{\alpha^2}}$
ReZ_2	$\dfrac{xy}{x+y}$	$m\,\dfrac{\delta}{2}$	$m\,\dfrac{\Delta}{2}$
$\mathrm{ReZ}_2^{2,1}$	$\dfrac{(xy)^2}{x+y}$	$m\,\dfrac{\delta^3}{2}$	$m\,\dfrac{\Delta^3}{2}$
$\mathrm{ReZ}_2^{1,2}$	$\dfrac{xy}{(x+y)^2}$	$m\,\dfrac{\delta\,\Delta}{(\delta+\Delta)^2}$	$m\,\dfrac{1}{4}$
$\mathrm{ReZ}_2^{\alpha,\alpha}$	$\left(\dfrac{xy}{x+y}\right)^\alpha$	$m\left(\dfrac{\delta}{2}\right)^\alpha$	$m\left(\dfrac{\Delta}{2}\right)^\alpha$
$\mathrm{GReZ}_2^{\alpha,\alpha}$	$\left(\dfrac{x^\alpha y^\alpha}{x^\alpha+y^\alpha}\right)^\alpha$	$m\,2^{-\alpha}\,\delta^{\alpha^2}$	$m\,2^{-\alpha}\,\Delta^{\alpha^2}$
ReZ_3	$xy(x+y)$	$2\,\delta^3\,m$	$2\,\Delta^3\,m$
$\mathrm{ReZ}_3^{2,1}$	$(xy)^2(x+y)$	$2\,\delta^5\,m$	$2\,\Delta^5\,m$
$\mathrm{ReZ}_3^{1,2}$	$xy(x+y)^2$	$4\,\delta^4\,m$	$4\,\Delta^4\,m$
$\mathrm{ReZ}_3^{\alpha,\alpha}$	$(xy)^\alpha(x+y)^\alpha$	$2^\alpha\delta^{3\alpha}\,m$	$2^\alpha\Delta^{3\alpha}\,m$
$\mathrm{GReZ}_3^{\alpha,\alpha}$	$(xy)^{\alpha^2}(x^\alpha+y^\alpha)^\alpha$	$2^\alpha\delta^{3\alpha^2}\,m$	$2^\alpha\Delta^{3\alpha^2}\,m$

ARTICLE IN PRESS

setting, where regularity leads to exact scaling rules and biregularity yields particularly transparent block structures.

4.5 Regular graphs: exact closed forms

For r–regular graphs the above bounds collapse to exact equalities. The following table gives a convenient closed–form summary for all redefined Zagreb families. This summary is especially useful because it allows the reader to identify immediately which families scale linearly, polynomially, or more strongly with the common degree parameter r.

Table 3 highlights the strong simplification that occurs in the regular case. Since every edge has the same degree pair (r, r), each redefined Zagreb quantity reduces to a constant multiple of the number of edges. Thus regular graphs provide the natural baseline model in which all local degree fluctuations disappear and the descriptor values are governed entirely by the common degree level.

The table also makes clear that the different families respond to regularity at different scales. The ReZ_1 family remains bounded or even decreases with increasing r, because it is driven by inverse-degree contributions, whereas the ReZ_2 and especially ReZ_3 families grow polynomially in r. In particular, the higher-order ReZ_3 variants amplify degree intensity much more strongly, which anticipates their greater sensitivity in the later spectral and descriptor-based analyses.

ARTICLE IN PRESS

Table 3: Exact values for an r–regular graph on n vertices ($m = \frac{nr}{2}$). Here $\alpha > 0$.

Variant	$F(r,r)$	$\sum_{uv\in E(G)} F(\delta(u),\delta(v)) = m\,F(r,r) = \frac{nr}{2}\,F(r,r)$
ReZ_1	$\frac{2}{r}$	n
$\mathrm{ReZ}_1^{2,1}$	4	$4m = 2nr$
$\mathrm{ReZ}_1^{1,2}$	$\frac{2}{r^3}$	$\frac{n}{r^2}$
$\mathrm{ReZ}_1^{\alpha,\alpha}$	$\frac{2^\alpha}{r^\alpha}$	$\frac{n\,2^{\alpha-1}}{r^{\alpha-1}}$
$\mathrm{GReZ}_1^{\alpha,\alpha}$	$\frac{2^\alpha}{r^{\alpha^2}}$	$\frac{n\,2^{\alpha-1}}{r^{\alpha^2-1}}$
ReZ_2	$\frac{r}{2}$	$\frac{nr^2}{4}$
$\mathrm{ReZ}_2^{2,1}$	$\frac{r^3}{2}$	$\frac{nr^4}{4}$
$\mathrm{ReZ}_2^{1,2}$	$\frac{1}{4}$	$\frac{nr}{8}$
$\mathrm{ReZ}_2^{\alpha,\alpha}$	$\left(\frac{r}{2}\right)^\alpha$	$\frac{n\,r^{\alpha+1}}{2^{\alpha+1}}$
$\mathrm{GReZ}_2^{\alpha,\alpha}$	$2^{-\alpha}r^{\alpha^2}$	$\frac{n^2}{2^{\alpha+1}}\,r^{\alpha^2+1}$
ReZ_3	$2r^3$	nr^4
$\mathrm{ReZ}_3^{2,1}$	$2r^5$	nr^6
$\mathrm{ReZ}_3^{1,2}$	$4r^4$	$2nr^5$
$\mathrm{ReZ}_3^{\alpha,\alpha}$	$2^\alpha r^{3\alpha}$	$n\,2^{\alpha-1}r^{3\alpha+1}$
$\mathrm{GReZ}_3^{\alpha,\alpha}$	$2^\alpha r^{3\alpha^2}$	$n\,2^{\alpha-1}r^{3\alpha^2+1}$

ARTICLE IN PRESS

These explicit expressions will be used in the subsequent sections to derive closed forms and extremal estimates for the weighted energies and entropy-type quantities associated with the redefined Zagreb families on regular and nearly regular graph structures. They also explain why regular graphs serve as canonical equality cases throughout the paper: once all edge types coincide, both the scalar indices and the associated weighted matrices become especially transparent.

5 Energy of redefined Zagreb indices for special graphs

In this section we study the energy corresponding to the redefined Zagreb matrices for several special graph classes. We begin with a general weighted–adjacency framework, and then specialize to the redefined first Zagreb matrix on paths and complete graphs. This section marks the transition from scalar degree-based descriptors to their spectral counterparts, which is one of the central novelties of the present work. In particular, the same kernel that defines a topological index at the scalar level will now be used to generate a symmetric weighted adjacency matrix whose eigenvalues encode additional global structural information.

5.1 Weighted topological index matrices and energy

Let $G = (V(G), E(G))$ be a simple graph with vertex set $V(G) = \{v_1, \ldots, v_n\}$ and degree function $\delta_G(v)$. Let $F : \mathbb{N} \times \mathbb{N} \to \mathbb{R}_{\geq 0}$ be a symmetric kernel in its arguments. The scalar topological index associated with F is

$$TI_F(G) \;=\; \sum_{uv\in E(G)} F\big(\delta_G(u), \delta_G(v)\big). \tag{5.1}$$

ARTICLE IN PRESS

To TI_F we associate the *F–weighted adjacency matrix* $W_F(G) = (w_{ij})_{1\le i,j\le n}$ defined by

$$w_{ij} = \begin{cases} F\big(\delta_G(v_i), \delta_G(v_j)\big), & v_iv_j \in E(G), \\ 0, & \text{otherwise.} \end{cases}$$

Clearly $W_F(G)$ is a real symmetric matrix and hence has real eigenvalues

$$\lambda_1(W_F) \ge \lambda_2(W_F) \ge \cdots \ge \lambda_n(W_F).$$

The *F–energy* of G is defined by

$$E_F(G) \;=\; \sum_{i=1}^{n} \big|\lambda_i(W_F)\big|. \tag{5.2}$$

Many well–known energies arise as particular choices of F: the Randić energy [34,35] corresponds to $F(x,y) = (xy)^{-1/2}$, the harmonic energy to $F(x,y) = \frac{2}{x+y}$ [40], the ABC energy to $F(x,y) = \sqrt{\frac{x+y-2}{xy}}$ [36], and the geometric–arithmetic energy to $F(x,y) = \frac{2\sqrt{xy}}{x+y}$ [37]. Hence the present framework should be viewed not as an isolated construction, but as a natural extension of a broader spectral tradition in which degree-based kernels induce weighted graph matrices and associated energies.

The advantage of this formulation is that it separates two complementary levels of information. The scalar quantity $TI_F(G)$ measures the total edgewise contribution of the kernel, whereas the spectrum of $W_F(G)$ reflects how these local contributions are arranged throughout the graph. Thus two graphs with comparable scalar index values may still exhibit different weighted spectral behaviors, which motivates the study of both aspects side by side.

5.2 Redefined Zagreb matrices as F–weighted adjacencies

Throughout this section we denote $\delta_i = \delta_G(v_i)$. On an edge $v_iv_j \in E(G)$ we abbreviate $x = \delta_i$ and $y = \delta_j$. The three basic redefined Zagreb kernels are

$$F_{ReZ_1}(x,y) = \frac{x+y}{xy}, \qquad F_{ReZ_2}(x,y) = \frac{xy}{x+y}, \qquad F_{ReZ_3}(x,y) = xy\,(x+y).$$

The corresponding matrices are

$$\big(M_{ReZ_1}(G)\big)_{ij} = \begin{cases} \dfrac{\delta_i+\delta_j}{\delta_i\,\delta_j}, & v_iv_j \in E(G), \\ 0, & \text{otherwise,} \end{cases}$$

$$\big(M_{ReZ_2}(G)\big)_{ij} = \begin{cases} \dfrac{\delta_i\,\delta_j}{\delta_i+\delta_j}, & v_iv_j \in E(G), \\ 0, & \text{otherwise,} \end{cases}$$

$$\big(M_{ReZ_3}(G)\big)_{ij} = \begin{cases} \delta_i\,\delta_j(\delta_i+\delta_j), & v_iv_j \in E(G), \\ 0, & \text{otherwise.} \end{cases}$$

By construction, $M_{ReZ_k}(G) = W_{F_{ReZ_k}}(G)$ for $k = 1,2,3$, and the corresponding energies $E_{ReZ_k}(G)$ are defined via (5.2). This identification is fundamental: once a redefined Zagreb index is written in kernel form, its weighted matrix, spectral radius, and energy arise automatically within the same formalism. Hyper, general, and generalized–general variants are obtained by replacing F_{ReZ_k} with the appropriate powers of x, y, and $(x+y)$; their spectra and energies are treated in the same framework and will not be repeated here.

ARTICLE IN PRESS

Hyper, general, and generalized–general redefined first Zagreb matrices. For the first family we set

$$\big(M_{ReZ_1^{2,1}(G)}\big)_{ij} = \begin{cases} \dfrac{(x+y)^2}{xy}, & v_iv_j \in E(G), \\ 0, & \text{otherwise}, \end{cases} \qquad \big(M_{ReZ_1^{1,2}(G)}\big)_{ij} = \begin{cases} \dfrac{x+y}{(xy)^2}, & v_iv_j \in E(G), \\ 0, & \text{otherwise}, \end{cases}$$

$$\big(M_{ReZ_1^{\alpha,\alpha}(G)}\big)_{ij} = \begin{cases} \dfrac{(x+y)^\alpha}{(xy)^\alpha}, & v_iv_j \in E(G), \\ 0, & \text{otherwise}, \end{cases} \qquad \big(M_{GReZ_1^{\alpha,\alpha}(G)}\big)_{ij} = \begin{cases} \dfrac{(x^\alpha+y^\alpha)^\alpha}{(xy)^{\alpha^2}}, & v_iv_j \in E(G), \\ 0, & \text{otherwise}. \end{cases}$$

Hyper, general, and generalized–general redefined second Zagreb matrices.

$$\big(M_{ReZ_2^{2,1}(G)}\big)_{ij} = \begin{cases} \dfrac{(xy)^2}{x+y}, & v_iv_j \in E(G), \\ 0, & \text{otherwise}, \end{cases} \qquad \big(M_{ReZ_2^{1,2}(G)}\big)_{ij} = \begin{cases} \dfrac{xy}{(x+y)^2}, & v_iv_j \in E(G), \\ 0, & \text{otherwise}, \end{cases}$$

$$\big(M_{ReZ_2^{\alpha,\alpha}(G)}\big)_{ij} = \begin{cases} \dfrac{(xy)^\alpha}{(x+y)^\alpha}, & v_iv_j \in E(G), \\ 0, & \text{otherwise}, \end{cases} \qquad \big(M_{GReZ_2^{\alpha,\alpha}(G)}\big)_{ij} = \begin{cases} \dfrac{(x^\alpha y^\alpha)^\alpha}{(x^\alpha+y^\alpha)^\alpha}, & v_iv_j \in E(G), \\ 0, & \text{otherwise}. \end{cases}$$

Hyper, general, and generalized–general redefined third Zagreb matrices.

$$\big(M_{ReZ_3^{2,1}(G)}\big)_{ij} = \begin{cases} (xy)^2(x+y), & v_iv_j \in E(G), \\ 0, & \text{otherwise}, \end{cases} \qquad \big(M_{ReZ_3^{1,2}(G)}\big)_{ij} = \begin{cases} xy(x+y)^2, & v_iv_j \in E(G), \\ 0, & \text{otherwise}, \end{cases}$$

$$\big(M_{ReZ_3^{\alpha,\alpha}(G)}\big)_{ij} = \begin{cases} (xy)^\alpha(x+y)^\alpha, & v_iv_j \in E(G), \\ 0, & \text{otherwise}, \end{cases} \qquad \big(M_{GReZ_3^{\alpha,\alpha}(G)}\big)_{ij} = \begin{cases} (x^\alpha y^\alpha)^\alpha(x^\alpha+y^\alpha)^\alpha, & v_iv_j \in E(G), \\ 0, & \text{otherwise}. \end{cases}$$

These matrix definitions also clarify the structural meaning of the three families. The first family places larger weights on edges incident with smaller degrees, the second balances product and sum effects, and the third strongly amplifies edges joining vertices of large degree. Consequently, one expects markedly different spectral responses across sparse, regular, branched, and hub-dominated graph classes.

In what follows we focus on the energies of the basic matrices $M_{ReZ_1}(G)$, $M_{ReZ_2}(G)$, and $M_{ReZ_3}(G)$ for some standard graph families. The hyper, general, and generalized–general variants are included above to make the framework complete, while the detailed calculations below are presented for the basic families in order to keep the exposition focused and readable.

5.3 A scaling rule for regular and biregular graphs

The following simple observation will be used repeatedly. It explains why regular and biregular graph families are especially tractable in the weighted spectral setting: once every edge carries the same degree pair, the corresponding weighted matrix becomes a constant multiple of the ordinary adjacency matrix.

Lemma 5.1. *Let G be a graph such that every edge has the same ordered degree pair (δ_1, δ_2), i.e.,*

$$\{\, (\delta_G(u), \delta_G(v)) : uv \in E(G) \,\} = \{(\delta_1, \delta_2), (\delta_2, \delta_1)\}.$$

Let F be a symmetric kernel and denote $c = F(\delta_1, \delta_2)$. Then the F–weighted adjacency matrix satisfies

$$W_F(G) = c\, A(G),$$

ARTICLE IN PRESS

where $A(G)$ is the usual adjacency matrix of G. Consequently,

$$\operatorname{spec}\big(W_F(G)\big) = c \cdot \operatorname{spec}\big(A(G)\big),$$

and the F–energy and spectral radius are given by

$$E_F(G) = |c|\; E(A(G)), \qquad \rho\big(W_F(G)\big) = |c|\; \rho\big(A(G)\big),$$

where $E(A(G)) = \sum_{i=1}^{n} |\lambda_i(A(G))|$.

Proof. Since all edges have the same degree pair (δ_1, δ_2), each nonzero off–diagonal entry of $W_F(G)$ equals $c = F(\delta_1, \delta_2)$, and $W_F(G)$ has zero diagonal. Thus $W_F(G)$ is obtained from the adjacency matrix $A(G)$ by multiplying every nonzero off–diagonal entry by c, i.e., $W_F(G) = c\,A(G)$. The relation between spectra then follows immediately, and the expressions for $E_F(G)$ and $\rho\big(W_F(G)\big)$ follow from (5.2) applied to $W_F(G) = cA(G)$. □

Typical examples for which Lemma 5.1 applies include d–regular graphs (with $\delta_1 = \delta_2 = d$), complete graphs K_n ($\delta_1 = \delta_2 = n-1$), complete bipartite graphs $K_{m,n}$ ($\delta_1 = m$, $\delta_2 = n$), cycles C_n ($\delta_1 = \delta_2 = 2$), stars $S_n = K_{1,n-1}$ ($\delta_1 = 1$, $\delta_2 = n-1$), and more generally any (r, s)–biregular bipartite graph.

For the usual adjacency matrix $A(G)$ we recall the classical spectra (see, e.g., [4]):

- K_n: $\operatorname{spec}(A) = \{\, n-1, -1^{(n-1)} \,\}$, hence $\rho(A) = n-1$ and $E(A) = 2(n-1)$.
- $K_{m,n}$: $\operatorname{spec}(A) = \{\sqrt{mn}, -\sqrt{mn}, 0^{(m+n-2)}\}$, hence $E(A) = 2\sqrt{mn}$.
- C_n: $\operatorname{spec}(A) = \{\, 2\cos(2\pi k/n) : k = 0, \ldots, n-1 \,\}$, hence

$$E(A(C_n)) = \sum_{k=0}^{n-1} \left| 2\cos\frac{2\pi k}{n} \right|.$$

Combining these with Lemma 5.1 yields closed forms for $E_F(G)$ once $c = F(\delta_1, \delta_2)$ is specified. In particular, for the redefined first Zagreb kernel

$$F_{ReZ_1}(x, y) = \frac{x+y}{xy}$$

we obtain immediately:

$$\begin{aligned} c(K_n) &= F_{ReZ_1}(n-1, n-1) = \frac{2}{n-1}, \\ c(K_{m,n}) &= F_{ReZ_1}(m, n) = \frac{m+n}{mn}, \\ c(C_n) &= F_{ReZ_1}(2, 2) = 1. \end{aligned}$$

Thus, for these families, the redefined Zagreb energy is obtained by a direct rescaling of the classical adjacency energy. This is one of the main structural reasons why regular and biregular graphs serve as natural benchmark classes throughout the paper.

5.4 Redefined first Zagreb energy of path graphs

We next treat the path P_n, whose endpoint degrees are 1 while all internal vertices have degree 2. In this case not all edges share the same degree pair, so Lemma 5.1 does not apply and we work directly with the corresponding tridiagonal weighted matrix. This makes the path graph the simplest nontrivial example in which endpoint effects perturb the uniform-weight behavior of regular families.

ARTICLE IN PRESS

Theorem 5.2. *Let P_n be the path graph on $n \geq 2$ vertices $V(P_n) = \{v_1, \ldots, v_n\}$, and let $M_{ReZ_1}(P_n)$ be its redefined first Zagreb matrix. Then $M_{ReZ_1}(P_n)$ is the $n \times n$ tridiagonal matrix*

$$M_{ReZ_1}(P_n) = \begin{bmatrix} 0 & \frac{3}{2} & 0 & \cdots & 0 & 0 \\ \frac{3}{2} & 0 & 1 & \cdots & 0 & 0 \\ 0 & 1 & 0 & \ddots & \vdots & \vdots \\ \vdots & \vdots & \ddots & \ddots & 1 & 0 \\ 0 & 0 & \cdots & 1 & 0 & \frac{3}{2} \\ 0 & 0 & \cdots & 0 & \frac{3}{2} & 0 \end{bmatrix}_{n \times n},$$

where the edge weights are

$$w_i = \begin{cases} \frac{3}{2}, & i = 1 \text{ or } i = n-1, \\ 1, & 2 \leq i \leq n-2. \end{cases}$$

Let $p_k(\lambda)$ be the characteristic polynomial of the leading principal $k \times k$ submatrix of $M_{ReZ_1}(P_n)$. Then

$$\begin{cases} p_0(\lambda) = 1, \\ p_1(\lambda) = \lambda, \\ p_k(\lambda) = \lambda\, p_{k-1}(\lambda) - w_{k-1}^2\, p_{k-2}(\lambda), \quad 2 \leq k \leq n. \end{cases} \tag{5.3}$$

The eigenvalues $\lambda_1, \ldots, \lambda_n$ of $M_{ReZ_1}(P_n)$ are the zeros of $p_n(\lambda)$, and the redefined first Zagreb energy of P_n is

$$E_{ReZ_1}(P_n) = \sum_{i=1}^{n} |\lambda_i|, \tag{5.4}$$

where $\lambda_1, \ldots, \lambda_n$ are the roots of p_n. In particular, for small n we have

$$E_{ReZ_1}(P_3) = 3\sqrt{2}, \qquad E_{ReZ_1}(P_4) = 2\sqrt{10}, \qquad E_{ReZ_1}(P_5) = \sqrt{17} + 3.$$

Proof. On P_n the degrees are $\delta_G(v_1) = \delta_G(v_n) = 1$ and $\delta_G(v_i) = 2$ for $2 \leq i \leq n-1$. Hence every edge incident with an endpoint has degree pair $(1, 2)$, while every internal edge has degree pair $(2, 2)$. Using $F_{ReZ_1}(x, y) = \frac{x+y}{xy}$ we obtain

$$F_{ReZ_1}(1, 2) = \frac{1+2}{1 \cdot 2} = \frac{3}{2}, \qquad F_{ReZ_1}(2, 2) = \frac{2+2}{2 \cdot 2} = 1,$$

which gives the claimed tridiagonal matrix and weights w_i.

The recurrence (5.3) follows from the standard determinant expansion for tridiagonal matrices:

$$p_k(\lambda) = \lambda\, p_{k-1}(\lambda) - w_{k-1}^2\, p_{k-2}(\lambda), \qquad k \geq 2,$$

with initial values $p_0(\lambda) = 1$ and $p_1(\lambda) = \lambda$. Thus the eigenvalues of $M_{ReZ_1}(P_n)$ are precisely the zeros of $p_n(\lambda)$, and (5.4) follows directly from the definition (5.2).

□

Remark 5.3. Since P_n is bipartite, the spectrum of $M_{ReZ_1}(P_n)$ is symmetric with respect to the origin, so

$$E_{ReZ_1}(P_n) = 2 \sum_{\lambda_i > 0} \lambda_i.$$

This symmetry reflects the bipartite structure of the path, while the endpoint weights $\frac{3}{2}$ produce a nonuniform perturbation of the constant-weight tridiagonal matrix associated with the ordinary path graph. In this sense, the path example illustrates how local degree irregularity influences the weighted spectrum even in a very simple graph family.

ARTICLE IN PRESS

5.5 Redefined first Zagreb energy of complete graphs

We next consider complete graphs, where Lemma 5.1 yields a particularly simple closed form. This case is important because it provides the clearest illustration of how the kernel-based weighted framework reduces to an exact rescaling of the ordinary adjacency matrix when the graph is regular.

Theorem 5.4. *Let K_n be the complete graph on $n \geq 2$ vertices. Then the redefined first Zagreb matrix $M_{ReZ_1}(K_n)$ has eigenvalues*

$$\lambda_1 = 2, \qquad \lambda_2 = \cdots = \lambda_n = -\frac{2}{n-1},$$

and its redefined first Zagreb energy is

$$E_{ReZ_1}(K_n) = 4. \tag{5.5}$$

Proof. In K_n every vertex has degree $\delta_G(v) = n-1$, so every edge has degree pair $(n-1, n-1)$. For the redefined first Zagreb kernel we have

$$c := F_{ReZ_1}(n-1, n-1) = \frac{(n-1)+(n-1)}{(n-1)^2} = \frac{2}{n-1}.$$

Hence, by Lemma 5.1,

$$M_{ReZ_1}(K_n) = W_{F_{ReZ_1}}(K_n) = c\, A(K_n) = \frac{2}{n-1}\big(J_n - I_n\big),$$

where J_n is the $n \times n$ all–ones matrix and I_n is the identity. The spectrum of $J_n - I_n$ is well known:

$$\operatorname{spec}(J_n - I_n) = \{\, n-1, -1^{(n-1)} \,\}.$$

Multiplying by $c = \frac{2}{n-1}$ gives

$$\lambda_1 = \frac{2}{n-1}(n-1) = 2, \qquad \lambda_2 = \cdots = \lambda_n = \frac{2}{n-1}(-1) = -\frac{2}{n-1},$$

as claimed. Therefore

$$E_{ReZ_1}(K_n) = |\lambda_1| + \sum_{i=2}^{n} |\lambda_i| = 2 + (n-1)\cdot\frac{2}{n-1} = 2 + 2 = 4.$$

□

Remark 5.5. The energy $E_{ReZ_1}(K_n)$ is independent of n, which is quite different from the usual adjacency energy $E(A(K_n)) = 2(n-1)$. This reflects a strong normalization effect: the inverse-degree factor in $F_{ReZ_1}(x,y) = \frac{x+y}{xy}$ compensates exactly for the growth of the common degree $n-1$. As a result, the weighted spectral energy remains constant even though the ordinary adjacency energy increases linearly with the graph size.

Remark 5.6. Using Lemma 5.1 and the explicit constants $c = F_{ReZ_1}(\delta_1, \delta_2)$ one similarly obtains closed expressions for $E_{ReZ_1}(K_{m,n})$, $E_{ReZ_1}(C_n)$, and the redefined energies of other regular or biregular families. For example,

$$E_{ReZ_1}(K_{m,n}) = 2\,\frac{m+n}{mn}\,\sqrt{mn} = \frac{2(m+n)}{\sqrt{mn}}, \qquad E_{ReZ_1}(C_n) = E(A(C_n)) = \sum_{k=0}^{n-1}\left|2\cos\frac{2\pi k}{n}\right|,$$

since every edge of C_n has degree pair $(2,2)$ and $F_{ReZ_1}(2,2) = 1$. These examples show that the first redefined Zagreb energy may either simplify dramatically or coincide with the classical adjacency energy, depending on how the degree kernel interacts with the underlying degree pattern.

ARTICLE IN PRESS

5.6 Redefined second and third Zagreb energies of complete graphs

In this subsection we compute the energies of the redefined second and third Zagreb matrices for complete graphs. We continue to use the kernel notation

$$F_{ReZ_2}(x,y) = \frac{xy}{x+y}, \qquad F_{ReZ_3}(x,y) = xy\,(x+y),$$

so that $M_{ReZ_k}(G) = W_{F_{ReZ_k}}(G)$ for $k = 2, 3$.

Theorem 5.7. *Let K_n be the complete graph on $n \geq 2$ vertices. Then:*

1. *The eigenvalues of the redefined second Zagreb matrix $M_{ReZ_2}(K_n)$ are*

$$\lambda_1 = \frac{(n-1)^2}{2}, \qquad \lambda_2 = \cdots = \lambda_n = -\frac{n-1}{2},$$

and its redefined second Zagreb energy is

$$E_{ReZ_2}(K_n) = (n-1)^2. \tag{5.6}$$

2. *The eigenvalues of the redefined third Zagreb matrix $M_{ReZ_3}(K_n)$ are*

$$\mu_1 = 2(n-1)^4, \qquad \mu_2 = \cdots = \mu_n = -2(n-1)^3,$$

and its redefined third Zagreb energy is

$$E_{ReZ_3}(K_n) = 4(n-1)^4. \tag{5.7}$$

Proof. In the complete graph K_n every vertex has degree $\delta(v) = n-1$, so every edge has degree pair $(n-1, n-1)$.

(i) Redefined second Zagreb matrix. For $F_{ReZ_2}(x,y) = \frac{xy}{x+y}$ we have

$$c_2 := F_{ReZ_2}(n-1, n-1) = \frac{(n-1)^2}{2(n-1)} = \frac{n-1}{2}.$$

By Lemma 5.1,

$$M_{ReZ_2}(K_n) = c_2\, A(K_n),$$

and since

$$\operatorname{spec}(A(K_n)) = \{\, n-1, -1^{(n-1)} \,\},$$

we obtain

$$\lambda_1 = c_2(n-1) = \frac{(n-1)^2}{2}, \qquad \lambda_2 = \cdots = \lambda_n = c_2(-1) = -\frac{n-1}{2}.$$

Therefore

$$E_{ReZ_2}(K_n) = |\lambda_1| + \sum_{i=2}^{n} |\lambda_i| = \frac{(n-1)^2}{2} + (n-1)\cdot\frac{n-1}{2} = (n-1)^2.$$

(ii) Redefined third Zagreb matrix. For $F_{ReZ_3}(x,y) = xy(x+y)$ we obtain

$$c_3 := F_{ReZ_3}(n-1, n-1) = (n-1)^2 \cdot 2(n-1) = 2(n-1)^3.$$

Again

$$M_{ReZ_3}(K_n) = c_3\, A(K_n),$$

ARTICLE IN PRESS

hence

$$\mu_1 = c_3(n-1) = 2(n-1)^4, \qquad \mu_2 = \cdots = \mu_n = c_3(-1) = -2(n-1)^3.$$

Thus

$$E_{ReZ_3}(K_n) = |\mu_1| + \sum_{i=2}^{n} |\mu_i| = 2(n-1)^4 + (n-1)\cdot 2(n-1)^3 = 4(n-1)^4,$$

which completes the proof. □

Remark 5.8. Comparing Theorems 5.4 and 5.7, we see that

$$E_{ReZ_1}(K_n) = 4, \qquad E_{ReZ_2}(K_n) = (n-1)^2, \qquad E_{ReZ_3}(K_n) = 4(n-1)^4,$$

so the normalization in M_{ReZ_1} completely removes the dependence on n, while M_{ReZ_2} and M_{ReZ_3} grow polynomially in the degree $n-1$. This comparison makes the hierarchy of the three families especially clear: the first family suppresses degree growth, the second records it at quadratic scale, and the third amplifies it much more strongly. Consequently, complete graphs provide a transparent model for understanding why higher-order redefined Zagreb energies become much more sensitive to high-degree concentration.

5.7 Redefined Zagreb energies of complete bipartite graphs

We now turn to complete bipartite graphs. Since $K_{m,n}$ is (n,m)–biregular, Lemma 5.1 applies directly and yields closed forms for all three basic redefined Zagreb energies.

Theorem 5.9. *Let $K_{m,n}$ be the complete bipartite graph with parts of sizes $m, n \geq 1$. Then*

$$E_{ReZ_1}(K_{m,n}) = \frac{2(m+n)}{\sqrt{mn}}, \qquad E_{ReZ_2}(K_{m,n}) = \frac{2(mn)^{3/2}}{m+n}, \qquad E_{ReZ_3}(K_{m,n}) = 2(mn)^{3/2}(m+n).$$

Proof. In $K_{m,n}$ each vertex in one part has degree n, while each vertex in the other part has degree m. Hence every edge has degree pair (m,n), and Lemma 5.1 gives

$$W_F(K_{m,n}) = F(m,n)\, A(K_{m,n}).$$

Since

$$\operatorname{spec}(A(K_{m,n})) = \{\, \sqrt{mn}, -\sqrt{mn}, 0^{(m+n-2)} \,\},$$

we have

$$E(A(K_{m,n})) = 2\sqrt{mn}.$$

Therefore,

$$E_F(K_{m,n}) = 2\,|F(m,n)|\,\sqrt{mn}.$$

Applying this identity to the three basic kernels,

$$F_{ReZ_1}(m,n) = \frac{m+n}{mn}, \qquad F_{ReZ_2}(m,n) = \frac{mn}{m+n}, \qquad F_{ReZ_3}(m,n) = mn(m+n),$$

we obtain

$$E_{ReZ_1}(K_{m,n}) = 2\frac{m+n}{mn}\sqrt{mn} = \frac{2(m+n)}{\sqrt{mn}},$$

$$E_{ReZ_2}(K_{m,n}) = 2\frac{mn}{m+n}\sqrt{mn} = \frac{2(mn)^{3/2}}{m+n},$$

and

$$E_{ReZ_3}(K_{m,n}) = 2\,mn(m+n)\sqrt{mn} = 2(mn)^{3/2}(m+n).$$

□

ARTICLE IN PRESS

Corollary 5.10. *Let $S_n = K_{1,n-1}$ be the star on n vertices. Then*

$$E_{ReZ_1}(S_n) = \frac{2n}{\sqrt{n-1}}, \qquad E_{ReZ_2}(S_n) = \frac{2(n-1)^{3/2}}{n}, \qquad E_{ReZ_3}(S_n) = 2n(n-1)^{3/2}.$$

Remark 5.11. The complete bipartite family illustrates how the three energies react differently to degree imbalance. The first redefined energy decreases with increasing balance-normalized degree, the second records an intermediate growth, and the third amplifies the joint degree scale much more strongly. In particular, the star graph S_n provides a simple extremal example in which one high-degree center and many pendant vertices produce markedly different magnitudes across the three families.

5.8 Redefined Zagreb energies of cycles

For cycles all vertices have degree 2, so every edge has degree pair $(2, 2)$ and Lemma 5.1 applies immediately.

Theorem 5.12. *Let C_n be the cycle on $n \geq 3$ vertices. Then*

$$E_{ReZ_1}(C_n) = E_{ReZ_2}(C_n) = E(A(C_n)) = \sum_{k=0}^{n-1} \left| 2\cos\frac{2\pi k}{n} \right|,$$

and

$$E_{ReZ_3}(C_n) = 16\, E(A(C_n)) = 16 \sum_{k=0}^{n-1} \left| 2\cos\frac{2\pi k}{n} \right|.$$

Proof. Since every vertex of C_n has degree 2, each edge has degree pair $(2, 2)$. The adjacency spectrum is

$$\operatorname{spec}(A(C_n)) = \left\{ 2\cos\frac{2\pi k}{n} : k = 0, 1, \ldots, n-1 \right\},$$

and therefore

$$E(A(C_n)) = \sum_{k=0}^{n-1} \left| 2\cos\frac{2\pi k}{n} \right|.$$

For the three basic kernels,

$$F_{ReZ_1}(2, 2) = 1, \qquad F_{ReZ_2}(2, 2) = 1, \qquad F_{ReZ_3}(2, 2) = 16.$$

Hence Lemma 5.1 gives

$$M_{ReZ_k}(C_n) = F_{ReZ_k}(2, 2)\, A(C_n), \qquad E_{ReZ_k}(C_n) = |F_{ReZ_k}(2, 2)|\, E(A(C_n)),$$

from which the stated formulas follow. □

Remark 5.13. The cycle family provides a useful contrast with complete graphs and stars. Because the degree pattern is perfectly uniform and fixed at 2, the first and second redefined Zagreb energies coincide exactly with the ordinary adjacency energy, whereas the third is simply a constant multiple of it. Thus, in uniformly sparse regular graphs, the kernel distinction appears only through scaling, not through any change in spectral shape.

Remark 5.14. As $n \to \infty$ it is known that

$$E(A(C_n)) \sim \frac{4}{\pi}\, n,$$

and therefore

$$E_{ReZ_1}(C_n) \sim \frac{4}{\pi}\, n, \qquad E_{ReZ_2}(C_n) \sim \frac{4}{\pi}\, n, \qquad E_{ReZ_3}(C_n) \sim \frac{64}{\pi}\, n.$$

Hence all three energies grow linearly with the cycle length, but with distinct constants determined by the kernel values at the common degree pair $(2, 2)$.

ARTICLE IN PRESS

6 Energy bounds for redefined Zagreb matrices and relations with other topological indices

In this section we derive general bounds for the energy of the F–weighted adjacency matrices associated with the redefined Zagreb families, and we relate these energies to classical and degree-based topological indices. To avoid repetition, we retain the graph-theoretic notation introduced earlier and focus here only on the energy estimates and their structural consequences.

Let $F : \mathbb{N} \times \mathbb{N} \to \mathbb{R}_{\geq 0}$ be a symmetric kernel, and let

$$\mathrm{Ind}_F(G) = \sum_{uv \in E(G)} F\big(\delta(u), \delta(v)\big)$$

be the associated scalar topological index. The corresponding F–weighted adjacency matrix is

$$W_F(G) = (w_{ij}), \qquad w_{ij} = \begin{cases} F\big(\delta(v_i), \delta(v_j)\big), & v_i v_j \in E(G), \\ 0, & \text{otherwise}, \end{cases}$$

and we denote its eigenvalues by $\lambda_1, \ldots, \lambda_n$. The *$F$–energy* is then defined by

$$E_F(G) = \sum_{i=1}^{n} |\lambda_i|.$$

For the redefined Zagreb families, the kernels F are those introduced earlier; for instance

$$F_{ReZ_1}(x, y) = \frac{x + y}{xy}, \qquad F_{ReZ_2}(x, y) = \frac{xy}{x + y}, \qquad F_{ReZ_3}(x, y) = xy(x + y),$$

with

$$\mathrm{ReZ}_1(G) = \mathrm{Ind}_{F_{ReZ_1}}(G), \qquad \mathrm{ReZ}_2(G) = \mathrm{Ind}_{F_{ReZ_2}}(G), \qquad \mathrm{ReZ}_3(G) = \mathrm{Ind}_{F_{ReZ_3}}(G),$$

and similarly for the hyper, general, and generalized–general variants.

ARTICLE IN PRESS

6.1 Two general energy bounds

We first record two general inequalities that hold for any symmetric nonnegative kernel F and will be used repeatedly.

Proposition 6.1. *Let*

$$S_2(G) = \sum_{uv \in E(G)} F\big(\delta(u), \delta(v)\big)^2.$$

Then

$$E_F(G) \;\leq\; \sqrt{n}\, \|W_F(G)\|_F = \sqrt{2n\, S_2(G)}. \tag{6.1}$$

In particular, if $F(x, y) \leq F^\star$ for all $x, y \in [\delta, \Delta]$, then $S_2(G) \leq m(F^\star)^2$ and

$$E_F(G) \;\leq\; \sqrt{2nm}\, F^\star.$$

Proof. Since $W_F(G)$ is real symmetric, its Frobenius norm satisfies

$$\|W_F(G)\|_F^2 = \sum_{i,j} w_{ij}^2 = \sum_{i=1}^{n} \lambda_i^2.$$

By Cauchy–Schwarz,

$$E_F(G) = \sum_{i=1}^{n} |\lambda_i| \leq \sqrt{n} \Big(\sum_{i=1}^{n} \lambda_i^2 \Big)^{1/2} = \sqrt{n}\, \|W_F(G)\|_F.$$

ARTICLE IN PRESS

Every edge contributes twice to the Frobenius sum, hence

$$\|W_F(G)\|_F^2 = 2 \sum_{uv \in E(G)} F(\delta(u), \delta(v))^2 = 2S_2(G),$$

which proves (6.1). The final estimate follows immediately from the bound $F(x, y) \le F^\star$ on the degree rectangle. □

Proposition 6.1 shows that the energy is controlled by the quadratic accumulation of the edge weights rather than only by their total sum. Consequently, kernels that strongly magnify large degree pairs produce much larger energy bounds than kernels based on inverse-degree normalization.

The next estimate is especially convenient in the bipartite setting.

Proposition 6.2. *Assume that G is bipartite. Then the spectrum of $W_F(G)$ is symmetric with respect to the origin, and*

$$E_F(G) = 2 \sum_{\lambda_i > 0} \lambda_i \;\ge\; 2\,\rho\big(W_F(G)\big), \tag{6.2}$$

where $\rho(\cdot)$ denotes the spectral radius. Moreover,

$$E_F(G) \;\ge\; 2\,\rho(W_F(G)) \;\ge\; \frac{4}{n}\,\mathrm{Ind}_F(G). \tag{6.3}$$

Proof. For a bipartite graph, $W_F(G)$ is permutation-similar to a block matrix of the form

$$\begin{bmatrix} 0 & B \\ B^\top & 0 \end{bmatrix},$$

and therefore its spectrum is symmetric about the origin. This gives

$$E_F(G) = 2 \sum_{\lambda_i > 0} \lambda_i \ge 2\rho(W_F(G)).$$

If s_i denotes the ith row sum of $W_F(G)$, then

$$\sum_{i=1}^{n} s_i = 2 \sum_{uv \in E(G)} F(\delta(u), \delta(v)) = 2\,\mathrm{Ind}_F(G).$$

Using the standard estimate

$$\rho(W_F(G)) \ge \frac{1}{n} \sum_{i=1}^{n} s_i,$$

we obtain

$$\rho(W_F(G)) \ge \frac{2}{n}\,\mathrm{Ind}_F(G),$$

and (6.3) follows. □

In contrast to the Frobenius bound, Proposition 6.2 is a lower estimate. It shows that for bipartite graphs the weighted energy cannot be too small relative to either the spectral radius or the underlying scalar index. This is particularly useful for families such as paths, stars, and complete bipartite graphs, where spectral symmetry is automatic.

ARTICLE IN PRESS

6.2 Consequences of the scaling rule

We shall repeatedly use the scaling rule established in Lemma 5.1. Rather than re-proving it here, we record the direct energy consequences for the regular and biregular situations most relevant to the present section.

Corollary 6.3. *Let G be d–regular. Then*

$$\rho\big(W_F(G)\big) = |F(d,d)|\, d, \qquad E_F(G) = |F(d,d)|\, E\big(A(G)\big).$$

In particular, for K_n one has $d = n-1$, for C_n one has $d = 2$, and for the d–dimensional hypercube Q_d every vertex has degree d.

Corollary 6.4. *Let G be (r,s)–biregular bipartite. Then*

$$\rho\big(W_F(G)\big) = |F(r,s)|\, \rho\big(A(G)\big), \qquad E_F(G) = |F(r,s)|\, E\big(A(G)\big).$$

If $G = K_{r,s}$, then

$$\rho\big(A(K_{r,s})\big) = \sqrt{rs}, \qquad E\big(A(K_{r,s})\big) = 2\sqrt{rs},$$

and therefore

$$\rho\big(W_F(K_{r,s})\big) = |F(r,s)|\, \sqrt{rs}, \qquad E_F(K_{r,s}) = 2\,|F(r,s)|\, \sqrt{rs}.$$

For the redefined Zagreb kernels, the relevant constants are obtained by substituting the corresponding degree pairs. For example, for ReZ_1 one finds

$$F_{ReZ_1}(n{-}1,n{-}1) = \frac{2}{n-1}, \qquad F_{ReZ_1}(2,2) = 1, \qquad F_{ReZ_1}(m,n) = \frac{m+n}{mn}, \qquad F_{ReZ_1}(1,n{-}1) = \frac{n}{n-1},$$

$F_{ReZ_1}(d,d) = \frac{2}{d}$. Hence

$$E_{\mathrm{ReZ}_1}(G) = |c|\, E(A(G))$$

for each of the standard regular or biregular families with the appropriate constant c.

These consequences show that, on regular and biregular families, the weighted spectral problem reduces completely to the classical adjacency spectrum. Thus the influence of the chosen redefined Zagreb kernel appears only through a single scaling factor, while the shape of the spectrum is inherited from the underlying graph.

6.3 Row–sum bounds for the spectral radius

We now derive degree–dependent bounds for the spectral radius $\rho(W_F(G))$, which can then be combined with the general energy estimates obtained earlier.

Let

$$s_i = \sum_j w_{ij} = \sum_{v_j \in N(v_i)} F\big(\delta(v_i), \delta(v_j)\big)$$

denote the row sum of $W_F(G)$ at the vertex v_i. By the Perron–Frobenius row–sum estimate,

$$\min_i s_i \;\le\; \rho(W_F(G)) \;\le\; \max_i s_i. \tag{6.4}$$

ARTICLE IN PRESS

Monotone increasing kernels

Assume that F is nondecreasing in each argument on $[\delta, \Delta]$. Then, for every v_i and every neighbour $v_j \in N(v_i)$,

$$F(\delta,\delta) \;\le\; F\big(\delta(v_i), \delta(v_j)\big) \;\le\; F(\Delta,\Delta),$$

and therefore

$$\delta\, F(\delta,\delta) \;\le\; s_i \;\le\; \Delta\, F(\Delta,\Delta).$$

Hence (6.4) yields

$$\delta\, F(\delta,\delta) \;\le\; \rho(W_F(G)) \;\le\; \Delta\, F(\Delta,\Delta). \tag{6.5}$$

This applies in particular to

$$\mathrm{ReZ}_2,\ \mathrm{ReZ}_2^{2,1},\ \mathrm{ReZ}_2^{\alpha,\alpha},\ \mathrm{GReZ}_2^{\alpha,\alpha},$$

and to the entire ReZ_3–family. For example,

F	$\delta\, F(\delta,\delta)$	$\Delta\, F(\Delta,\Delta)$
$\mathrm{ReZ}_2(x,y) = \dfrac{xy}{x+y}$	$\dfrac{\delta^2}{2}$	$\dfrac{\Delta^2}{2}$
$\mathrm{ReZ}_3(x,y) = xy(x+y)$	$2\delta^4$	$2\Delta^4$
$\mathrm{ReZ}_2^{2,1}(x,y) = \dfrac{(xy)^2}{x+y}$	$\dfrac{\delta^4}{2}$	$\dfrac{\Delta^4}{2}$

so that

$$\frac{\delta^2}{2} \;\le\; \rho\big(W_{\mathrm{ReZ}_2}(G)\big) \;\le\; \frac{\Delta^2}{2}, \qquad 2\delta^4 \;\le\; \rho\big(W_{\mathrm{ReZ}_3}(G)\big) \;\le\; 2\Delta^4.$$

These estimates show that kernels built from degree products produce spectral radii that grow rapidly with the extremal degrees. In particular, the ReZ_3 family is much more sensitive to high-degree concentration than the ReZ_2 family.

The unimodal kernel $\mathrm{ReZ}_2^{1,2}$

For

$$\mathrm{ReZ}_2^{1,2}(x,y) = \frac{xy}{(x+y)^2},$$

coordinatewise monotonicity fails on the whole rectangle $[\delta,\Delta]^2$, but the extremal values are easy to identify:

$$\min_{(x,y)\in[\delta,\Delta]^2} \mathrm{ReZ}_2^{1,2}(x,y) = \mathrm{ReZ}_2^{1,2}(\delta,\Delta) = \frac{\delta\Delta}{(\delta+\Delta)^2}, \qquad \max_{(x,y)\in[\delta,\Delta]^2} \mathrm{ReZ}_2^{1,2}(x,y) = \frac{1}{4},$$

since

$$\frac{\delta\Delta}{(\delta+\Delta)^2} \le \frac{1}{4}$$

by $(\delta-\Delta)^2 \ge 0$. Therefore

$$\delta\,\frac{\delta\Delta}{(\delta+\Delta)^2} \;\le\; s_i \;\le\; \Delta\cdot\frac{1}{4},$$

and hence

$$\frac{\delta^2\Delta}{(\delta+\Delta)^2} \;\le\; \rho\big(W_{\mathrm{ReZ}_2^{1,2}}(G)\big) \;\le\; \frac{\Delta}{4}.$$

ARTICLE IN PRESS

The special structure of ReZ_1

For ReZ_1 one has

$$F_{\mathrm{ReZ}_1}(x,y) = \frac{x+y}{xy} = \frac{1}{x} + \frac{1}{y},$$

so the row sum at v_i becomes

$$s_i = \sum_{v_j \in N(v_i)} \left(\frac{1}{\delta(v_i)} + \frac{1}{\delta(v_j)} \right) = 1 + \sum_{v_j \in N(v_i)} \frac{1}{\delta(v_j)}.$$

Using $\delta \le \delta(v_j) \le \Delta$, we obtain

$$1 + \frac{\delta}{\Delta} \;\le\; s_i \;\le\; 1 + \frac{\Delta}{\delta},$$

and therefore

$$1 + \frac{\delta}{\Delta} \;\le\; \rho\big(W_{\mathrm{ReZ}_1}(G)\big) \;\le\; 1 + \frac{\Delta}{\delta}. \tag{6.6}$$

Unlike the higher families, the first redefined Zagreb kernel separates additively into inverse-degree contributions. This produces a much milder dependence on δ and Δ, consistent with the normalizing role of ReZ_1 observed earlier.

Envelope bounds for decreasing or mixed kernels

If a kernel is decreasing in each argument, or more generally bounded on $[\delta, \Delta]^2$, one may use the envelopes

$$F^\star = \max_{x,y \in [\delta,\Delta]} F(x,y), \qquad F_\star = \min_{x,y \in [\delta,\Delta]} F(x,y),$$

to obtain

$$\delta\, F_\star \;\le\; \rho(W_F(G)) \;\le\; \Delta\, F^\star.$$

For example,

$$\begin{aligned}
\mathrm{ReZ}_1^{2,1}(x,y) = \frac{(x+y)^2}{xy} \quad &\Rightarrow \quad 4\,\delta \;\le\; \rho\big(W_{\mathrm{ReZ}_1^{2,1}}(G)\big) \;\le\; \Delta\big(2 + \tfrac{\Delta}{\delta} + \tfrac{\delta}{\Delta}\big), \\
\mathrm{ReZ}_1^{1,2}(x,y) = \frac{x+y}{(xy)^2} \quad &\Rightarrow \quad \frac{2\delta}{\Delta^3} \;\le\; \rho\big(W_{\mathrm{ReZ}_1^{1,2}}(G)\big) \;\le\; \frac{2\Delta}{\delta^3}, \\
\mathrm{ReZ}_1^{\alpha,\alpha}(x,y) = \frac{(x+y)^\alpha}{(xy)^\alpha} \quad &\Rightarrow \quad \delta\left(\tfrac{2}{\Delta}\right)^\alpha \;\le\; \rho\big(W_{\mathrm{ReZ}_1^{\alpha,\alpha}}(G)\big) \;\le\; \Delta\left(\tfrac{2}{\delta}\right)^\alpha.
\end{aligned}$$

Indeed, for $\mathrm{ReZ}_1^{2,1}$ one uses

$$4 \;\le\; \frac{(x+y)^2}{xy} \;\le\; 2 + \frac{\Delta}{\delta} + \frac{\delta}{\Delta},$$

while for $\mathrm{ReZ}_1^{1,2}$ the kernel is strictly decreasing in each argument, so

$$\frac{2}{\Delta^3} = \mathrm{ReZ}_1^{1,2}(\Delta,\Delta) \;\le\; \mathrm{ReZ}_1^{1,2}(x,y) \;\le\; \mathrm{ReZ}_1^{1,2}(\delta,\delta) = \frac{2}{\delta^3},$$

and for $\mathrm{ReZ}_1^{\alpha,\alpha}$,

$$\mathrm{ReZ}_1^{\alpha,\alpha}(\Delta,\Delta) = \frac{2^\alpha}{\Delta^\alpha} \;\le\; \mathrm{ReZ}_1^{\alpha,\alpha}(x,y) \;\le\; \frac{2^\alpha}{\delta^\alpha} = \mathrm{ReZ}_1^{\alpha,\alpha}(\delta,\delta).$$

Analogous envelope estimates hold for the generalized variants $\mathrm{GReZ}_1^{\alpha,\alpha}$, $\mathrm{GReZ}_2^{\alpha,\alpha}$, and $\mathrm{GReZ}_3^{\alpha,\alpha}$.

Together with the Frobenius upper bound and the bipartite lower estimate established earlier, these row–sum bounds give a practical degree-based toolkit for controlling both the spectral radius and the energy of the weighted matrices associated with the redefined Zagreb families.

ARTICLE IN PRESS

ARTICLE IN PRESS

6.4 Relations with the classical adjacency energy

Rather than repeating previously established degree–extreme and spectral estimates, we now focus only on the part that adds new information, namely the explicit connection between the classical adjacency energy and the scalar redefined Zagreb indices.

Recall that

$$E(A(G)) = \sum_{i=1}^{n} |\mu_i|,$$

where $\mu_1, \dots, \mu_n$ are the eigenvalues of $A(G)$. A convenient starting point is the identity

$$\sum_{v \in V} \sqrt{\delta(v)} = \sum_{uv \in E(G)} \left(\frac{1}{\sqrt{\delta(u)}} + \frac{1}{\sqrt{\delta(v)}} \right),$$

together with the general estimate

$$E(A(G)) \;\le\; \sum_{uv \in E(G)} \left(\frac{1}{\sqrt{\delta(u)}} + \frac{1}{\sqrt{\delta(v)}} \right). \tag{6.7}$$

If, for a given symmetric kernel F, one has

$$\frac{1}{\sqrt{x}} + \frac{1}{\sqrt{y}} \;\le\; C_F(\delta, \Delta)\, \sqrt{F(x,y)} \qquad (x, y \in [\delta, \Delta]),$$

then Cauchy–Schwarz yields

$$E(A(G)) \;\le\; C_F(\delta, \Delta)\, \sqrt{m\, \mathrm{Ind}_F(G)}. \tag{6.8}$$

Thus the problem reduces to finding effective constants $C_F(\delta, \Delta)$ for kernels of interest. For the present paper, the most useful cases are the second and third redefined Zagreb kernels, because they lead to explicit and reasonably sharp bounds with direct structural interpretation.

Corollary 6.5. *Let G be a graph with minimum degree $\delta \ge 1$. Then:*

1. *For*

$$\mathrm{ReZ}_2(G) = \sum_{uv \in E(G)} \frac{\delta(u)\delta(v)}{\delta(u) + \delta(v)},$$

one has

$$E(A(G)) \;\le\; \frac{2\sqrt{2}}{\delta} \sqrt{m\, \mathrm{ReZ}_2(G)}. \tag{6.9}$$

2. *For*

$$\mathrm{ReZ}_3(G) = \sum_{uv \in E(G)} \delta(u)\delta(v)\big(\delta(u) + \delta(v)\big),$$

one has

$$E(A(G)) \;\le\; \frac{\sqrt{2}}{\delta} \sqrt{m\, \mathrm{ReZ}_3(G)}. \tag{6.10}$$

Proof. Both bounds follow from (6.7) and Cauchy–Schwarz after estimating

$$\frac{1}{\sqrt{x}} + \frac{1}{\sqrt{y}}$$

in terms of $\sqrt{F(x,y)}$ on $[\delta, \Delta]^2$. Indeed, for all $x, y \in [\delta, \Delta]$ one has

$$\frac{1}{\sqrt{x}} + \frac{1}{\sqrt{y}} \;\le\; \frac{2\sqrt{2}}{\delta} \sqrt{\frac{xy}{x+y}}, \qquad \frac{1}{\sqrt{x}} + \frac{1}{\sqrt{y}} \;\le\; \frac{\sqrt{2}}{\delta} \sqrt{xy(x+y)}.$$

ARTICLE IN PRESS

Summing over all edges and using

$$\sum_{uv\in E(G)} \sqrt{F(\delta(u),\delta(v))} \;\le\; \sqrt{m}\,\sqrt{\mathrm{Ind}_F(G)},$$

gives (6.9) and (6.10). □

Remark 6.6. Corollary 6.5 gives a direct theoretical rationale for linking adjacency energy with higher-order redefined Zagreb quantities. Since ReZ_2 and especially ReZ_3 amplify contributions from larger endpoint degrees, large values of these indices force large adjacency energy. In this sense, they quantify how degree concentration and branching intensity influence global spectral behavior.

6.5 Bipartite graphs: direct lower bounds

For bipartite graphs, the general estimate (6.3) immediately yields lower bounds for the redefined Zagreb energies in terms of their scalar counterparts.

Corollary 6.7. *Let G be a bipartite graph of order n. Then, for every redefined Zagreb kernel F,*

$$E_F(G) \;\ge\; \frac{4}{n}\,\mathrm{Ind}_F(G).$$

In particular,

$$E_{ReZ_1}(G) \;\ge\; \frac{4}{n}\mathrm{ReZ}_1(G), \qquad E_{ReZ_2}(G) \;\ge\; \frac{4}{n}\mathrm{ReZ}_2(G), \qquad E_{ReZ_3}(G) \;\ge\; \frac{4}{n}\mathrm{ReZ}_3(G).$$

Proof. This is a direct specialization of (6.3). □

Corollary 6.8. *Let G be a connected (r,s)–biregular bipartite graph and let F be any redefined Zagreb kernel. Then*

$$\rho\big(W_F(G)\big) = |F(r,s)|\,\sqrt{rs}, \qquad E_F(G) = |F(r,s)|\,E(A(G)) \;\ge\; 2\,|F(r,s)|\,\sqrt{rs}.$$

Proof. The first identity follows from the scaling rule of Lemma 5.1, together with the fact that

$$\rho(A(G)) = \sqrt{rs}$$

for connected (r,s)–biregular bipartite graphs. The lower bound follows from the bipartite inequality

$$E(A(G)) \ge 2\rho(A(G)).$$

□

Remark 6.9. For complete bipartite graphs, the corresponding explicit formulas have already been derived in Theorem 5.9, so they need not be repeated here. This keeps the presentation concise while preserving the main structural message: in the biregular bipartite case, the weighted energies are exact rescalings of the classical adjacency energy.

Closing observation. The results of this section show that the energy of the redefined Zagreb matrices is controlled from two complementary directions: from above through Frobenius-type and row–sum estimates, and from below in the bipartite setting through the scalar indices themselves. The most informative new link is the one established above between $E(A(G))$ and the scalar indices $\mathrm{ReZ}_2(G)$ and $\mathrm{ReZ}_3(G)$, since it directly connects classical spectral energy with higher-order degree-based structure.

ARTICLE IN PRESS

7 Analytical Descriptor Study of Anticancer Drug-Like Molecules Using Redefined Zagreb Indices and Their Energy-Based Analogues

7.1 Data set and computational methodology

7.1.1 Molecular data set

The present analytical descriptor study was carried out on a curated data set of 22 anticancer drug-like molecules. The compounds were selected from the public chemical databases PubChem [74], SwissADME [75], and ChEMBL [76], using standard identifiers and curated structural annotations. Canonical SMILES strings and primary structural information were obtained mainly from PubChem, while physicochemical and drug-likeness descriptors were retrieved from SwissADME and cross-checked against ChEMBL whenever available. Two-dimensional depictions of the molecules were prepared using ACD/ChemSketch [77].

The selected set comprises clinically used or investigational anticancer agents spanning a broad range of chemotypes and mechanisms of action, including alkylating agents, antimetabolites, platinum-based complexes, topoisomerase inhibitors, taxanes, vinca alkaloids, and targeted tyrosine-kinase inhibitors. This chemical diversity provides a meaningful test bed for examining the sensitivity and discriminative behavior of the proposed redefined Zagreb indices and their energy-based analogues across structurally heterogeneous anticancer molecules. At the same time, the sample size remains modest, so the results in this section should be interpreted as exploratory descriptor-level evidence rather than as a basis for broad predictive generalization.

7.1.2 Computation of redefined Zagreb indices and energies

All graph-theoretical calculations were performed in a Python environment (Google Colab) using custom scripts based on **networkx** and **numpy**. For each molecular graph G, we computed the three basic redefined Zagreb indices

$$\mathrm{ReZ}_1(G), \quad \mathrm{ReZ}_2(G), \quad \mathrm{ReZ}_3(G),$$

together with their hyper, general, and generalized–general variants

$$\mathrm{ReZ}_1^{2,1},\ \mathrm{ReZ}_1^{1,2},\ \mathrm{ReZ}_1^{\alpha,\alpha},\ \mathrm{GReZ}_1^{\alpha,\alpha},$$

$$\mathrm{ReZ}_2^{2,1},\ \mathrm{ReZ}_2^{1,2},\ \mathrm{ReZ}_2^{\alpha,\alpha},\ \mathrm{GReZ}_2^{\alpha,\alpha},$$

$$\mathrm{ReZ}_3^{2,1},\ \mathrm{ReZ}_3^{1,2},\ \mathrm{ReZ}_3^{\alpha,\alpha},\ \mathrm{GReZ}_3^{\alpha,\alpha},$$

as defined in Section 3.

For each kernel F in the redefined Zagreb families, the corresponding F-weighted adjacency matrix $W_F(G)$ was constructed as described in Section 5. The associated spectral energy was then computed as

$$E_F(G) = \sum_{i=1}^{n} |\lambda_i(W_F(G))|\,,$$

where $\lambda_i(W_F(G))$ denotes the eigenvalues of $W_F(G)$. Eigenvalue calculations were performed using the standard **numpy.linalg.eig** routine. In this way, each molecule is represented not only by scalar degree-based descriptors but also by weighted spectral quantities that capture how the same local degree information is distributed across the molecular graph. This procedure yields, in particular, the energy-based descriptors

$$E_{M_{\mathrm{ReZ}_1}},\ E_{M_{\mathrm{ReZ}_2}},\ E_{M_{\mathrm{ReZ}_3}},\ E_{M_{\mathrm{ReZ}_1^{2,1}}},\ E_{M_{\mathrm{ReZ}_1^{1,2}}},\ \ldots,\ E_{M_{\mathrm{ReZ}_3^{2,1}}},\ E_{M_{\mathrm{ReZ}_3^{1,2}}},$$

which are analysed in Sections 5 and 6.

ARTICLE IN PRESS

7.1.3 Physicochemical descriptors and UFF energies

Standard physicochemical descriptors, namely molecular weight (MW), number of heavy atoms (HA), number of aromatic heavy atoms (AHA), number of rotatable bonds (RB), topological polar surface area (TPSA), molar refractivity (MR), number of hydrogen-bond acceptors (HBA), number of hydrogen-bond donors (HBD), and fraction of sp^3 carbons (Frac. Csp^3), were extracted from PubChem and SwissADME, and were recomputed or verified in Python using the RDKit cheminformatics library when necessary.

For each compound, the minimum universal force-field energy UFF_{min} was obtained by first generating a three-dimensional structure from the SMILES representation, then performing UFF geometry optimization, and finally evaluating the optimized force-field energy. These calculations were carried out with RDKit (version 2025.9.2) in the Google Colab environment. In the present manuscript, UFF_{min} is used only as an auxiliary analytical endpoint for descriptor comparison and structural interpretation, not as the basis of a fully developed predictive QSPR model. This framing is intentional, because the size and composition of the anticancer set make it more suitable for comparative descriptor analysis than for claiming broad predictive performance.

7.1.4 Statistical analysis

The statistical analysis was carried out in Python using **pandas**, **numpy**, **scipy**, and **scikit-learn**, with the primary aim of identifying descriptor-level trends and structure–property associations. Pearson correlation coefficients were used to quantify linear associations between variables. For each pair (P, I), where P denotes either a physicochemical property or UFF_{min}, and I denotes a single redefined Zagreb index or its energy-based analogue, three univariate regression models were considered:

- linear: $P = a_1 I + a_0$,
- quadratic: $P = b_2 I^2 + b_1 I + b_0$,
- logarithmic: $P = c_0 + c_1 \ln(I)$.

For each (P, I) pair, the model with the largest coefficient of determination R^2 was retained.

In addition, a multiple linear regression model was fitted for UFF_{min} using all nine basic redefined Zagreb indices, as reported in (7.6). Model performance was assessed using standard goodness-of-fit statistics, including R^2, adjusted R^2, residual standard error S, the F-statistic, and the corresponding p-value. The condition number of the design matrix was also monitored in order to diagnose multicollinearity. Because of the limited sample size and the strong dependence among several descriptors, these regression results are interpreted as exploratory rather than confirmatory. Accordingly, the anticancer section is intended to highlight comparative descriptor behavior and mechanistic structure–index–property tendencies, whereas the more fully validated predictive QSPR analysis is presented later for the alcohol-compound data set.

For the two platinum-containing compounds, UFF_{min} values were not available in the present workflow; accordingly, these entries were retained in the descriptor tables but excluded from analyses involving UFF_{min}.

7.2 Correlation Analysis and Exploratory Structure–Property Modeling

We next examine the association structure linking the physicochemical descriptors in Table 4, the redefined Zagreb indices in Table 5, the corresponding energy-based descriptors in Table 6, and the auxiliary endpoint UFF_{min}. In keeping with the scope of this anticancer section, the analysis is intended to identify descriptor trends, redundancy patterns, and promising univariate structure–property relationships rather than to establish a fully validated predictive QSPR model.

The regression forms considered here are exactly those introduced in Section 7.1; accordingly, we do not repeat them in full. For each descriptor–response pair, the reported fit corresponds to the model form with the largest observed coefficient of determination R^2.

ARTICLE IN PRESS

Table 4: Physicochemical descriptors of the anticancer drug-like molecules.

Formula	MW	HA	AHA	RB	TPSA	MR	HBA	HBD	Frac. Csp^3	UFF_{min}
$C_{15}H_{18}N_4O_5$	334.33	24	0	4	146.89	86.95	6	3	0.53	404.16
$C_{10}H_{13}FN_5O_7P$	365.21	24	9	4	195.88	73.54	11	5	0.50	73.72
$C_{43}H_{59}NO_{17}$	861.93	61	12	14	252.14	214.40	17	8	0.56	244.46
$C_5H_4N_4S$	152.18	10	9	0	89.45	39.07	2	2	0.00	54.67
$C_6H_{14}O_6S_2$	246.30	14	0	7	103.50	51.05	6	0	1.00	10.90
$C_9H_{13}N_3O_5$	243.22	17	6	2	130.83	55.85	6	4	0.56	31.92
$C_7H_{15}Cl_2N_2O_2P$	261.09	14	0	5	51.38	62.60	4	1	1.00	15.59
$C_{22}H_{24}ClFN_4O_3$	446.90	31	16	8	68.74	121.66	7	1	0.36	66.55
$C_{46}H_{60}N_4O_{13}S$	909.05	64	15	10	237.08	246.75	15	5	0.59	262.02
$C_{20}H_{24}N_8O_6$	472.45	34	16	10	219.77	121.45	10	6	0.25	56.18
$C_5H_5N_5S$	167.19	11	9	0	115.47	43.48	2	3	0.00	55.15
$C_{20}H_{16}N_2O_4$	348.35	26	16	1	81.42	95.31	5	1	0.25	79.88
$Cl_2H_6N_2Pt$	300.05	5	0	0	6.48	21.16	5	1	0.25	–
$C_{20}H_{16}N_2O_5$	364.35	27	16	1	101.65	97.34	6	2	0.25	80.68
$C_{14}H_{19}Cl_2NO_2$	304.21	19	6	9	40.54	81.01	2	1	0.50	25.76
$C_{27}H_{29}NO_{11}$	543.52	39	12	5	206.07	132.66	12	6	0.44	98.65
$C_{27}H_{30}ClNO_{10}$	563.98	39	12	4	185.84	138.47	11	5	0.44	95.75
$C_6H_{12}N_2O_4Pt$	371.25	13	0	0	59.08	38.49	6	2	0.67	–
$C_{47}H_{51}NO_{14}$	853.91	62	18	15	221.29	218.96	14	4	0.45	252.23
$C_{29}H_{31}N_7O$	493.60	37	24	8	86.28	154.50	6	2	0.24	87.98
$C_{46}H_{58}N_4O_{14}S$	923.04	65	15	11	254.15	247.33	16	5	0.57	238.48
$C_7H_{17}Cl_2N_2O_3P$	279.10	15	0	5	60.61	65.65	5	2	1.00	18.49

Abbreviations and units: MW – molecular weight ($g\,mol^{-1}$); HA – number of heavy atoms; AHA – number of aromatic heavy atoms; RB – number of rotatable bonds; TPSA – topological polar surface area ($Å^2$); MR – molar refractivity ($cm^3\,mol^{-1}$); HBA – number of hydrogen-bond acceptors; HBD – number of hydrogen-bond donors; Frac. Csp^3 – fraction of sp^3 carbons (dimensionless); UFF_{min} – minimum UFF energy ($kcal\,mol^{-1}$).

ARTICLE IN PRESS

7.3 Correlation structure of physicochemical descriptors, redefined Zagreb indices, and their energies

Table 7 reports the Pearson correlation coefficients between the physicochemical descriptors

$$\{\mathrm{MW}, \mathrm{HA}, \mathrm{AHA}, \mathrm{RB}, \mathrm{TPSA}, \mathrm{MR}, \mathrm{HBA}, \mathrm{HBD}, \text{Frac. } \mathrm{Csp}^3\}$$

and the nine redefined Zagreb indices

$$\{\mathrm{ReZ}_1, \mathrm{ReZ}_2, \mathrm{ReZ}_3, \mathrm{ReZ}_1^{2,1}, \mathrm{ReZ}_1^{1,2}, \mathrm{ReZ}_2^{2,1}, \mathrm{ReZ}_2^{1,2}, \mathrm{ReZ}_3^{2,1}, \mathrm{ReZ}_3^{1,2}\}.$$

The dominant pattern is that molecular weight (MW), number of heavy atoms (HA), and molar refractivity (MR) are very strongly and positively correlated with nearly all redefined Zagreb indices, in most cases with $r > 0.95$. This is consistent with the degree-based construction of the descriptors: larger and more highly connected molecular graphs contribute more edges and larger endpoint degrees, so the corresponding index values increase in a largely monotone way with molecular size and overall connectivity. By contrast, the fraction of sp^3 carbons exhibits almost no linear association with these indices, indicating that the present descriptors are much more sensitive to global connectivity and branching than to hybridization-related composition.

ARTICLE IN PRESS

Table 5: Redefined Zagreb indices of the anticancer drug-like molecules.

Formula	ReZ_1	ReZ_2	ReZ_3	$ReZ_1^{2,1}$	$ReZ_1^{1,2}$	$ReZ_2^{2,1}$	$ReZ_2^{1,2}$	$ReZ_3^{2,1}$	$ReZ_3^{1,2}$
$C_{15}H_{18}N_4O_5$	24.00	33.34	1060.00	118.25	5.41	255.91	6.24	9154.00	6238.00
$C_{10}H_{13}FN_5O_7P$	24.00	30.03	836.00	118.08	5.08	196.57	5.86	5918.00	4526.00
$C_{43}H_{59}NO_{17}$	58.00	74.13	2278.00	286.33	12.52	536.27	14.19	19390.00	13364.00
$C_5H_4N_4S$	10.00	12.55	304.00	46.00	2.15	74.05	2.65	1984.00	1552.00
$C_6H_{14}O_6S_2$	14.00	12.47	296.00	66.50	3.31	60.53	2.65	1568.00	1496.00
$C_9H_{13}N_3O_5$	17.00	20.57	550.00	79.00	4.12	132.23	4.15	3910.00	2944.00
$C_7H_{15}Cl_2N_2O_2P$	14.00	14.91	368.00	60.67	3.83	86.17	3.27	2624.00	1984.00
$C_{22}H_{24}ClFN_4O_3$	31.00	38.57	916.00	142.00	6.80	222.23	8.18	5728.00	4600.00
$C_{46}H_{60}N_4O_{13}S$	64.00	85.47	2674.00	314.75	14.44	632.47	16.29	22792.00	15754.00
$C_{20}H_{24}N_8O_6$	33.00	39.10	970.00	153.67	7.43	231.10	8.07	6214.00	4960.00
$C_5H_5N_5S$	11.00	13.70	344.00	51.67	2.37	82.70	2.81	2252.00	1772.00
$C_{20}H_{16}N_2O_4$	26.00	36.63	1068.00	128.08	5.33	257.74	7.10	8382.00	6002.00
$Cl_2H_6N_2Pt$	3.00	1.33	12.00	9.00	1.50	2.67	0.44	24.00	36.00
$C_{20}H_{16}N_2O_5$	27.00	37.78	1108.00	133.75	5.55	266.39	7.27	8650.00	6222.00
$C_{14}H_{19}Cl_2NO_2$	19.00	19.93	426.00	81.00	5.07	102.27	4.49	2406.00	2040.00
$C_{27}H_{29}NO_{11}$	39.00	51.41	1510.00	189.00	8.88	362.67	9.92	11746.00	8472.00
$C_{27}H_{30}ClNO_{10}$	38.00	50.30	1486.00	185.67	8.44	356.39	9.65	11590.00	8352.00
$C_6H_{12}N_2O_4Pt$	11.00	14.00	412.00	52.17	2.45	97.38	2.79	3472.00	2404.00
$C_{47}H_{51}NO_{14}$	62.00	80.25	2390.00	300.92	13.42	569.35	15.64	20084.00	13854.00
$C_{29}H_{31}N_7O$	37.00	46.55	1094.00	172.00	7.64	264.05	9.82	6590.00	5420.00
$C_{46}H_{58}N_4O_{14}S$	65.00	86.59	2698.00	318.08	14.88	638.75	16.56	22948.00	15874.00
$C_7H_{17}Cl_2N_2O_3P$	14.00	14.91	368.00	60.67	3.83	86.17	3.27	2624.00	1984.00

A closely related pattern is observed for the energy-based redefined Zagreb descriptors (Table 8). Again, MW, HA, and MR display strong positive correlations with nearly all spectral quantities, showing that the energy-based descriptors largely preserve the same size- and connectivity-related information encoded by the underlying combinatorial indices.

The correlation matrix between each redefined Zagreb index and its corresponding energy-based analogue is summarized in Table 9. All pairs exhibit extremely strong linear relationships, with correlation coefficients typically very close to unity. For the present anticancer dataset, this indicates that the energy transformation acts mainly as a structured rescaling of the underlying combinatorial information rather than as a source of substantially independent descriptor content. This observation is important for interpreting later regression results, because it implies that any multivariate model including both raw indices and their energy analogues is naturally prone to strong multicollinearity.

Taken together, Tables 7–9 suggest three main points: first, the redefined Zagreb descriptors primarily encode molecular size and connectivity; second, they are less informative for hybridization-related composition variables such as Frac. Csp^3; and third, the corresponding spectral energies largely preserve the same ordering information as the underlying indices. This makes the energy-based quantities mathematically interesting and spectrally interpretable, but in this small-data anticancer setting they should be viewed as closely related companion descriptors rather than fully independent predictor families.

7.4 Relationship between UFF_{min}, physicochemical descriptors, and redefined Zagreb indices

To examine the analytical usefulness of the proposed descriptors, we next study how the available physicochemical variables and redefined Zagreb indices relate to the auxiliary endpoint UFF_{min}. Because

ARTICLE IN PRESS

Table 6: Energy-based redefined Zagreb indices of the anticancer drug-like molecules.

Formula	$E_{M_{\mathrm{ReZ}_1}}$	$E_{M_{\mathrm{ReZ}_2}}$	$E_{M_{\mathrm{ReZ}_3}}$	$E_{M_{\mathrm{ReZ}_1^{2,1}}}$	$E_{M_{\mathrm{ReZ}_1^{1,2}}}$	$E_{M_{\mathrm{ReZ}_2^{2,1}}}$	$E_{M_{\mathrm{ReZ}_2^{1,2}}}$	$E_{M_{\mathrm{ReZ}_3^{2,1}}}$	$E_{M_{\mathrm{ReZ}_3^{1,2}}}$
$C_{15}H_{18}N_4O_5$	30.13	36.30	1134.35	138.77	8.12	275.64	7.02	9960.77	6699.93
$C_{10}H_{13}FN_5O_7P$	28.52	33.05	922.33	134.64	6.87	219.51	6.55	6823.50	5058.51
$C_{43}H_{59}NO_{17}$	70.60	80.93	2454.22	331.20	17.40	586.49	15.91	21859.58	14553.58
$C_5H_4N_4S$	12.33	14.67	350.08	55.19	2.87	85.72	3.14	2313.98	1788.88
$C_6H_{14}O_6S_2$	16.02	14.05	331.06	74.07	3.94	70.67	3.06	1964.24	1705.34
$C_9H_{13}N_3O_5$	21.79	23.30	619.93	95.36	6.29	150.36	4.82	4560.04	3353.68
$C_7H_{15}Cl_2N_2O_2P$	18.54	17.79	418.02	75.96	5.75	99.47	4.07	3089.80	2250.38
$C_{22}H_{24}ClFN_4O_3$	38.77	45.44	1060.63	172.07	9.34	258.41	9.82	6727.93	5332.60
$C_{46}H_{60}N_4O_{13}S$	78.60	93.75	2826.20	363.75	20.77	672.38	18.57	24182.72	16576.23
$C_{20}H_{24}N_8O_6$	40.60	44.93	1113.84	183.04	10.09	267.63	9.41	7451.94	5768.64
$C_5H_5N_5S$	13.26	15.61	391.92	60.47	3.19	94.97	3.24	2635.50	2034.20
$C_{20}H_{16}N_2O_4$	32.27	41.11	1176.77	151.12	7.66	285.98	8.18	9475.51	6645.70
$Cl_2H_6N_2Pt$	4.24	1.89	16.97	12.73	2.12	3.77	0.63	33.94	50.91
$C_{20}H_{16}N_2O_5$	33.26	42.04	1218.73	156.44	8.03	295.26	8.28	9800.03	6893.09
$C_{14}H_{19}Cl_2NO_2$	24.01	23.80	499.90	99.17	7.06	120.61	5.46	2862.48	2395.40
$C_{27}H_{29}NO_{11}$	49.43	57.03	1664.71	224.55	13.57	403.62	11.30	13414.28	9437.32
$C_{27}H_{30}ClNO_{10}$	47.28	55.49	1636.61	218.19	12.42	396.55	10.88	13269.83	9308.03
$C_6H_{12}N_2O_4Pt$	12.79	14.95	435.45	57.55	3.32	104.56	3.05	3811.55	2561.30
$C_{47}H_{51}NO_{14}$	76.53	89.06	2600.45	354.09	18.67	627.30	17.86	22681.13	15185.67
$C_{29}H_{31}N_7O$	45.75	54.83	1271.20	207.36	10.19	308.04	11.75	7778.05	6310.42
$C_{46}H_{58}N_4O_{14}S$	80.09	95.19	2851.59	368.36	21.53	678.74	18.95	24304.13	16688.73
$C_7H_{17}Cl_2N_2O_3P$	18.07	17.64	417.33	74.50	5.58	99.34	4.01	3088.80	2249.10

$\mathrm{UFF}_{\min}$ is available only for the subset of molecules for which the optimization workflow returned a value, all analyses in this subsection are based on that reduced subset.

Selected Pearson correlations are reported in Table 10. Among the standard physicochemical variables, the strongest univariate associations with $\mathrm{UFF}_{\min}$ are obtained for HA, MR, and MW, with R^2 values around 0.42–0.45. Several redefined Zagreb descriptors show stronger linear associations, particularly $\mathrm{ReZ}_3^{2,1}$, $\mathrm{ReZ}_3^{1,2}$, and $\mathrm{ReZ}_2^{2,1}$, whose R^2 values lie near 0.53–0.57. This pattern is consistent with the structure of these higher-order descriptors: because they place greater weight on products and mixed powers of endpoint degrees, they respond more strongly to branching intensity, local degree heterogeneity, and the concentration of connectivity around highly connected vertices. These features are plausibly more relevant to the optimized UFF energy landscape than size-oriented descriptors alone.

Representative univariate models for the standard physicochemical variables are

$$\mathrm{UFF}_{\min} = 0.0341\,\mathrm{HA}^2 + 1.2698\,\mathrm{HA} + 27.4225, \qquad (R^2 = 0.447,\ S \approx 84.47), \tag{7.1}$$

$$\mathrm{UFF}_{\min} = 0.2800\,\mathrm{MW} - 15.2194, \qquad (R^2 = 0.417,\ S \approx 84.26), \tag{7.2}$$

$$\mathrm{UFF}_{\min} = 1.0328\,\mathrm{MR} - 8.5949, \qquad (R^2 = 0.418,\ S \approx 84.22). \tag{7.3}$$

Among the graph-based descriptors, the strongest univariate fit is obtained for $\mathrm{ReZ}_3^{2,1}$:

$$\mathrm{UFF}_{\min} = 0.0114\,\mathrm{ReZ}_3^{2,1} + 12.2489, \qquad (R^2 = 0.569,\ S \approx 72.50), \tag{7.4}$$

$$\mathrm{UFF}_{\min} = -1.0 \times 10^{-4}\,(\mathrm{ReZ}_3^{2,1})^2 + 0.0187\,\mathrm{ReZ}_3^{2,1} - 13.9663, \qquad (R^2 = 0.582,\ S \approx 73.46). \tag{7.5}$$

Comparable, though slightly weaker, trends are observed for $\mathrm{ReZ}_3^{1,2}$, $\mathrm{ReZ}_2^{2,1}$, ReZ_3, and ReZ_2. From a structural point of view, this reinforces the interpretation that descriptors emphasizing mixed degree interactions are better aligned with the nonuniform connectivity patterns that influence force-field stabilization.

ARTICLE IN PRESS

Table 7: Pearson correlation coefficients between physicochemical descriptors and redefined Zagreb indices.

	ReZ_1	ReZ_2	ReZ_3	$\mathrm{ReZ}_1^{2,1}$	$\mathrm{ReZ}_1^{1,2}$	$\mathrm{ReZ}_2^{2,1}$	$\mathrm{ReZ}_2^{1,2}$	$\mathrm{ReZ}_3^{2,1}$	$\mathrm{ReZ}_3^{1,2}$
MW	0.965	0.958	0.958	0.965	0.971	0.956	0.957	0.952	0.956
HA	0.999	0.995	0.984	0.998	0.994	0.984	0.995	0.966	0.976
AHA	0.669	0.677	0.610	0.661	0.620	0.618	0.699	0.542	0.573
RB	0.788	0.736	0.696	0.770	0.804	0.691	0.759	0.667	0.681
TPSA	0.823	0.822	0.833	0.834	0.814	0.831	0.807	0.825	0.831
MR	0.992	0.986	0.971	0.989	0.992	0.971	0.991	0.950	0.961
HBA	0.891	0.883	0.894	0.898	0.893	0.890	0.872	0.890	0.894
HBD	0.661	0.660	0.671	0.670	0.657	0.670	0.646	0.664	0.668
Frac. Csp^3	0.011	−0.024	0.003	0.007	0.060	−0.008	−0.028	0.031	0.021

Table 8: Pearson correlation coefficients between physicochemical descriptors and energy-based redefined Zagreb indices.

	$E_{M_{\mathrm{ReZ}_1}}$	$E_{M_{\mathrm{ReZ}_2}}$	$E_{M_{\mathrm{ReZ}_3}}$	$E_{M_{\mathrm{ReZ}_1^{2,1}}}$	$E_{M_{\mathrm{ReZ}_1^{1,2}}}$	$E_{M_{\mathrm{ReZ}_2^{2,1}}}$	$E_{M_{\mathrm{ReZ}_2^{1,2}}}$	$E_{M_{\mathrm{ReZ}_3^{2,1}}}$	$E_{M_{\mathrm{ReZ}_3^{1,2}}}$
MW	0.963	0.955	0.958	0.962	0.965	0.956	0.953	0.954	0.957
HA	0.998	0.995	0.988	0.998	0.988	0.988	0.993	0.972	0.981
AHA	0.669	0.696	0.633	0.672	0.600	0.639	0.711	0.559	0.594
RB	0.787	0.746	0.705	0.775	0.775	0.702	0.767	0.679	0.691
TPSA	0.817	0.811	0.833	0.827	0.814	0.831	0.793	0.832	0.835
MR	0.993	0.989	0.975	0.990	0.985	0.974	0.993	0.954	0.965
HBA	0.886	0.873	0.892	0.891	0.891	0.889	0.860	0.896	0.896
HBD	0.659	0.649	0.673	0.666	0.665	0.673	0.630	0.677	0.676
Frac. Csp^3	0.011	−0.032	−0.010	0.002	0.067	−0.019	−0.030	0.023	0.009

ARTICLE IN PRESS

A multiple linear regression model including all nine basic redefined Zagreb indices yields

$$\begin{aligned}\mathrm{UFF}_{\min} = {} & 44.0441 - 4589.2838\,\mathrm{ReZ}_1 + 2.121\times10^4\,\mathrm{ReZ}_2 - 1705.3393\,\mathrm{ReZ}_3 + 937.7913\,\mathrm{ReZ}_1^{2,1} \\ & + 5134.4318\,\mathrm{ReZ}_1^{1,2} + 1747.9341\,\mathrm{ReZ}_2^{2,1} - 4.82\times10^4\,\mathrm{ReZ}_2^{1,2} - 40.3631\,\mathrm{ReZ}_3^{2,1} + 207.6543\,\mathrm{ReZ}_3^{1,2},\end{aligned} \tag{7.6}$$

with $R^2 = 0.864$, adjusted $R^2 = 0.741$, $F = 7.05$, and $\mathrm{Prob}(F) = 0.0026$. Although the fit appears numerically strong, the very large condition number ($\approx 1.8\times10^7$) reveals severe multicollinearity, so the model should not be interpreted as a stable predictive equation. Rather, it mainly confirms the strong redundancy structure already visible in the correlation analysis. Accordingly, the anticancer data support using a small number of informative descriptors for interpretation, while more fully validated predictive modeling is deferred to the larger alcohol-compound study.

Discussion and practical implications. The main message of this analysis is comparative rather than predictive. Several higher-order redefined Zagreb descriptors, especially $\mathrm{ReZ}_3^{2,1}$, $\mathrm{ReZ}_3^{1,2}$, and $\mathrm{ReZ}_2^{2,1}$, show stronger univariate association with $\mathrm{UFF}_{\min}$ than standard size-related variables such as MW, HA, and MR. At the same time, the small sample size and the strong dependence among descriptors require caution: these results identify promising structure–descriptor relationships, but they do not by themselves establish a robust predictive QSPR model.

ARTICLE IN PRESS

Table 9: Pearson correlation coefficients between redefined Zagreb indices and their associated energy-based descriptors.

	$E_{M_{\mathrm{ReZ}_1}}$	$E_{M_{\mathrm{ReZ}_2}}$	$E_{M_{\mathrm{ReZ}_3}}$	$E_{M_{\mathrm{ReZ}_1^{2,1}}}$	$E_{M_{\mathrm{ReZ}_1^{1,2}}}$	$E_{M_{\mathrm{ReZ}_2^{2,1}}}$	$E_{M_{\mathrm{ReZ}_2^{1,2}}}$	$E_{M_{\mathrm{ReZ}_3^{2,1}}}$	$E_{M_{\mathrm{ReZ}_3^{1,2}}}$
ReZ_1	1.000	0.997	0.989	1.000	0.990	0.988	0.996	0.971	0.981
ReZ_2	0.996	0.999	0.996	0.998	0.986	0.997	0.996	0.981	0.990
ReZ_3	0.984	0.988	0.999	0.988	0.982	0.999	0.980	0.996	0.999
$\mathrm{ReZ}_1^{2,1}$	0.998	0.997	0.993	1.000	0.988	0.993	0.994	0.978	0.987
$\mathrm{ReZ}_1^{1,2}$	0.996	0.988	0.982	0.993	0.997	0.981	0.989	0.967	0.976
$\mathrm{ReZ}_2^{2,1}$	0.984	0.989	0.999	0.988	0.981	0.999	0.981	0.995	0.999
$\mathrm{ReZ}_2^{1,2}$	0.998	1.000	0.990	0.998	0.985	0.991	0.999	0.970	0.981
$\mathrm{ReZ}_3^{2,1}$	0.965	0.969	0.991	0.969	0.969	0.990	0.957	0.999	0.997
$\mathrm{ReZ}_3^{1,2}$	0.975	0.979	0.996	0.979	0.976	0.995	0.968	0.999	0.999

Table 10: Selected Pearson correlation coefficients between $\mathrm{UFF}_{\mathrm{min}}$ and physicochemical or ReZ-type descriptors.

Predictor X	$r(\mathrm{UFF}_{\mathrm{min}}, X)$	R^2
$\mathrm{ReZ}_3^{2,1}$	0.754	0.569
$\mathrm{ReZ}_3^{1,2}$	0.741	0.549
$\mathrm{ReZ}_2^{2,1}$	0.729	0.531
ReZ_3	0.728	0.530
ReZ_2	0.691	0.477
$\mathrm{ReZ}_1^{2,1}$	0.678	0.460
$\mathrm{ReZ}_2^{1,2}$	0.670	0.449
ReZ_1	0.664	0.441
HA	0.663	0.440
MR	0.647	0.419
MW	0.646	0.417
TPSA	0.610	0.372
HBA	0.583	0.340

ARTICLE IN PRESS

7.5 Relationship between $\mathrm{UFF}_{\mathrm{min}}$ and energy-based redefined Zagreb indices

The association between $\mathrm{UFF}_{\mathrm{min}}$ and the energy-based redefined Zagreb descriptors is summarized in Table 11. The strongest correlations again occur for the higher-order mixed descriptors, namely $E_{M_{\mathrm{ReZ}_3^{2,1}}}$, $E_{M_{\mathrm{ReZ}_3^{1,2}}}$, and $E_{M_{\mathrm{ReZ}_2^{2,1}}}$.

Among the energy-based descriptors, the best univariate fit is again obtained for $E_{M_{\mathrm{ReZ}_3^{2,1}}}$:

$$\mathrm{UFF}_{\mathrm{min}} = 0.0105\, E_{M_{\mathrm{ReZ}_3^{2,1}}} + 8.7194, \qquad (R^2 = 0.559,\ S \approx 73.28), \tag{7.7}$$

and

$$\mathrm{UFF}_{\mathrm{min}} = -1.0 \times 10^{-4}\, E^2_{M_{\mathrm{ReZ}_3^{2,1}}} + 0.0153\, E_{M_{\mathrm{ReZ}_3^{2,1}}} - 10.8553, \qquad (R^2 = 0.566,\ S \approx 74.87). \tag{7.8}$$

These values are very close to those obtained for the corresponding combinatorial descriptor $\mathrm{ReZ}_3^{2,1}$. Thus, in the present anticancer dataset, the energy transformation preserves the same explanatory signal but

ARTICLE IN PRESS

Table 11: Pearson correlation coefficients between $\mathrm{UFF}_{\mathrm{min}}$ and energy-based redefined Zagreb descriptors.

Energy descriptor E	$r(\mathrm{UFF}_{\mathrm{min}}, E)$
$E_{M_{\mathrm{ReZ}_3^{2,1}}}$	0.748
$E_{M_{\mathrm{ReZ}_3^{1,2}}}$	0.735
$E_{M_{\mathrm{ReZ}_2^{2,1}}}$	0.720
$E_{M_{\mathrm{ReZ}_3}}$	0.719
$E_{M_{\mathrm{ReZ}_2}}$	0.679
$E_{M_{\mathrm{ReZ}_1^{2,1}}}$	0.673
$E_{M_{\mathrm{ReZ}_1}}$	0.664
$E_{M_{\mathrm{ReZ}_1^{1,2}}}$	0.663
$E_{M_{\mathrm{ReZ}_2^{1,2}}}$	0.658

does not provide a substantial gain in univariate performance. From a practical viewpoint, this favors the combinatorial forms when interpretability and parsimony are preferred.

Figures 1, 2, and 3 visually support these numerical observations. Figures 2 and 3 show that both combinatorial and energy-based ReZ descriptors exhibit clearer trends with $\mathrm{UFF}_{\mathrm{min}}$ than the standard physicochemical variables shown in Figure 1.

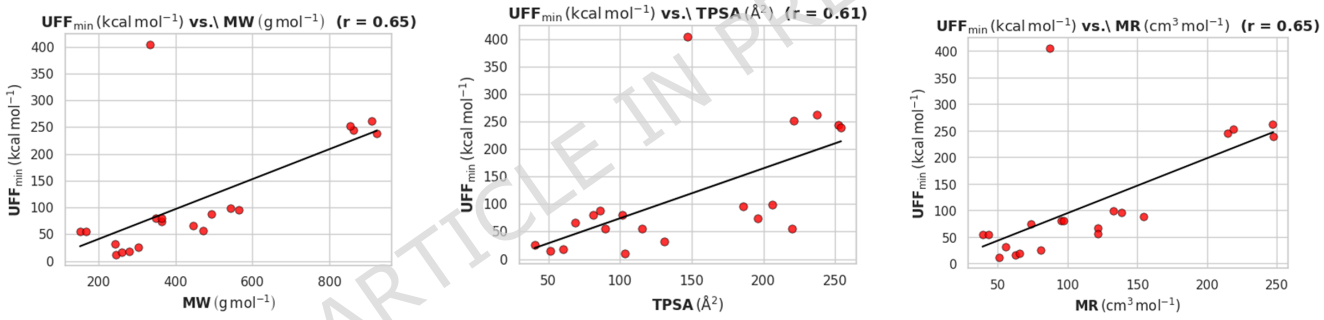

(a) (b) (c)

Figure 1: Representative scatter plots of $\mathrm{UFF}_{\mathrm{min}}$ against selected physicochemical descriptors. The broader scatter is consistent with the more modest univariate associations reported in Table 10.

Overall, the anticancer dataset supports a consistent analytical picture: higher-order redefined Zagreb descriptors, especially $\mathrm{ReZ}_3^{2,1}$ and closely related variants, capture structure–energy tendencies more effectively than the standard physicochemical variables considered here, whereas their energy-based counterparts largely reproduce the same information. This makes the combinatorial descriptors the more economical choice for interpretation in the present small-sample setting.

ARTICLE IN PRESS

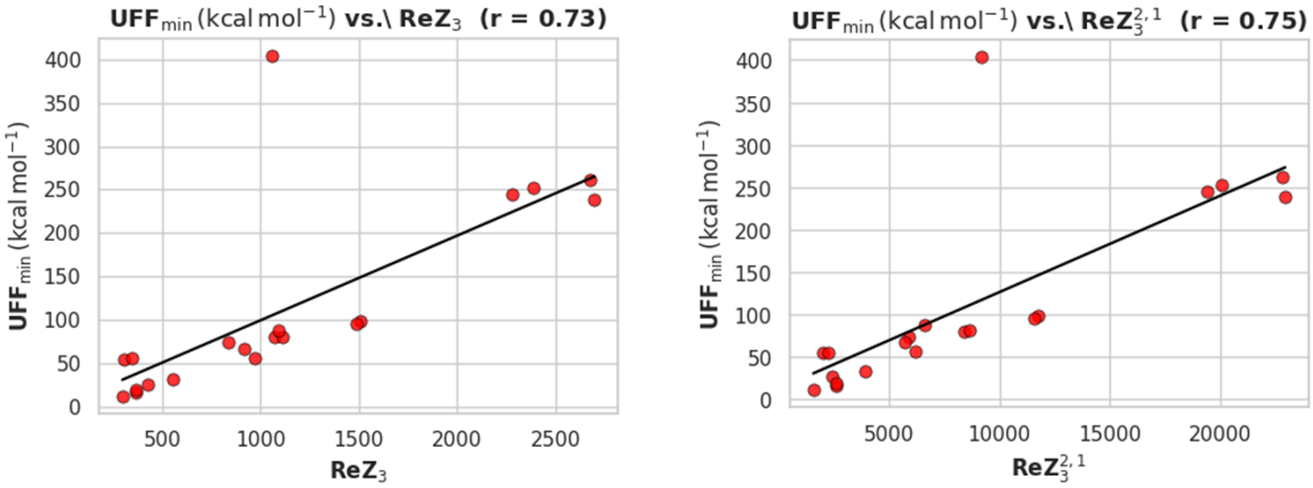

(a) (b)

Figure 2: Representative relationships between $\mathrm{UFF_{min}}$ and selected redefined Zagreb descriptors, including $\mathrm{ReZ_3^{2,1}}$ and $\mathrm{ReZ_3}$. The clearer trends are consistent with the stronger univariate associations observed for the higher-order descriptors.

Table 12: Selected best univariate linear descriptor models for the minimum UFF energy $\mathrm{UFF_{min}}$ of the studied anticancer drug-like molecules. Each model has the form $\mathrm{UFF_{min}} = a\,x + b$. Here R^2 is the coefficient of determination, $S = \sqrt{\mathrm{MSE_{resid}}}$ is the standard error of estimate, F is the F-statistic, and p_F is the corresponding significance level.

Type	Model ID	x	Equation	R^2	S	F	p_F
Physicochemical	P1	HA	$\mathrm{UFF_{min}} \approx 3.87\,\mathrm{HA} - 9.88$	0.439	82.69	14.09	1.5×10^{-3}
ReZ index	R1	$\mathrm{ReZ_3^{2,1}}$	$\mathrm{UFF_{min}} \approx 0.0114\,\mathrm{ReZ_3^{2,1}} + 12.25$	0.569	72.50	23.73	1.0×10^{-4}
ReZ index	R2	$\mathrm{ReZ_3^{1,2}}$	$\mathrm{UFF_{min}} \approx 0.0166\,\mathrm{ReZ_3^{1,2}} + 7.04$	0.549	74.12	21.93	2.0×10^{-4}
ReZ index	R3	$\mathrm{ReZ_2^{2,1}}$	$\mathrm{UFF_{min}} \approx 0.4125\,\mathrm{ReZ_2^{2,1}} + 1.00$	0.532	75.55	20.44	3.0×10^{-4}
Energy ReZ	E1	$E_{M_{\mathrm{ReZ_3^{2,1}}}}$	$\mathrm{UFF_{min}} \approx 0.0105\,E_{M_{\mathrm{ReZ_3^{2,1}}}} + 8.72$	0.559	73.28	22.85	1.0×10^{-4}
Energy ReZ	E2	$E_{M_{\mathrm{ReZ_3^{1,2}}}}$	$\mathrm{UFF_{min}} \approx 0.0156\,E_{M_{\mathrm{ReZ_3^{1,2}}}} + 3.57$	0.540	74.90	21.11	2.0×10^{-4}
Energy ReZ	E3	$E_{M_{\mathrm{ReZ_2^{2,1}}}}$	$\mathrm{UFF_{min}} \approx 0.3827\,E_{M_{\mathrm{ReZ_2^{2,1}}}} - 2.09$	0.519	76.58	19.41	3.0×10^{-4}

8 QSPR Performance of Redefined Zagreb-Based Descriptors and Their Derivatives for Alcohol Compounds

8.1 Dataset, physicochemical endpoints, and descriptor sets

The QSPR investigation was conducted on a curated dataset of $n = 100$ alcohol compounds. For each compound, standard molecular identifiers were retained, including the compound name, molecular formula, canonical SMILES, InChI, and InChIKey. The dataset covers structurally diverse aliphatic alcohols and substituted alcohol derivatives, thus providing a chemically coherent yet sufficiently heterogeneous benchmark for assessing the predictive utility of redefined Zagreb-based molecular descriptors.

Physicochemical property values were compiled from the Cheméo database and retained in the original units reported by the source. For reproducibility, the physicochemical property values for the $n = 100$ compounds were compiled from Cheméo on 24 Feb 2026. Seventeen continuous physicochemical properties

ARTICLE IN PRESS

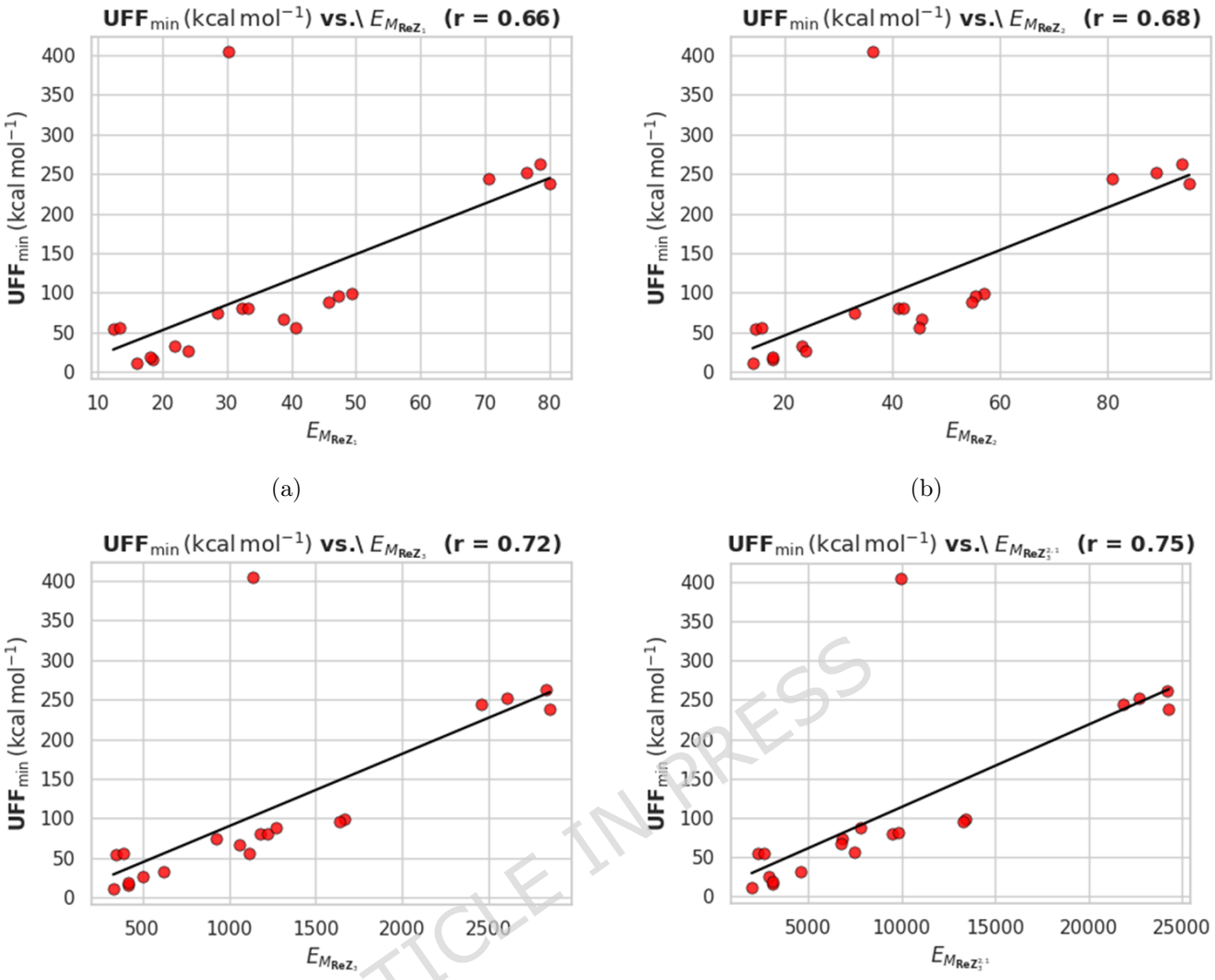

Figure 3: Representative relationships between $\mathrm{UFF}_{\mathrm{min}}$ and selected energy-based redefined Zagreb descriptors. Their behavior closely mirrors that of the corresponding combinatorial descriptors, again indicating limited independence at the descriptor level.

were considered as QSPR targets, namely molecular weight (MW), ideal-gas heat capacity ($C_{p,\mathrm{gas}}$), dynamic viscosity (η), standard Gibbs free energy of formation ($\Delta_f G^\circ$), standard enthalpy of formation in the gas phase ($\Delta_f H^\circ_{\mathrm{gas}}$), standard enthalpy of fusion ($\Delta_{\mathrm{fus}} H^\circ$), enthalpy of fusion at a given temperature ($\Delta_{\mathrm{fus}} H$), standard enthalpy of vaporization ($\Delta_{\mathrm{vap}} H^\circ$), enthalpy of vaporization at a given temperature ($\Delta_{\mathrm{vap}} H$), logarithm of water solubility ($\log_{10} WS$), octanol/water partition coefficient ($\log P_{\mathrm{oct/wat}}$), McGowan characteristic volume (McVol), critical pressure (P_c), normal boiling temperature (T_{boil}), critical temperature (T_c), normal melting point (T_{fus}), and critical volume (V_c). A representative summary of the physicochemical data is provided in Table 13, while the complete dataset is supplied in the Supplementary Material.

To evaluate how effectively the redefined Zagreb framework captures chemically meaningful structure–property signals across this broad set of endpoints, we considered three descriptor configurations. The aim is not merely to identify a single "winning" descriptor block, but rather to assess the overall predictive capacity of the redefined Zagreb descriptors, their derivative forms, and their combined representation across seventeen physicochemical properties.

For clarity, we denote the first configuration by *Redefined Zagreb_6* (abbreviated ReZ_6). It consists of

ARTICLE IN PRESS

the six basic redefined Zagreb descriptors

$$\mathrm{ReZ}_1, \quad \mathrm{ReZ}_2, \quad \mathrm{ReZ}_3, \quad E_M(\mathrm{ReZ}_1), \quad E_M(\mathrm{ReZ}_2), \quad E_M(\mathrm{ReZ}_3).$$

The second configuration is denoted by *Derivatives Redefined Zagreb_ 12* (abbreviated $DReZ_{12}$). It contains the twelve derivative descriptors associated with the parameter pairs $(2,1)$ and $(1,2)$, namely

$$\mathrm{ReZ}_1^{(2,1)},\ \mathrm{ReZ}_1^{(1,2)},\ \mathrm{ReZ}_2^{(2,1)},\ \mathrm{ReZ}_2^{(1,2)},\ \mathrm{ReZ}_3^{(2,1)},\ \mathrm{ReZ}_3^{(1,2)},$$

$$E_M\big(\mathrm{ReZ}_1^{(2,1)}\big),\ E_M\big(\mathrm{ReZ}_1^{(1,2)}\big),\ E_M\big(\mathrm{ReZ}_2^{(2,1)}\big),\ E_M\big(\mathrm{ReZ}_2^{(1,2)}\big),\ E_M\big(\mathrm{ReZ}_3^{(2,1)}\big),\ E_M\big(\mathrm{ReZ}_3^{(1,2)}\big).$$

A representative summary of these descriptors is given in Table 14. The third configuration, $Combined_{18}$, merges ReZ_6 and $DReZ_{12}$ into a single descriptor block of dimension 18. This combined setting is included to examine whether the derivative descriptors provide complementary information when used together with the basic redefined Zagreb descriptors.

Let $\mathbf{X} \in \mathbb{R}^{n\times p}$ denote the descriptor matrix, where $n = 100$ and $p \in \{6, 12, 18\}$ according to the descriptor set under consideration. For each physicochemical endpoint, the response vector is denoted by $\mathbf{y} \in \mathbb{R}^n$, and each QSPR task is treated as an independent scalar regression problem. In this way, the alcohol-compound study functions as a broad descriptor-evaluation framework for determining how well the redefined Zagreb family and its derivatives reproduce a wide spectrum of physicochemical behavior, ranging from size-dominated properties to more structurally sensitive thermodynamic and transport-related endpoints.

Table 13: Representative physicochemical properties of the alcohol compound set $C_1, \ldots, C_{100}$. The complete property table is provided in the Supplementary Material.

Compound	MW	$C_{p,\mathrm{gas}}$	η ($\times 10^{-5}$ Pa · s)	$\Delta_f G^\circ$	$\Delta_f H^\circ_{\mathrm{gas}}$	$\Delta_{\mathrm{fus}} H^\circ$	$\Delta_{\mathrm{fus}} H$	$\Delta_{\mathrm{vap}} H^\circ$	$\Delta_{\mathrm{vap}} H$	$\log_{10} WS$	$\log P_{\mathrm{oct/wat}}$	McVol	P_c	T_{boil}	T_c	T_{fus}	V_c
C_1	144.25	405.56	13.37	-116.80	-391.88	16.11	16.11	51.53	51.53	-2.72	2.584	143.540	2566.29	496.62	661.81	222.01	0.546
C_2	158.28	456.11	11.09	-108.38	-412.52	18.70	18.70	53.76	53.76	-3.14	2.974	157.630	2333.78	478.15	683.75	233.28	0.603
C_3	158.28	457.87	10.48	-110.82	-417.80	15.17	15.17	53.37	53.37	-2.90	2.830	157.630	2351.92	519.06	686.37	218.28	0.597
C_4	130.23	356.45	16.09	-125.22	-371.24	13.52	13.52	49.31	54.80	-2.30	2.194	129.450	2835.36	433.15	639.93	210.74	0.490
C_5	114.19	307.10	21.79	-112.02	-306.06	10.88	10.88	47.97	47.97	-1.78	1.557	104.500	3782.33	466.62	659.09	232.61	0.379
C_6	114.19	307.10	21.79	-112.02	-306.06	10.88	10.88	65.50	65.50	-1.78	1.557	104.500	3782.33	444.35	659.09	232.61	0.379
C_7	114.19	307.10	21.79	-112.02	-306.06	10.88	10.88	47.97	47.97	-1.78	1.557	104.500	3782.33	466.62	659.09	232.61	0.379
C_8	144.25	405.56	13.37	-116.80	-391.88	16.11	16.11	51.53	51.53	-2.72	2.584	143.540	2566.29	496.62	661.81	222.01	0.546
C_9	158.28	456.11	11.09	-108.38	-412.52	18.70	18.70	53.76	53.76	-3.14	2.974	157.630	2333.78	519.50	683.75	233.28	0.603
C_{10}	214.39	673.32	4.87	77.14	-500.36	25.54	25.54	62.27	62.27	-4.57	4.390	213.990	1671.43	533.15	775.11	263.36	0.821
C_{11}	130.23	356.45	16.09	-125.22	-371.24	13.52	13.52	49.31	46.50	-2.30	2.194	129.450	2835.36	440.65	621.20	181.90	0.490
C_{12}	186.33	561.31	7.61	-91.54	-453.80	23.88	23.88	58.21	58.21	-3.98	3.754	185.810	1954.41	565.26	728.05	255.82	0.715
C_{13}	172.31	508.04	9.19	-99.96	-433.16	21.29	21.29	55.98	55.98	-3.56	3.364	171.720	2131.49	542.38	705.81	244.55	0.658
C_{14}	100.16	255.97	29.61	-108.34	-279.26	10.39	10.39	45.58	45.58	-1.36	1.167	90.410	4135.61	424.00	626.67	224.86	0.331
C_{15}	130.23	356.45	16.09	-125.22	-371.24	13.52	13.52	49.31	47.60	-2.30	2.194	129.450	2835.36	438.65	639.93	210.74	0.490
⋮	⋮	⋮	⋮	⋮	⋮	⋮	⋮	⋮	⋮	⋮	⋮	⋮	⋮	⋮	⋮	⋮	⋮
C_{96}	114.19	307.10	21.79	-112.02	-306.06	10.88	10.88	47.97	47.97	-1.78	1.557	104.500	3782.33	440.60	659.09	232.61	0.379
C_{97}	142.24	408.69	15.24	-97.62	-352.62	12.54	12.54	52.04	52.04	-2.38	2.194	132.680	3052.41	511.94	704.02	240.15	0.484
C_{98}	142.24	408.69	15.24	-97.62	-352.62	12.54	12.54	52.04	52.04	-2.38	2.194	132.680	3052.41	511.94	704.02	240.15	0.484
C_{99}	142.24	408.69	15.24	-97.62	-352.62	12.54	12.54	52.04	52.04	-2.38	2.194	132.680	3052.41	511.94	704.02	240.15	0.484
C_{100}	142.24	408.69	15.24	-97.62	-352.62	12.54	12.54	52.04	52.04	-2.38	2.194	132.680	3052.41	511.94	704.02	240.15	0.484

Abbreviations: MW = Molecular Weight (g/mol); $C_{p,\mathrm{gas}}$ = ideal gas heat capacity (J/mol×K); η = dynamic viscosity ($\times 10^{-5}$ Pa·s); $\Delta_f G^\circ$ = standard Gibbs free energy of formation (kJ/mol); $\Delta_f H^\circ_{\mathrm{gas}}$ = enthalpy of formation at standard conditions (gas phase, kJ/mol); $\Delta_{\mathrm{fus}} H^\circ$ = enthalpy of fusion at standard conditions (kJ/mol); $\Delta_{\mathrm{fus}} H$ = enthalpy of fusion at a given temperature (kJ/mol); $\Delta_{\mathrm{vap}} H^\circ$ = enthalpy of vaporization at standard conditions (kJ/mol); $\Delta_{\mathrm{vap}} H$ = enthalpy of vaporization at a given temperature (kJ/mol); $\log_{10} WS = \log_{10}$ of water solubility in mol/L; $\log P_{\mathrm{oct/wat}}$ = octanol/water partition coefficient; McVol = McGowan's characteristic volume (mL/mol); P_c = critical pressure (kPa); T_{boil} = normal boiling point temperature (K); T_c = critical temperature (K); T_{fus} = normal melting (fusion) point (K); V_c = critical volume (m^3/kmol).

8.2 Scope and interpretation of the QSPR tasks

The seventeen physicochemical endpoints considered in this study play two complementary roles in assessing descriptor quality. Some properties, such as molecular weight, McGowan characteristic volume, and critical volume, are strongly associated with overall molecular size and therefore serve primarily as *structural validation targets*. Accurate prediction of such responses indicates that the redefined Zagreb-based descriptors successfully encode global size, branching, and topological bulk information in a chemically meaningful manner.

ARTICLE IN PRESS

Table 14: Representative values of the newly proposed lifted redefined Zagreb descriptors and their corresponding energies for the alcohol compound set $C_1, \ldots, C_{100}$. The complete descriptor table is provided in the Supplementary Material.

Compound	$\mathrm{ReZ}_1^{(2,1)}$	$\mathrm{ReZ}_1^{(1,2)}$	$\mathrm{ReZ}_2^{(2,1)}$	$\mathrm{ReZ}_2^{(1,2)}$	$\mathrm{ReZ}_3^{(2,1)}$	$\mathrm{ReZ}_3^{(1,2)}$	$E_M(\mathrm{ReZ}_1^{(2,1)})$	$E_M(\mathrm{ReZ}_1^{(1,2)})$	$E_M(\mathrm{ReZ}_2^{(2,1)})$	$E_M(\mathrm{ReZ}_2^{(1,2)})$	$E_M(\mathrm{ReZ}_3^{(2,1)})$	$E_M(\mathrm{ReZ}_3^{(1,2)})$
C_1	41.000	3.000	37.683	2.005	788.000	740.000	50.888	4.306	45.848	2.457	989.968	896.134
C_2	45.000	3.250	41.683	2.255	852.000	804.000	54.934	4.525	50.681	2.725	1065.495	973.864
C_3	47.333	3.028	44.050	2.148	964.000	904.000	56.603	4.023	53.022	2.523	1228.638	1091.246
C_4	37.000	2.750	33.683	1.755	724.000	676.000	44.446	3.837	40.403	2.078	897.970	808.786
C_5	35.333	1.944	41.300	1.835	920.000	824.000	41.993	2.633	50.332	2.168	1150.013	1000.162
C_6	35.333	1.944	41.300	1.835	920.000	824.000	41.993	2.633	50.332	2.168	1150.013	1000.162
C_7	35.333	1.944	41.300	1.835	920.000	824.000	41.993	2.633	50.332	2.168	1150.013	1000.162
C_8	41.000	3.000	37.683	2.005	788.000	740.000	51.210	4.316	46.250	2.466	1014.450	910.368
C_9	45.000	3.250	41.683	2.255	852.000	804.000	57.570	4.784	51.503	2.835	1095.552	994.078
C_{10}	62.000	4.417	64.617	3.197	1404.000	1272.000	76.665	6.469	77.058	3.913	1694.943	1509.820
C_{11}	36.333	2.944	35.967	1.779	816.000	732.000	47.613	4.892	43.665	2.261	1020.068	886.175
C_{12}	53.000	3.750	49.683	2.755	980.000	932.000	67.657	5.406	61.686	3.469	1258.721	1156.984
C_{13}	49.000	3.500	45.683	2.505	916.000	868.000	61.899	5.084	56.541	3.117	1180.164	1075.070
C_{14}	31.333	1.694	37.300	1.585	856.000	760.000	37.820	2.414	44.344	1.871	1049.013	903.359
C_{15}	37.000	2.750	33.683	1.755	724.000	676.000	47.605	4.211	41.458	2.205	936.584	834.543
⋮	⋮	⋮	⋮	⋮	⋮	⋮	⋮	⋮	⋮	⋮	⋮	⋮
C_{96}	35.000	1.991	44.400	1.855	1110.000	912.000	44.436	2.961	54.994	2.284	1447.526	1132.916
C_{97}	44.333	2.509	60.150	2.293	1632.000	1284.000	53.549	3.408	70.781	2.727	1967.698	1509.303
C_{98}	44.333	2.509	60.150	2.293	1632.000	1284.000	53.549	3.408	70.781	2.727	1967.698	1509.303
C_{99}	44.333	2.509	60.150	2.293	1632.000	1284.000	53.549	3.408	70.781	2.727	1967.698	1509.303
C_{100}	44.333	2.509	60.150	2.293	1632.000	1284.000	53.549	3.408	70.781	2.727	1967.698	1509.303

Abbreviations: $\mathrm{ReZ}_1^{(2,1)}, \mathrm{ReZ}_1^{(1,2)}, \mathrm{ReZ}_2^{(2,1)}, \mathrm{ReZ}_2^{(1,2)}, \mathrm{ReZ}_3^{(2,1)}, \mathrm{ReZ}_3^{(1,2)}$ denote the six redefined Zagreb indices under the parameter pairs $(2,1)$ and $(1,2)$; $E_M(\cdot)$ denotes the corresponding energy of the associated index.

By contrast, properties such as dynamic viscosity, water solubility, octanol/water partition coefficient, critical pressure, and phase-change enthalpies are more sensitive to finer structural and intermolecular effects. These responses are therefore regarded as more demanding *nontrivial property targets*. Strong predictive performance on such endpoints provides more compelling evidence that the redefined Zagreb framework and its derivative descriptors capture chemically relevant structural information beyond simple size effects.

Accordingly, the present QSPR analysis is not intended as a substitute for direct physicochemical measurement or high-level property calculation. Rather, it is designed as a controlled descriptor-evaluation framework for examining how effectively the ReZ_6, $DReZ_{12}$, and $Combined_{18}$ representations encode structural signals relevant to a broad spectrum of chemically meaningful physicochemical behavior. In this sense, the section should be read primarily as an assessment of descriptor capability across seventeen endpoints, not merely as a competition between three alternative blocks.

8.3 Computational setup and leakage-safe grouped evaluation

All experiments were carried out in Python within a reproducible machine-learning workflow. To ensure a fair and leakage-safe comparison across the three descriptor configurations, namely ReZ_6, $DReZ_{12}$, and $Combined_{18}$, the same evaluation logic was applied to each endpoint and each descriptor block.

Before splitting, compounds were grouped according to a rounded descriptor signature constructed from the active predictor set. Thus, compounds sharing identical descriptor signatures were assigned the same **Signature_Group_ID**. This grouping step was introduced to prevent structurally indistinguishable descriptor patterns from appearing simultaneously in both training and test partitions, thereby eliminating a major source of descriptor-level leakage.

External assessment was performed by repeated group-aware hold-out validation. For each descriptor set, **GroupShuffleSplit** was applied with a test fraction of 0.20 over 30 repeated runs, using seeds

$$\mathbf{random_state} = 42 + \mathbf{repeat}, \qquad \mathbf{repeat} = 1, \ldots, 30.$$

Accordingly, all reported external-test results are based on repeated hold-out evaluation under group-aware

ARTICLE IN PRESS

separation. This design is intended to measure not only predictive strength, but also the stability of that strength under repeated leakage-safe external assessment.

8.4 Regression models, model selection, and performance metrics

For each endpoint and each descriptor set, we considered a diverse panel of linear and nonlinear regression models:

- Linear Regression,
- Ridge Regression,
- Lasso Regression,
- Elastic Net,
- Partial Least Squares (PLS),
- Support Vector Regression with radial basis function kernel (SVR-RBF),
- Random Forest,
- Extra Trees.

For models requiring feature scaling, the regressor was embedded in a **Pipeline** with **StandardScaler**. Model selection was performed using grouped cross-validation on the full dataset prior to repeated external testing. Specifically, **GroupKFold** was used to evaluate candidate models in a leakage-safe manner, and the model achieving the largest grouped cross-validation R^2 was selected as the representative model for the corresponding endpoint and descriptor set. This strategy was adopted to obtain a stable and computationally efficient comparison across the three descriptor spaces.

After model preselection, the chosen model for each endpoint–descriptor-set pair was evaluated over 30 repeated group-aware external splits. Predictive performance was quantified using the coefficient of determination R^2, mean absolute error (MAE), and root mean squared error (RMSE). The final assessment is based primarily on the mean and standard deviation of the external-test R^2 across the repeated grouped splits, while MAE and RMSE serve as supporting error measures.

ARTICLE IN PRESS

8.5 Direct comparison of descriptor sets

The principal comparison table summarizes, for each physicochemical target, the predictive behavior of the three descriptor blocks: ReZ_6, $DReZ_{12}$, and $Combined_{18}$. For each target, the table reports the selected best model together with the grouped cross-validation R^2, the mean external-test R^2, and the corresponding standard deviation over repeated grouped splits. In this way, the comparison reflects average generalization behavior under repeated leakage-safe evaluation rather than the outcome of a single train/test realization.

The central purpose of this comparison is to determine how well the redefined Zagreb family as a whole reproduces a wide range of physicochemical properties, and to examine whether the derivative descriptors contribute useful complementary structure–property information. In particular, ReZ_6 measures the predictive value of the basic redefined Zagreb descriptors and their energies, $DReZ_{12}$ isolates the contribution of the derivative descriptors associated with the parameter pairs $(2, 1)$ and $(1, 2)$, and $Combined_{18}$ tests whether the joint representation improves performance by combining both types of information.

Accordingly, the comparison should not be interpreted solely as a search for a single universally dominant descriptor set. Rather, it provides a structured way to evaluate the breadth, robustness, and complementarity of the redefined Zagreb descriptors and their derivatives across seventeen chemically meaningful regression tasks.

ARTICLE IN PRESS

Table 15: Direct comparison of the predictive performance of the ReZ_6, $DReZ_{12}$, and $Combined_{18}$ descriptor sets for the alcohol dataset under repeated group-aware external validation. Reported values are mean ± standard deviation of the external-test R^2 over 30 grouped splits.

Target property	ReZ_6	$DReZ_{12}$	$Combined_{18}$	**Highest mean**
Molecular Weight	1.000 ± 0.000	1.000 ± 0.000	1.000 ± 0.000	$Combined_{18}$
$C_{p,\mathrm{gas}}$: Ideal gas heat capacity (J/mol×K)	0.996 ± 0.003	0.995 ± 0.002	0.995 ± 0.002	ReZ_6
V_c: Critical volume (m^3/kmol)	0.995 ± 0.009	0.995 ± 0.005	0.995 ± 0.005	$Combined_{18}$
McVol: McGowan's characteristic volume (mL/mol)	0.995 ± 0.010	0.996 ± 0.005	0.996 ± 0.004	$Combined_{18}$
T_c: Critical temperature (K)	0.954 ± 0.034	0.953 ± 0.035	0.954 ± 0.035	ReZ_6
$\log_{10} WS$: Log_{10} of water solubility (mol/L)	0.900 ± 0.168	0.911 ± 0.113	0.911 ± 0.115	$Combined_{18}$
P_c: Critical pressure (kPa)	0.891 ± 0.043	0.887 ± 0.119	0.881 ± 0.056	ReZ_6
$\log P_{\mathrm{oct/wat}}$: Octanol/water partition coefficient	0.883 ± 0.211	0.854 ± 0.168	0.855 ± 0.168	ReZ_6
$\Delta_{\mathrm{fus}} H^\circ$: Enthalpy of fusion at standard conditions (kJ/mol)	0.876 ± 0.061	0.850 ± 0.111	0.854 ± 0.099	ReZ_6
$\Delta_{\mathrm{fus}} H$: Enthalpy of fusion at a given temperature (kJ/mol)	0.876 ± 0.061	0.850 ± 0.111	0.854 ± 0.099	ReZ_6
$\Delta_f H^\circ_{\mathrm{gas}}$: Enthalpy of formation in the gas phase (kJ/mol)	0.776 ± 0.294	0.747 ± 0.263	0.744 ± 0.266	ReZ_6
η: Dynamic viscosity (Pa·s)	0.632 ± 0.402	0.602 ± 0.305	0.595 ± 0.312	ReZ_6
T_{fus}: Normal melting point (K)	0.630 ± 0.179	0.562 ± 0.150	-0.334 ± 3.288	ReZ_6
T_{boil}: Normal boiling point temperature (K)	0.486 ± 0.299	0.455 ± 0.271	0.454 ± 0.285	ReZ_6
$\Delta_{\mathrm{vap}} H$: Enthalpy of vaporization at a given temperature (kJ/mol)	0.325 ± 0.320	0.256 ± 0.399	0.301 ± 0.368	ReZ_6
$\Delta_{\mathrm{vap}} H^\circ$: Enthalpy of vaporization at standard conditions (kJ/mol)	0.361 ± 0.357	0.244 ± 0.462	0.291 ± 0.385	ReZ_6
$\Delta_f G^\circ$: Standard Gibbs free energy of formation (kJ/mol)	0.328 ± 0.660	0.121 ± 0.779	0.144 ± 0.770	ReZ_6
Mean over all targets	**0.759**	**0.722**	**0.676**	ReZ_6
Median over all targets	**0.876**	**0.850**	**0.854**	ReZ_6
Targets with mean test $R^2 \geq 0.90$	**5**	**6**	**6**	—
Targets with mean test $R^2 \geq 0.75$	**11**	**10**	**10**	—
Targets with mean test $R^2 < 0$	**0**	**0**	**1**	—

ARTICLE IN PRESS

8.6 Comparative QSPR performance of ReZ_6, $DReZ_{12}$, and $Combined_{18}$

To provide a transparent comparison of the predictive behavior of the investigated descriptor spaces, we analyzed the ReZ_6, $DReZ_{12}$, and $Combined_{18}$ sets using repeated group-aware external validation. In this framework, compounds sharing identical descriptor signatures within a given descriptor space were assigned to the same group, thereby preventing leakage between training and test subsets. Predictive performance was summarized through the mean and standard deviation of the external-test R^2 over 30 repeated grouped splits, together with graphical summaries of overall accuracy, predictive stability, and relative change with respect to the ReZ_6 baseline.

Table 15 and Figure 4 show that the redefined Zagreb descriptor family as a whole has substantial QSPR capability across the seventeen physicochemical targets. A large fraction of the reported external-test results lie above 0.80, and several size-, volume-, and critical-property-related endpoints are predicted with very high accuracy. In particular, Molecular Weight is reproduced essentially perfectly by all three descriptor spaces, while $C_{p,\mathrm{gas}}$, V_c, McVol, T_c, and $\log_{10} WS$ also exhibit strong predictive behavior.

ARTICLE IN PRESS

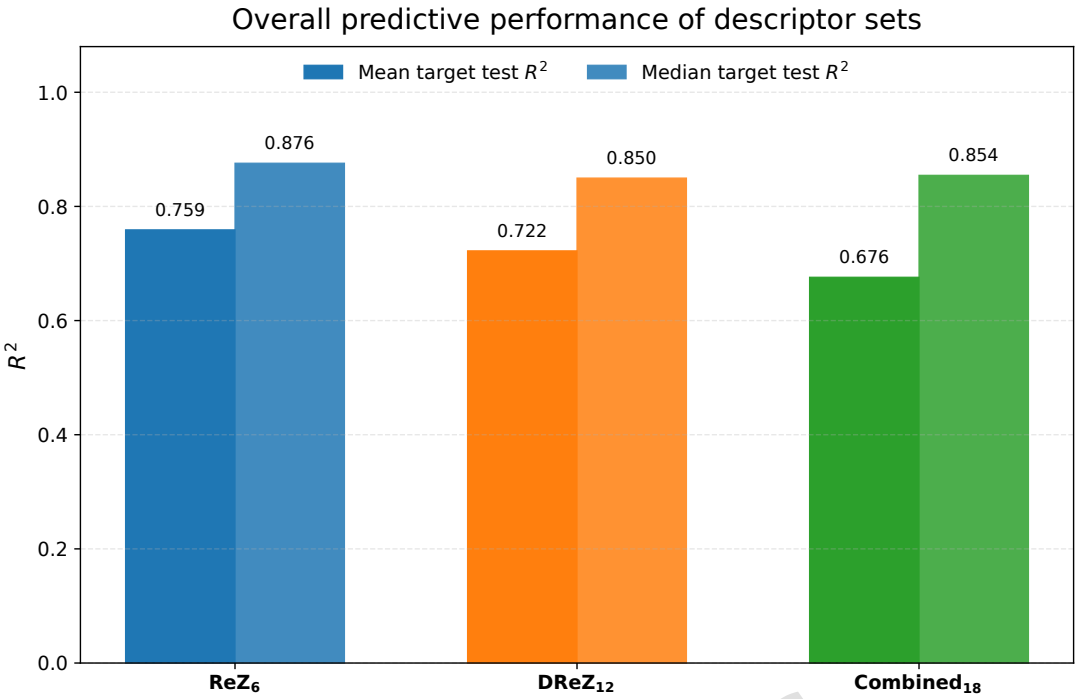

Figure 4: Overall predictive performance of the ReZ_6, $DReZ_{12}$, and $Combined_{18}$ descriptor sets across the 17 physicochemical targets of the alcohol dataset. The bars represent the mean and median target-level external-test R^2 obtained from repeated group-aware external validation.

These results indicate that both the basic redefined Zagreb descriptors and their derivative forms capture chemically meaningful structural information over a broad range of property classes. The strongest outcomes are observed for endpoints closely linked to molecular size, branching, bulk structure, and critical behavior, which is fully consistent with the graph-theoretical nature of the descriptor families.

A target-wise comparison is reported in Table 15. The numerical results show that ReZ_6, $DReZ_{12}$, and $Combined_{18}$ all provide useful predictive information, but with slightly different strengths across endpoint categories. Rather than interpreting the table only as a ranking exercise, it is more informative to view it as evidence that the redefined Zagreb framework remains predictive in multiple descriptor realizations. The derivative descriptors are therefore not introduced as replacements for the basic family, but as meaningful extensions that preserve strong QSPR performance and, for selected targets, contribute complementary information.

This complementary behavior is most visible for Molecular Weight, McGowan characteristic volume, critical volume, and water solubility, where $Combined_{18}$ attains the highest mean external-test R^2, although in some of these cases the numerical differences are very small. In practical terms, this suggests that the derivative descriptors can enrich the original redefined Zagreb representation, especially for targets governed by bulk structural and volume-related effects.

The robustness of these observations is highlighted in Figure 5, where predictive performance is shown as mean external-test $R^2\pm$ standard deviation over repeated grouped splits. The strongest endpoints, such as Molecular Weight, $C_{p,\mathrm{gas}}$, McVol, V_c, and T_c, display both high accuracy and relatively small variability, confirming that these relationships are stable and reproducible. In contrast, weaker endpoints are accompanied by larger uncertainty, indicating stronger split sensitivity and reduced robustness. This is especially evident for the combined descriptor block in the case of T_{fus}, where the mean external-test performance becomes negative and the standard deviation is exceptionally large. The broken-axis display in Figure 5 is therefore useful, since it preserves readability while explicitly retaining this unstable outlier.

The relative behavior of the derivative descriptor spaces is shown more directly in Figure 6, which

ARTICLE IN PRESS

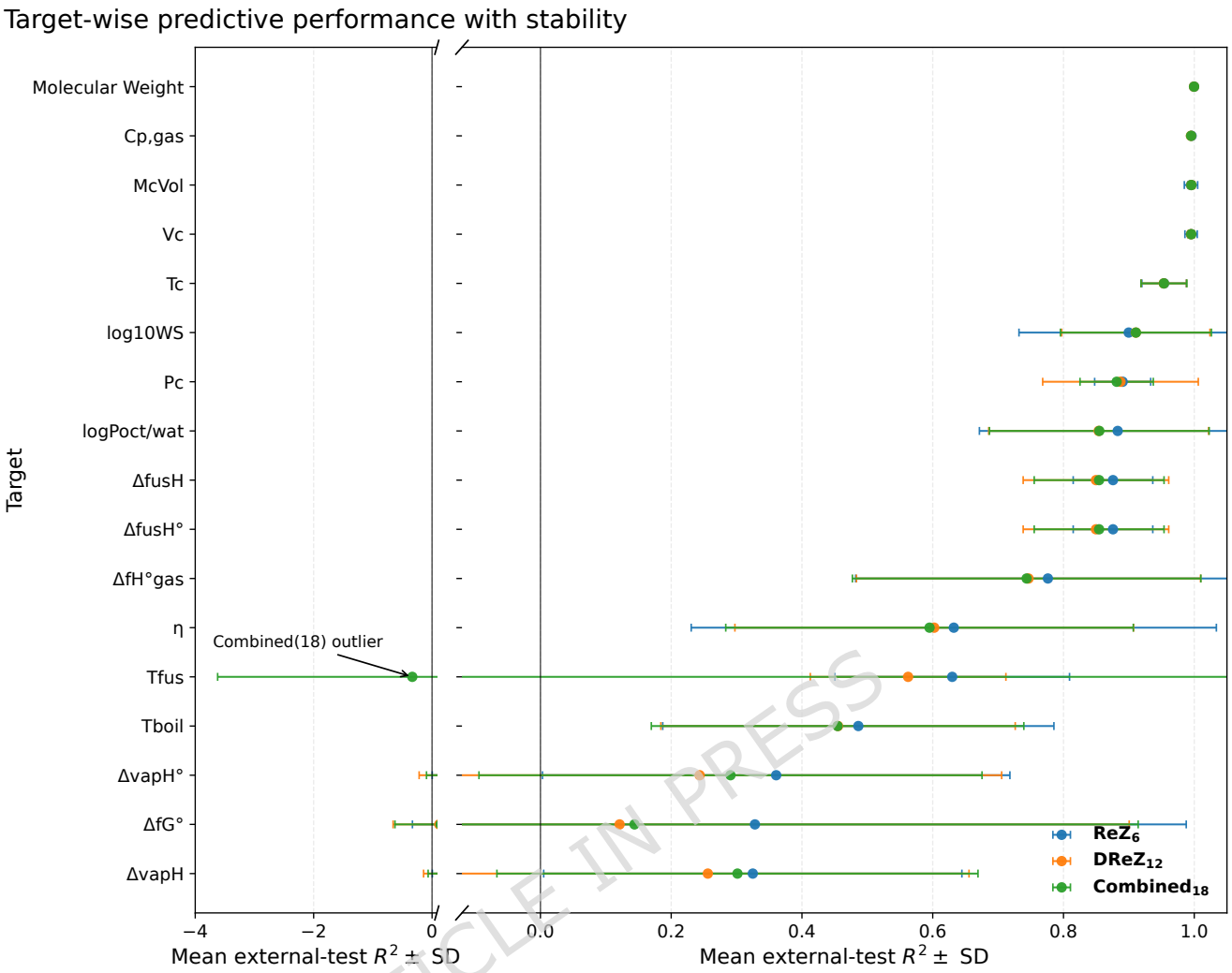

Figure 5: Target-wise predictive performance with stability, reported as mean external-test $R^2\pm$ standard deviation over repeated group-aware splits. A broken x-axis is used to preserve readability while explicitly retaining the negative outlier associated with the $Combined_{18}$ descriptor set for T_{fus}.

reports the change in mean external-test R^2 relative to the ReZ_6 baseline. The figure confirms that the derivative and combined representations do not act as uniformly dominant alternatives, but they do provide localized improvements for a subset of important endpoints. This is precisely the type of behavior expected from complementary descriptor extensions: their value lies in broadening the structural representation, not necessarily in outperforming the baseline for every target.

Overall, the repeated leakage-safe grouped evaluation supports a balanced conclusion. The ReZ_6 descriptors, the derivative $DReZ_{12}$ descriptors, and their union in $Combined_{18}$ all demonstrate substantial QSPR usefulness for alcohol compounds. The strongest and most stable results are obtained for many of the seventeen physicochemical properties, with several targets showing mean external-test R^2 values well above 0.80. The derivative descriptors therefore contribute genuine QSPR value and should be interpreted as meaningful extensions of the redefined Zagreb family, while the combined representation illustrates where additional complementary information can be gained without implying that one descriptor block must universally dominate the others.

For completeness, additional graphical summaries are provided in the Supplementary Material. These include a heatmap of target-wise performance, the number of targets won by each descriptor set, the agreement between grouped cross-validation and external-test performance, and an accuracy–stability

ARTICLE IN PRESS

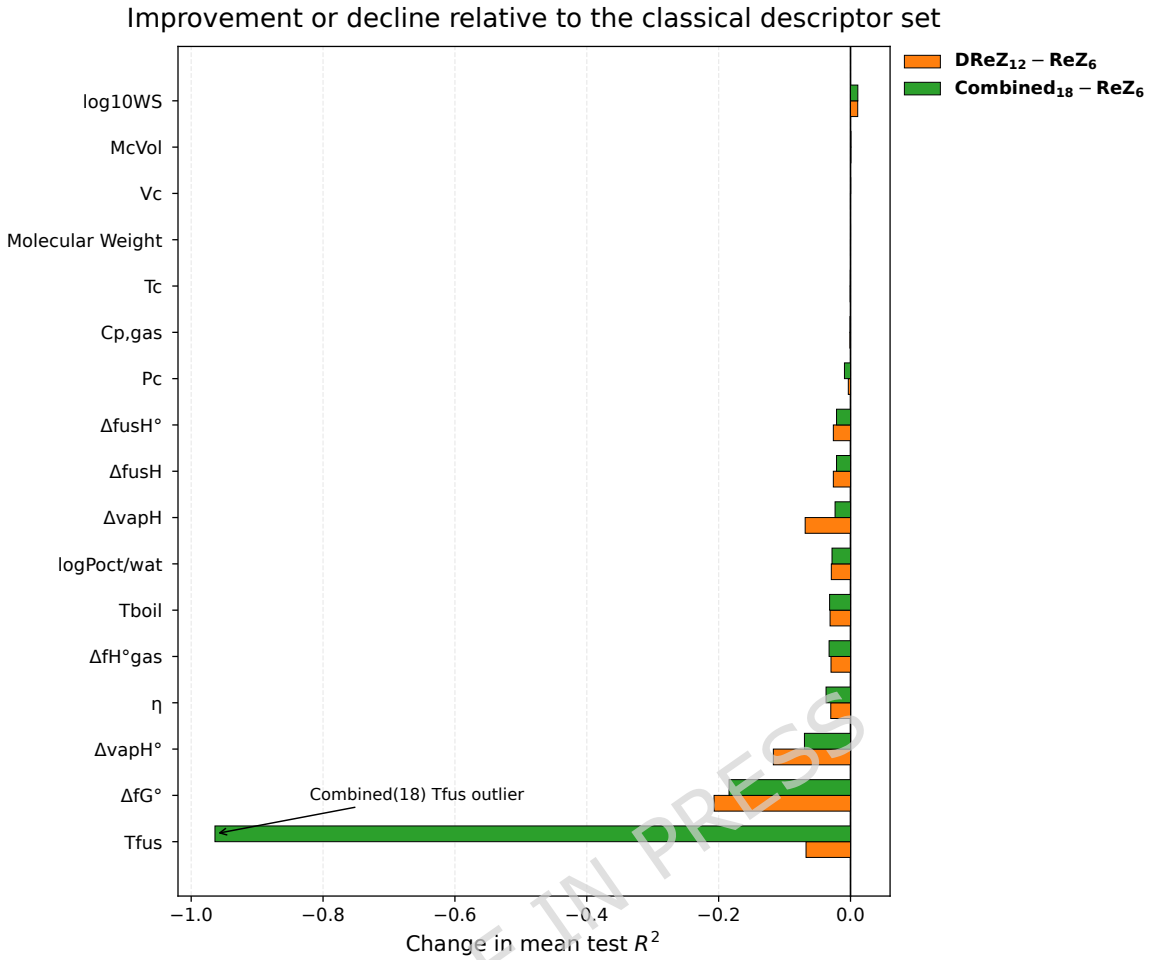

Figure 6: Improvement or decline in mean external-test R^2 relative to the ReZ_6 baseline. Positive values indicate that the $DReZ_{12}$ or $Combined_{18}$ descriptor sets outperform the baseline, whereas negative values indicate lower mean performance.

ARTICLE IN PRESS

landscape summarizing the balance between predictive strength and variability.

Discussion

The present article develops the redefined Zagreb framework along three complementary directions: explicit graph-theoretical formulas for several classical graph families, a spectral interpretation through weighted adjacency matrices and their associated energies, and two chemically distinct descriptor applications. Taken together, these components show that the redefined Zagreb family is not merely a formal extension of degree-based indices, but a flexible framework linking combinatorial structure, spectral behaviour, and molecular-property analysis.

From the theoretical perspective, the closed expressions obtained for paths, cycles, complete graphs, stars, wheels, complete bipartite graphs, and friendship graphs clarify how the basic, hyper, general, and generalized-general redefined Zagreb indices respond to different degree patterns. In regular and biregular settings, these formulas reduce to especially transparent forms, whereas in mixed-degree families they reveal how the indices amplify interactions between low- and high-degree vertices. The derived bounds further place these descriptors within the broader landscape of degree-based topological indices, showing that the redefined Zagreb family remains closely connected to classical graph invariants while providing a

ARTICLE IN PRESS

refined measure of degree heterogeneity and edge-degree interaction.

A second major contribution is the spectral reinterpretation of the redefined Zagreb kernels. By associating each kernel F with a weighted adjacency matrix $W_F(G)$, the paper extends the classical concept of graph energy to a family of redefined Zagreb energies. This viewpoint makes it possible to derive upper and lower bounds in terms of Frobenius-type estimates, degree extremes, and row-sum constraints, and to obtain exact expressions for highly structured families whenever $W_F(G)$ reduces to a scalar multiple of the adjacency matrix. In this way, the work makes explicit the interplay between degree structure, topological complexity, and spectral behaviour.

The first application, carried out on 22 anticancer drug-like molecules, should be interpreted as an analytical descriptor study rather than as a fully developed predictive QSPR model. Within that scope, the redefined Zagreb descriptors and their energy-based analogues are strongly correlated with classical size-related physicochemical quantities such as MW, HA, and MR. At the same time, several higher-order mixed descriptors—most notably $\mathrm{ReZ}_3^{2,1}$, $\mathrm{ReZ}_3^{1,2}$, and $\mathrm{ReZ}_2^{2,1}$—show stronger univariate association with $\mathrm{UFF}_{\min}$ than the conventional physicochemical descriptors examined here. Among them, $\mathrm{ReZ}_3^{2,1}$ provides the strongest individual performance, suggesting that branching intensity and high-degree connectivity are more closely linked to the UFF energy landscape than molecular size alone. However, the near-perfect correlations between each redefined Zagreb index and its energy-based analogue show that, for this dataset, the spectral transformation behaves largely as a monotone rescaling rather than as an independent source of descriptor information. This observation is fully consistent with the severe multicollinearity seen in the full multiple regression model.

The second study, based on 100 alcohol compounds and 17 physicochemical endpoints, provides a broader and more rigorous QSPR assessment of the descriptor family. Under repeated leakage-safe grouped external validation, the ReZ_6, $DReZ_{12}$, and $Combined_{18}$ descriptor spaces all exhibit substantial predictive usefulness across a wide range of endpoints. Many properties are modeled with strong external-test accuracy, and several results exceed the 0.80 level. The strongest performance is observed for endpoints related to molecular size, volume, and critical-property behaviour, which is consistent with the graph-theoretical content of the descriptors. The derivative descriptors are therefore clearly chemically meaningful and predictive, even though they do not uniformly dominate the basic redefined Zagreb representation. Instead, the evidence suggests that the derivative forms act mainly as complementary extensions that broaden the structural representation and provide localized improvements for selected endpoints, while the combined block illustrates where such complementary information can be beneficial and where it may reduce stability for more difficult targets.

Viewed together, the two applications lead to a balanced interpretation of the redefined Zagreb framework. On the one hand, the family is clearly chemically informative: in the anticancer dataset it yields descriptors more strongly associated with $\mathrm{UFF}_{\min}$ than several standard physicochemical variables, and in the alcohol dataset it provides a broadly useful descriptor system across a diverse set of physicochemical properties. On the other hand, the practical role of the different variants is context-dependent. In the anticancer study, $\mathrm{ReZ}_3^{2,1}$ emerges as the most informative individual descriptor, whereas in the alcohol study the basic and derivative forms should be viewed together as a predictive family whose strengths vary across endpoint classes. Thus, the derivative descriptors are best regarded as meaningful extensions of the redefined Zagreb framework rather than as universal replacements for the original descriptors.

Overall, the article shows that the redefined Zagreb framework is mathematically rich and chemically relevant. It yields explicit formulas and structural inequalities for important graph classes, admits a natural spectral-energy formulation, and provides practically meaningful topological descriptors for molecular structure–property analysis. The strongest general conclusion is therefore not that a single new descriptor universally dominates, but that the redefined Zagreb family offers a unified combinatorial and spectral framework whose usefulness depends on the graph class, the molecular domain, and the endpoint under consideration.

ARTICLE IN PRESS

Conclusion

In this work, we developed a unified framework for the redefined Zagreb family that combines graph-theoretical, spectral, and applied structure–property perspectives. Starting from the edge-weight kernels

$$F(\delta(u), \delta(v)),$$

which generate the basic, hyper, general, and generalized-general redefined Zagreb indices, we introduced the associated F-weighted adjacency matrices $W_F(G)$ and studied their spectra, energies, and related structural properties. This approach allowed us to interpret redefined Zagreb energies as matrix energies, derive general upper and lower bounds in terms of degree parameters, Frobenius-type estimates, and row-sum arguments, and obtain exact closed forms for several regular and biregular graph families through the scaling relation $W_F(G) = cA(G)$ whenever all edges share the same degree pair.

Within this framework, we established explicit formulas for the redefined Zagreb variants on important graph classes, together with degree-extreme bounds and comparison inequalities linking these quantities to classical degree-based indices and to adjacency energy. These results show that the redefined Zagreb family is mathematically tractable, structurally informative, and naturally connected to the broader spectral theory of graphs. The entropy viewpoint developed in the paper further extends this picture by showing that the same descriptor family can also be interpreted from an information-theoretic perspective.

The first application, carried out on 22 anticancer drug-like molecules, showed that the redefined Zagreb descriptors and their energy-based analogues are strongly associated with classical size-related physicochemical quantities such as MW, HA, and MR, while remaining essentially uncorrelated with the fraction of sp^3 carbons. Among the examined quantities, the mixed higher-order descriptor $\mathrm{ReZ}_3^{2,1}$, together with its energy analogue $E_{M_{\mathrm{ReZ}_3^{2,1}}}$, exhibited the strongest univariate association with the auxiliary endpoint $\mathrm{UFF}_{\min}$. At the same time, the near-perfect correlation between each redefined Zagreb index and its energy-based counterpart indicates that, for this dataset, the spectral transformation acts mainly as a monotone rescaling rather than as a qualitatively independent source of descriptor information. Because of the limited sample size and strong multicollinearity, this part of the study is best interpreted as an analytical descriptor investigation rather than a definitive predictive QSPR model.

The second study, based on 100 alcohol compounds and 17 physicochemical endpoints, provided a broader comparative validation of the descriptor family under repeated leakage-safe grouped external evaluation. The results showed that the ReZ_6, $DReZ_{12}$, and $Combined_{18}$ descriptor spaces all possess clear QSPR utility. Many endpoints were predicted with strong external-test performance, especially those related to molecular size, volume, and critical-property behaviour. The derivative descriptors are therefore chemically meaningful and predictive, while the combined block illustrates where additional complementary information can be gained. At the same time, the results also show that descriptor expansion does not automatically imply uniformly better generalization across all targets.

Taken together, the two applied studies support a balanced overall conclusion. The redefined Zagreb framework is chemically informative: in the anticancer dataset it yields descriptors more strongly associated with $\mathrm{UFF}_{\min}$ than several standard physicochemical variables, while in the alcohol dataset it provides a broad and predictive descriptor system across a wide range of physicochemical properties. The main contribution of the paper is therefore not the universal superiority of a single new descriptor, but the development of a mathematically rich and chemically relevant family of descriptors whose combinatorial, spectral, and predictive roles can be studied in a unified way.

Several natural directions arise from the present work. On the theoretical side, it would be worthwhile to extend the F-weighted matrix approach to other degree-based or distance-based kernels, to investigate extremal problems for redefined Zagreb energies under additional structural constraints, and to study the asymptotic behaviour of these quantities on graph families relevant to chemical nanostructures. On the applied side, the present results motivate broader QSPR/QSAR validation on larger and chemically more diverse datasets, the development of regularized multivariate models that explicitly address multicollinearity, and systematic comparisons between redefined Zagreb energies and other spectral descriptors. We hope

ARTICLE IN PRESS

that the methods and results developed here will provide a useful foundation for future work at the intersection of chemical graph theory, spectral graph invariants, information-theoretic descriptors, and molecular informatics.

Author contributions

Conceptualization: Y.Z., E.C., M.A.; Methodology: E.C., M.A.; Validation: Y.Z., M.A.; Investigation: E.C., M.A.; Resources: Y.Z., E.C.; Writing-original draft: M.A.; Writing-review and editing: Y.Z., E.C. All authors have read and agreed to the published version of the manuscript.

Conflict of interest

The authors declare no conflicts of interest.

Source of Funding

No source of funding for this work.

Availability of data and materials

All physicochemical property values for the $n = 100$ compounds were compiled from Cheméo (https://www.chemeo.com/) on 24 Feb 2026 (units as reported by the source). All data, scripts, and materials needed to reproduce the QSPR analyses in this study are provided as supplementary material.

ARTICLE IN PRESS

References

[1] West, D. B. (2001). *Introduction to graph theory* (2nd ed.). Upper Saddle River, NJ: Prentice Hall.

[2] Bapat, R. B. (2010). *Graphs and matrices*. New Delhi, India: Hindustan Book Agency.

[3] Brouwer, A. E., & Haemers, W. H. (2011). *Spectra of graphs*. New York, NY: Springer.

[4] Cvetković, D., Rowlinson, P., & Simić, S. (2010). *An introduction to the theory of graph spectra*. Cambridge, UK: Cambridge University Press.

[5] Horn, R. A., & Johnson, C. R. (2012). *Matrix analysis* (2nd ed.). Cambridge, UK: Cambridge University Press.

[6] Gutman, I., & Trinajstić, N. (1972). Graph theory and molecular orbitals. Total π-electron energy of alternant hydrocarbons. *Chemical Physics Letters*, **17**(4), 535–538.

[7] Gutman, I., Li, X., & Zhang, J. (2009). Graph energy. In M. Dehmer & F. Emmert-Streib (Eds.), *Analysis of complex networks: From biology to linguistics* (pp. 145–174). Weinheim, Germany: Wiley-VCH.

[8] Li, X., Shi, Y., & Gutman, I. (2012). *Graph energy*. New York, NY: Springer.

[9] Balakrishnan, R. (2004). The energy of a graph. *Linear Algebra and Its Applications*, **387**, 287–295.

[10] Gutman, I., & Furtula, B. (2019). Graph energies and their applications. *Bulletin, Classe des Sciences mathématiques et naturelles, Sciences mathématiques*, **44**, 29–45.

ARTICLE IN PRESS

[11] Gutman, I., & Ramane, H. (2020). Research on graph energies in 2019. *MATCH Communications in Mathematical and in Computer Chemistry*, **84**, 277–292.

[12] Estrada, E., & Benzi, M. (2017). What is the meaning of the graph energy after all? *Discrete Applied Mathematics*, **230**, 71–77.

[13] Das, K. C., Gutman, I., Milovanović, I., Milovanović, E., & Furtula, B. (2018). Degree-based energies of graphs. *Linear Algebra and Its Applications*, **554**, 185–204.

[14] Hosamani, S. M., & Ramane, H. S. (2016). On degree sum energy of a graph. *European Journal of Pure and Applied Mathematics*, **9**, 340–345.

[15] Gutman, I., Ruščić, B., Trinajstić, N., & Wilcox, C. F. (1975). Graph theory and molecular orbitals. XII. Acyclic polyenes. *Journal of Chemical Physics*, **62**, 3399–3405.

[16] Nikolić, S., Kovačević, G., Miličević, A., & Trinajstić, N. (2003). The Zagreb indices 30 years after. *Croatica Chemica Acta*, **76**(2), 113–124.

[17] Gutman, I., & Das, K. C. (2004). The first Zagreb index 30 years after. *MATCH Communications in Mathematical and in Computer Chemistry*, **50**, 83–92.

[18] Xu, K., Liu, M., Das, K. C., Gutman, I., & Furtula, B. (2017). A survey on Zagreb indices. *MATCH Communications in Mathematical and in Computer Chemistry*, **78**(1), 17–56.

[19] Gutman, I. (2013). Degree-based topological indices. *Croatica Chemica Acta*, **86**(4), 351–361.

[20] Borovićanin, B., Das, K. C., Furtula, B., & Gutman, I. (2017). Bounds for Zagreb indices. *MATCH Communications in Mathematical and in Computer Chemistry*, **78**, 17–100.

[21] Das, K. C. (2011). Sharp bounds for Zagreb indices. *Chemical Physics Letters*, **511**(4–6), 452–454.

[22] Borovićanin, B., Das, K. C., Furtula, B., & Gutman, I. (2017). Zagreb indices: Bounds and extremal graphs. In I. Gutman, B. Furtula, K. C. Das, E. Milovanović, & I. Milovanović (Eds.), *Bounds in chemical graph theory – Basics* (pp. 67–153). Kragujevac, Serbia: University of Kragujevac.

[23] Li, J., Shi, Y., & Gutman, I. (2020). Nordhaus–Gaddum-type results for Zagreb indices. *Discrete Applied Mathematics*, **284**, 396–402.

[24] Gagarin, A., Chellali, K., & Makinde, O. D. (2022). Generalized Zagreb indices and their applications. *Discrete Mathematics Letters*, **8**, 30–38.

[25] Zhu, X., Huang, Q., & Deng, H. (2020). New generalizations of the Zagreb indices and their extremal properties. *Journal of Mathematical Chemistry*, **58**(4), 1095–1114.

[26] Shirdel, G. H., Rezapour, H., & Sayadi, A. M. (2013). The hyper–Zagreb index of graph operations. *Iranian Journal of Mathematical Chemistry*, **4**, 213–220.

[27] Gutman, I. (2017). On hyper–Zagreb index and coindex. *Bulletin, Classe des Sciences mathématiques et naturelles, Sciences mathématiques*, **42**, 1–8.

[28] Basavanagoud, B., & Patil, S. (2016). A note on hyper–Zagreb index of graph operations. *Iranian Journal of Mathematical Chemistry*, **7**, 89–92.

[29] Pattabiraman, K., & Vijayaragavan, M. (2017). Hyper Zagreb indices and its coindices of graphs. *Bulletin of the International Mathematical Virtual Institute*, **7**, 31–41.

ARTICLE IN PRESS

ARTICLE IN PRESS

[30] Hayat, S., Khan, M. A., Khan, A., Jamil, H., & Malik, M. Y. H. (2023). Extremal hyper-Zagreb index of trees of given segments with applications to regression modeling in QSPR studies. *Alexandria Engineering Journal*, **80**, 259–268.

[31] Liu, J. B., Wang, C., Wang, S., et al. (2019). Zagreb indices and multiplicative Zagreb indices of Eulerian graphs. *Bulletin of the Malaysian Mathematical Sciences Society*, **42**, 67–78.

[32] Zhang, J., Wang, H., & Zhang, X. D. (2026). On extremal connected graphs with respect to the forgotten topological index. *MATCH Communications in Mathematical and in Computer Chemistry*, **95**(1), 39–62.

[33] Zhang, X. M., Zhang, X. D., Bass, R., & Wang, H. (2017). Extremal trees with respect to functions on adjacent vertex degrees. *MATCH Communications in Mathematical and in Computer Chemistry*, **78**(2), 307–322.

[34] Bozkurt, Ş. B., Güngör, A. D., Gutman, I., & Çevik, A. S. (2010). Randić matrix and Randić energy. *MATCH Communications in Mathematical and in Computer Chemistry*, **64**, 239–250.

[35] Bozkurt, Ş. B., Güngör, A. D., & Gutman, I. (2010). Randić spectral radius and Randić energy. *MATCH Communications in Mathematical and in Computer Chemistry*, **64**, 321–334.

[36] Estrada, E. (2017). The ABC matrix. *Journal of Mathematical Chemistry*, **55**, 1021–1033.

[37] Rodríguez, J. M., & Sigarreta, J. M. (2016). Spectral properties of geometric–arithmetic index. *Applied Mathematics and Computation*, **277**, 142–153.

[38] Arif, A., Hayat, S., & Khan, A. (2023). On irregularity indices and main eigenvalues of graphs and their applicability. *Journal of Applied Mathematics and Computing*, **69**, 2549–2571.

[39] Liu, J. B., Tang, X. J., Cai, G. J., & Cao, J. (2026). Spectrum and coherence analysis in networks with noise disturbance. *Journal of Complex Networks*, **14**(2), cnaf046.

[40] Hosamani, S. M., Kulkarni, B. B., Boli, R. G., & Gadag, V. M. (2017). QSPR analysis of certain graph theoretical matrices and their corresponding energy. *Applied Mathematics and Nonlinear Sciences*, **2**, 131–150.

[41] Hayat, S., & Liu, J.-B. (2025). Comparative analysis of temperature-based graphical indices for correlating the total π-electron energy of benzenoid hydrocarbons. *International Journal of Modern Physics B*, **39**(7), 2550047.

[42] Deng, H., Radenković, S., & Gutman, I. (2009). The Estrada index. In D. Cvetković & I. Gutman (Eds.), *Applications of graph spectra* (pp. 123–140). Belgrade, Serbia: Mathematical Institute.

[43] Zhou, B., & Du, Z. (2010). Some lower bounds for Estrada index. *Iranian Journal of Mathematical Chemistry*, **1**, 67–72.

[44] Gutman, I. (2001). The energy of a graph: Old and new results. In A. Betten, A. Kohnert, R. Laue, & A. Wassermann (Eds.), *Algebraic combinatorics and applications* (pp. 196–211). Berlin, Germany: Springer.

[45] Majstorović, S., Klobučar, A., & Gutman, I. (2009). Selected topics from the theory of graph energy: Hypoenergetic graphs. In D. Cvetković & I. Gutman (Eds.), *Applications of graph spectra* (pp. 65–105). Belgrade, Serbia: Mathematical Institute.

[46] Das, K. C., Gutman, I., Çevik, A. S., & Zhou, B. (2013). On Laplacian energy. *MATCH Communications in Mathematical and in Computer Chemistry*, **70**, 689–696.

ARTICLE IN PRESS

ARTICLE IN PRESS

[47] Stevanović, D., Milošević, M., Hic, P., & Pokorny, M. (2013). Proof of a conjecture on distance energy of complete multipartite graphs. *MATCH Communications in Mathematical and in Computer Chemistry*, **70**, 157–162.

[48] Ji, S., Li, X., & Shi, Y. (2013). Extremal matching energy of bicyclic graphs. *MATCH Communications in Mathematical and in Computer Chemistry*, **70**, 697–706.

[49] Gutman, I. (2021). Geometric approach to degree-based topological indices: Sombor indices. *MATCH Communications in Mathematical and in Computer Chemistry*, **86**(1), 11–16.

[50] Cruz, R., Gutman, I., & Rada, J. (2021). Sombor index of chemical graphs. *Applied Mathematics and Computation*, **399**, 126018.

[51] Ghanbari, N., & Alikhani, S. (2021). Sombor index of certain graphs. *Iranian Journal of Mathematical Chemistry*, **12**(1), 27–37.

[52] Das, K. C., Çevik, A. S., Cangul, I. N., & Shang, Y. (2021). On Sombor index. *Symmetry*, **13**(1), 140.

[53] Ghanbari, N. (2022). On the Sombor characteristic polynomial and Sombor energy of a graph. *Computational and Applied Mathematics*, **41**, 242.

[54] Deng, H., Tang, Z., & Wu, R. (2021). Molecular trees with extremal values of Sombor indices. *International Journal of Quantum Chemistry*, **121**(7), e26622.

[55] Wang, Z., Mao, Y., Li, Y., & Furtula, B. (2022). On relations between Sombor and other degree-based indices. *Journal of Applied Mathematics and Computing*, **68**, 1–17.

[56] Chen, H., Li, W., & Wang, J. (2022). Extremal values on the Sombor index of trees. *MATCH Communications in Mathematical and in Computer Chemistry*, **87**, 23–49.

[57] Li, S., Wang, Z., & Zhang, M. (2022). On the extremal Sombor index of trees with a given diameter. *Applied Mathematics and Computation*, **416**, 126731.

[58] Hayat, S., Arshad, M., & Khan, A. (2024). Graphs with given connectivity and their minimum Sombor index having applications to QSPR studies of monocarboxylic acids. *Heliyon*, **10**(1), e23392.

[59] Huang, R. R., Azam, S., Aslam, A., et al. (2025). Topological indices and QSPR modeling of gonalgia-associated drug molecules via M-polynomials. *European Physical Journal E*, **48**, 63.

[60] Zhang, X., Yousaf, S., Naeem, A., Tawfiq, F. M., & Aslam, A. (2024). Analyzing topological descriptors of guar gum and its derivatives for predicting physical properties in carbohydrates. *Chemometrics and Intelligent Laboratory Systems*, **253**, 105203.

[61] Espinal, C., Gutman, I., & Rada, J. (2025). Elliptic Sombor index of chemical graphs. *Communications in Combinatorics and Optimization*, **10**(4), 989–999.

[62] Redžepović, I. (2021). Chemical applicability of Sombor indices. *Journal of the Serbian Chemical Society*, **86**, 445–457.

[63] Jafari Rad, N., Jahanbani, A., & Gutman, I. (2018). Zagreb energy and Zagreb Estrada index of graphs. *MATCH Communications in Mathematical and in Computer Chemistry*, **79**(2), 371–386.

[64] Yang, Y., Jin, B. B., Lu, M., et al. (2023). Computing the expected subtree number of random hexagonal and phenylene chains based on probability matrices. *Discrete Applied Mathematics*, **339**, 184–201.

ARTICLE IN PRESS

ARTICLE IN PRESS

[65] Knor, M., Sedlar, J., Škrekovski, R., et al. (2026). The subpath number of cactus graphs. *Computational and Applied Mathematics*, **45**, 102.

[66] Cambié, S., Wagner, S., & Wang, H. (2021). On the maximum mean subtree order of trees. *European Journal of Combinatorics*, **97**, 103388.

[67] Furtula, B., & Gutman, I. (2015). A forgotten topological index. *Journal of Mathematical Chemistry*, **53**(4), 1184–1190.

[68] Randić, M. (1975). On characterization of molecular branching. *Journal of the American Chemical Society*, **97**(23), 6609–6615.

[69] Zhong, L. (2012). The harmonic index for graphs. *Applied Mathematics Letters*, **25**(3), 561–566.

[70] Zhou, B., & Trinajstić, N. (2009). On a novel connectivity index. *Journal of Mathematical Chemistry*, **46**(4), 1252–1270.

[71] Vukičević, D., & Furtula, B. (2009). Topological index based on the ratios of geometrical and arithmetical means of end-vertex degrees of edges. *Journal of Mathematical Chemistry*, **46**(4), 1369–1376.

[72] Estrada, E., Torres, L., Rodríguez, L., & Gutman, I. (1998). An atom-bond connectivity index: Modelling the enthalpy of formation of alkanes. *Indian Journal of Chemistry, Section A*, **37A**, 849–855.

[73] Ranjini, P. S., Lokesha, V., & Usha, A. (2013). Relation between phenylene and hexagonal squeeze using harmonic index. *International Journal of Graph Theory*, **1**, 116–121.

[74] Kim, S., Chen, J., Cheng, T., Gindulyte, A., He, J., He, S., Li, Q., Shoemaker, B. A., Thiessen, P. A., Yu, B., Zaslavsky, L., Zhang, J., & Bolton, E. E. (2021). PubChem in 2021: New data content and improved web interfaces. *Nucleic Acids Research, 49*(D1), D1388–D1395. https://doi.org/10.1093/nar/gkaa971

[75] Daina, A., Michielin, O., & Zoete, V. (2017). SwissADME: A free web tool to evaluate pharmacokinetics, drug-likeness and medicinal chemistry friendliness of small molecules. *Scientific Reports, 7*, 42717. https://doi.org/10.1038/srep42717

[76] Gaulton, A., Bellis, L. J., Bento, A. P., Chambers, J., Davies, M., Hersey, A., Light, Y., McGlinchey, S., Michalovich, D., Al-Lazikani, B., & Overington, J. P. (2012). ChEMBL: A large-scale bioactivity database for drug discovery. *Nucleic Acids Research, 40*(Database issue), D1100–D1107. https://doi.org/10.1093/nar/gkr777

[77] Advanced Chemistry Development, Inc. (ACD/Labs). (2023). *ACD/ChemSketch, version 2023* [Computer software]. Advanced Chemistry Development, Inc.

....